

## INFORMATION TO USERS

The most advanced technology has been used to photograph and reproduce this manuscript from the microfilm master. UMI films the text directly from the original or copy submitted. Thus, some thesis and dissertation copies are in typewriter face, while others may be from any type of computer printer.

The quality of this reproduction is dependent upon the quality of the copy submitted. Broken or indistinct print, colored or poor quality illustrations and photographs, print bleedthrough, substandard margins, and improper alignment can adversely affect reproduction.

In the unlikely event that the author did not send UMI a complete manuscript and there are missing pages, these will be noted. Also, if unauthorized copyright material had to be removed, a note will indicate the deletion.

Oversize materials (e.g., maps, drawings, charts) are reproduced by sectioning the original, beginning at the upper left-hand corner and continuing from left to right in equal sections with small overlaps. Each original is also photographed in one exposure and is included in reduced form at the back of the book. These are also available as one exposure on a standard 35mm slide or as a 17" x 23" black and white photographic print for an additional charge.

Photographs included in the original manuscript have been reproduced xerographically in this copy. Higher quality 6" x 9" black and white photographic prints are available for any photographs or illustrations appearing in this copy for an additional charge. Contact UMI directly to order.

# U·M·I

University Microfilms International  
A Bell & Howell Information Company  
300 North Zeeb Road, Ann Arbor, MI 48106-1346 USA  
313/761-4700 800/521-0600



Order Number 8914742

**Computer simulation study of the conduction properties of  
conducting polymer fiber films**

**Barve, Chandralekha Shrish, Ph.D.**

**City University of New York, 1988**

**U·M·I**  
300 N. Zeeb Rd.  
Ann Arbor, MI 48106



COMPUTER SIMULATION STUDY OF  
THE CONDUCTION PROPERTIES OF  
CONDUCTING POLYMER FIBER FILMS

by

CHANDRALEKHA S. BARVE <sup>A</sup>

A dissertation presented to  
the Graduate Faculty in Physics  
in partial fulfillment of the requirements  
for the degree of Doctor of Philosophy,  
City University of New York.

1988.

This manuscript has been read and accepted for the Graduate Faculty in Physics in satisfaction of the dissertation requirement for the degree of Doctor of Philosophy.

5/9/88  
Date

M. Tomkiewicz  
Prof. Micha Tomkiewicz  
Chairman of Examining Committee

5/10/88  
Date

Joe Gordon  
Executive Officer

Pabitra Sen  
Dr. Pabitra Sen, Schlumberger-Doll Research

St. Greenbaum  
Prof. Steven Greenbaum, Hunter College

Yeddyah Langsam  
Prof. Yeddyah Langsam, Brooklyn College

Alvin Halpern  
Prof. Alvin Halpern, Brooklyn College

Supervisory Committee.

The City University of New York.

Abstract

COMPUTER SIMULATION STUDY OF  
THE CONDUCTION PROPERTIES OF  
CONDUCTING POLYMER FIBER FILMS.

by

Chandralekha S. Barve

Adviser: Professor Micha Tomkiewicz

We employ Computer Simulation techniques to study the effect of morphology on the conductivity properties of polymer fiber films. A Random Network Model is introduced where a model fibrous film is represented by an equivalent electrical network. The resulting complex random network problem is solved to determine the impedance of the system for various frequencies. We have analyzed the response of the system to see how various processes of conduction, and structural factors, contribute to the electrical properties of the system. For heavily doped films, the low and the high frequency behaviour of the impedance can be represented by passive networks; whereas, in mid-frequency range the system shows Constant Phase Angle (CPA) behaviour. The CPA slope  $\beta$  is found to be related to the fractal dimension  $D$  by a simple relation  $\beta = D-1$ . Both  $\beta$  and  $D$  change linearly with the fractional vol-

ume occupied by the fibers. For lightly doped films, using Monte Carlo simulation of Kivelson's hopping model (Ki82), the conductivity of a single fiber is determined. The Random Network Model is then utilized to calculate the conductivity of the film. The dc conductivity is determined for various morphologies of the film, and a relationship between the dc conductivity of a fiber and that of the film is established. The complex conductivity  $\sigma(\omega)$  is calculated in the frequency range 1 Hz to 1 MHz for various temperatures. The results are compared with experimental data.

To my parents  
with love and appreciation

## Acknowledgements

I wish to express my deepest gratitude to Professor Micha Tomkiewicz, my thesis adviser, for his guidance and encouragement. He was always accessible for any kind of help or discussion, and his constant interest in my progress has given me more than one could hope for in a mentor.

I would like to thank my senior colleague Doctor Michael Kramer, who took special interest in my project, for teaching me tricks of the trade and also for introducing me to the CUNY computer system.

Special thanks to Doctor Pabitra Sen of Schlumberger-Doll Research, Professor Alvin Halpern and Professor Yedidyah Langsam, both of Brooklyn College, and Professor Steven Greenbaum of Hunter College for agreeing to work on my thesis committee.

I wish to acknowledge with gratitude the financial support offered by the Physics Department of Brooklyn College and by the Research Foundation of CUNY during my graduate studies. I am also grateful to the Computer Center of the Brooklyn College and to CUNY University Computing Center for allowing me to use their facilities.

Words can not express my appreciation of my husband, Shrish, for his constant support, from the days of my undergraduate studies and throughout my graduate carrier. Being a Physicist himself, he has

gone through every finer detail of my work and has helped me understand the physical aspects of my problem. Without his encouragement, and prodding, this work would never have seen the light of the day. Finally, to my son Vivek, who is probably the most wonderful thing that could have happened to me during my graduate studies (and who loves saying "yoouu welcome"), thanks!

## CONTENTS

ABSTRACT	iii
ACKNOWLEDGEMENT	vi
LIST OF FIGURES	ix
INTRODUCTION.	1
CH. 1 : CONDUCTING ORGANIC POLYMERS.	4
1.1 : Physical Structure of Polyacetylene.	6
1.2 : Band Structure of Polyacetylene.	9
1.3 : Solitons in Polyacetylene.	13
1.4 : Electrical Transport Properties.	16
1.5 : Other Conducting Polymers.	19
CH. 2 : ELECTRONIC CONDUCTION IN POLYMERS: THEORETICAL TOOLS.	20
2.1 : Hopping of Electrons Between Localized States	20
2.2 : Electron Hopping in a Soliton Band.	23
2.3 : Fluctuation-Induced Tunneling Conduction.	28
2.4 : Effective Medium Theory and Resistor Networks.	32
CH. 3 : A COMPUTER SIMULATION MODEL.	36
3.1 : Search for an Alternative.	36
3.2 : Random Network Model.	38
3.3 : Computer Simulation of a Single Fiber.	46
CH. 4 : RESULTS AND DISCUSSION.	52
4.1 : Lightly Doped Polyacetylene.	52
4.2 : Behaviour of the Equivalent Electrical Network.	62
4.3 : CPA Behaviour and Fractal Nature of the Film.	72
SUMMARY AND CONCLUSIONS.	83
APPENDICES.	
A : The Definition of the Equivalent Electrical Network.	87
B : Program Listings.	92
REFERENCES.	128

## LIST OF FIGURES

Figure	Caption	Page
1.1	Molecular structure of Trans and Cis isomers of polyacetylene.	7
1.2	Electron micrograph of polyacetylene film.	8
1.3	Perfectly dimerized Trans-Polyacetylene; a) A phase, b) B phase.	10
1.4	Band structure of perfectly dimerized Trans-Polyacetylene.	11
1.5	a) Schematic diagram of soliton separating A and B phases. b) Soliton energy as a function of wall width for three values of $E_g$ .	14
1.6	Electrical conductivity (room temperature) as a function of dopant concentration.	17
2.1	Schematic representation of soliton conduction. a) Free-soliton conduction in which a bound charged soliton is thermally liberated. b) Electron hopping between soliton bound states.	25
2.2	a) Tunneling junction between two conducting segments. b) Representation of a junction as a parallel plate capacitor.	30
3.1	A typical system of fibers with its equivalent network.	41
3.2	Real and imaginary impedences for different sizes of film, compared with those for a film of size $L/d = 120$ .	45
4.1	Dc conductivity as a function of concentration.	54
4.2	The ratio of the conductivity of the film to that of the fiber as a function of $\cos^2 \theta$ .	57
4.3	The real part of the conductivity plotted against frequency for various temperatures.	59

4.4	Temperature dependence of the ratio of the real part of the conductivity to the imaginary part at $10^4$ Hz.	61
4.5	Input parameters of the Random Network Model.	64
4.6	A typical frequency response for $v = 0.3$ .	65
4.7	The current flow in a typical system a) at low frequency b) at high frequency.	67
4.8	The low and the high frequency capacitances as a function of resistivity of fiber.	69
4.9	a) The low frequency capacitance as a function of fractional volume. b) The high frequency capacitance as a function of fractional volume.	71
4.10	CPA behaviour in mid-frequency range.	73
4.11	Vanishing of CPA behaviour for large values of fiber resistance.	74
4.12	CPA slope as a function of fractional volume.	76
4.13	Liu's Cantor bar model of rough electrode and its equivalent circuit.	78
4.14	log-log plot of number of intersection points and the size of the square.	79
4.15	Fractal dimension as a function of fractional volume.	80

## INTRODUCTION.

After the birth of quantum mechanics, our understanding of the solid state, especially the crystalline solids, grew very rapidly. The theory of the electrical conductivity of metals was particularly successful. The concept of phonon helped us in comprehending elastic, thermal, and electronic properties of the solids. The band theory has neatly classified materials into insulators, metals and semiconductors. Semiconductor physics, due to its successful applications in fabricating electronic devices has revolutionized the world. The natural consequence of this revolution is the interest in studying and synthesizing new materials, with specific mechanical and electrical properties, that can be tailored in accordance with the demands of millions of applications.

The study of charge transport in these materials is of fundamental interest; both, from the point of view of basic physics and for its applications in electronic devices. On the one hand, the analysis of the transport phenomena throws light on the electronic interactions in the material, on band structure etc. On the other hand, modern electronics, which depends heavily on the sophisticated knowledge of many aspects of charge transport in the semiconductors, seems to have ceaselessly growing influence on human activities.

Charge transport is in general a difficult problem; from both, a mathematical and physical point of view. In fact, the integrodifferential Boltzmann equation that describes the problem, does not offer analytical solutions except for a very few special cases. In most materials, the electronic transport is controlled by various microscopic physical processes, whose relative importance is not known. For some physical systems, under special conditions, it is possible to formulate microscopic models for charge transport; but the analytical solutions based on such models are generally very complex. With the advent of large computers with fast processors, computer simulation may well be the only feasible approach to deal with this problem.

Conducting organic polymers have been investigated extensively in the present decade, because of their wide spectrum of applications. The polymer fiber films have been used in fabricating light weight rechargeable batteries, solar cells, photoelectrochemical cells etc. In this work, we have applied computer simulation techniques to study the polymer fiber films; particularly, the conduction mechanism and the effect of morphology of the film on charge transport.

Chapter 1 presents an overview of conducting organic polymers. In Chapter 2 we describe theoretical models that have been developed in order to understand the conduction mechanism in polymer fiber films. Chapter 3 introduces our computer simulation model. The results of our

calculations for lightly doped and heavily doped systems have been presented in Chapter 4 along with some discussion. Finally we make some concluding remarks.

## Chapter 1.

## CONDUCTING ORGANIC POLYMERS.

Polyenes consist of a carbon backbone formed by C-C sigma bonds and pi bonds. Three out of the four valence electrons of a carbon atom are in  $sp^2$  hybridized orbitals. The linear combination of the 2s orbital with the two in-plane 2p orbitals produces three  $\sigma$  bonds. Two of the  $\sigma$  bonds are links in the backbone chain, while the third forms a bond with some side group [for example H in  $(CH)_x$ ]. The remaining valence electron forms a  $\pi$  bond in which charge density is perpendicular to the plane of the molecule. The  $\sigma$  bonds form low lying completely filled bands, whereas the  $\pi$  bond gives rise to a half filled band. Hence if there is negligibly small distortion of the carbon chain, the system should behave like a metal.

The electronic structure of polyenes has been a subject of interest for many years. In an earlier theoretical study based on the Huckel theory of molecular orbitals, J. E. Lennard-Jones (Le37) concluded that, in the limit of infinite chain length, C-C bonds in polyene tend to a constant length of 1.38 Å. This was later supported by Coulson(Co38). But the agreement between this and the experimental observations was not satisfactory. In optical studies of long polyenes, it was found that the frequency of maximum absorption, first decreases

with increasing chain length as expected from free electron or molecular orbital theory; however it then saturates at about 2 eV. This suggests that the system of long polyenes is a semiconductor with a band gap of 2 eV.

Higgins and Salem carried out an analysis with a well defined model, and found that the uniform infinite chain is unstable with respect to bond alternation. For an infinite polyene the stable configuration is one of unequal bond lengths. This is nothing but a restatement of the one dimensional Peierls instability (Pe55) for a special case. A distortion of the chain in which every molecule moves a little bit, so that the lattice constant becomes twice that of the undistorted chain, leads to a small band gap at the fermi energy.

Ovchinnikov et al. (Ov78) have argued that the electronic gap in long chain polyenes is due to correlations in polyenes, with Peierls effect playing no important role. There is no general agreement on this point.

In the context of the above discussion, polyacetylene  $(CH)_x$ , the simplest conjugated polymer, is of special interest. In 1974, Ito, Shirakawa, and Ikeda (It74) succeeded in obtaining flexible silvery films of  $(CH)_x$ . Interest in this semiconducting polymer has been stimulated by the successful demonstration of doping, with the associated control of electrical properties over a wide range. Chiang et al. (Ch77) have

shown that, the electrical conductivity of  $(\text{CH})_x$  films can be varied over 12 orders of magnitude from that of an insulator through semiconductor to a metal. Since then, the various physical, chemical, and structural properties of polyacetylene have been studied extensively. In the following sections of this chapter we summarize these properties.

### 1.1 Physical Structure Of Polyacetylene.

Polyacetylene  $(\text{CH})_x$  is the simplest linear conjugated polymer. It is ideally a planar compound composed of a succession of CH units joined by alternating single and double bonds. It exists in two isomeric forms Cis-Polyacetylene and Trans-Polyacetylene as shown in Figure (1.1). The Cis and Trans content of polyacetylene are strongly dependent on the polymerization temperature. For example, if the preparation of polyacetylene is carried out at room temperature, the film has approximately 60% Cis and 40% Trans. By heating, Cis isomer may be conveniently converted to the thermodynamically more stable Trans isomer. This is known as Cis-Trans isomerization.

Electron micrograph of Polyacetylene film [Figure (1.2)] shows a fleece of randomly oriented fibers with diameters of about 200 Å and indefinite length. The bulk density of  $(\text{CH})_x$  film obtained from weight and physical volume ranges from 0.3 to 0.6 gm/cm<sup>3</sup>; whereas its flotation density is 1.15 gm/cm<sup>3</sup>. This indicates that only one fourth to one

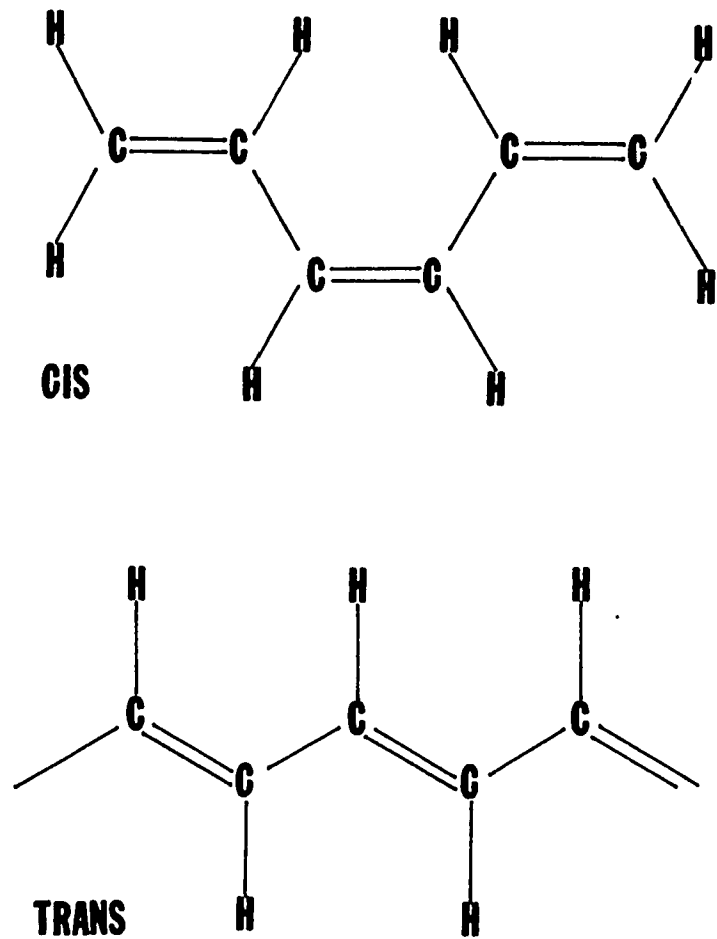


Fig. 1.1 Molecular Structure of Cis and Trans isomers of Polyacetylene.

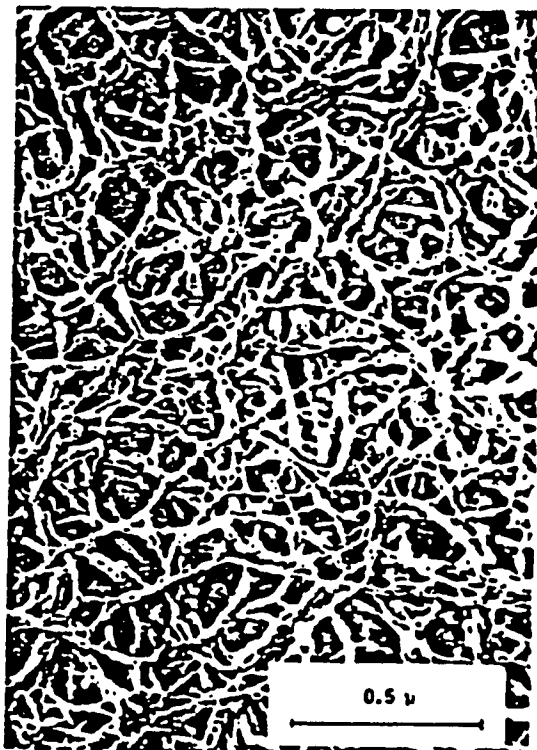


Fig. 1.2 Electron Micrograph Of Polyacetylene film [after ref. (Mo82)].

half of the film volume is occupied by the fibers. Partial orientation of the polyacetylene fibers can be achieved by stretch alignment of the films with combined mechanical and thermal treatment. Stretch oriented polyacetylene films exhibit considerable electrical and optical anisotropy.

## 1.2 Band Structure Of Polyacetylene.

The  $\pi$ -system transfer integral for polyacetylene can be deduced from theoretical and spectroscopic studies as  $|t| \approx 2-2.5$  eV. This implies a large overall bandwidth  $W_{\parallel} \sim 8-10$  eV. However, the transverse bandwidth due to interchain coupling is much less. The nearest neighbour interchain spacing of  $4.39 \text{ \AA}$  implies the transverse bandwidth  $W_{\perp} \sim 0.1$  eV. Hence the polyacetylene system may be regarded as quasi-one-dimensional. We consider a model for Trans-Polyacetylene in which  $\pi$  electrons are treated in a tight binding approximation, and  $\sigma$  electrons are assumed to move adiabatically with the nuclei.

Let  $u_n$  be a configuration coordinate for displacement of the  $n^{\text{th}}$  CH group along the molecular symmetry axis as shown in Figure (1.3a).  $u_n = 0$  for the undimerized chain. The Hamiltonian is

$$H = - \sum_{ns} ( t_{n+1,n} c_{n+1,s}^{\dagger} c_{n,s} + \text{h.c.} ) + \sum_n \frac{1}{2} K (u_{n+1} - u_n)^2 + \sum_n \frac{1}{2} M u_n^2, \quad (1.1)$$

where to first order in the  $u$ 's,

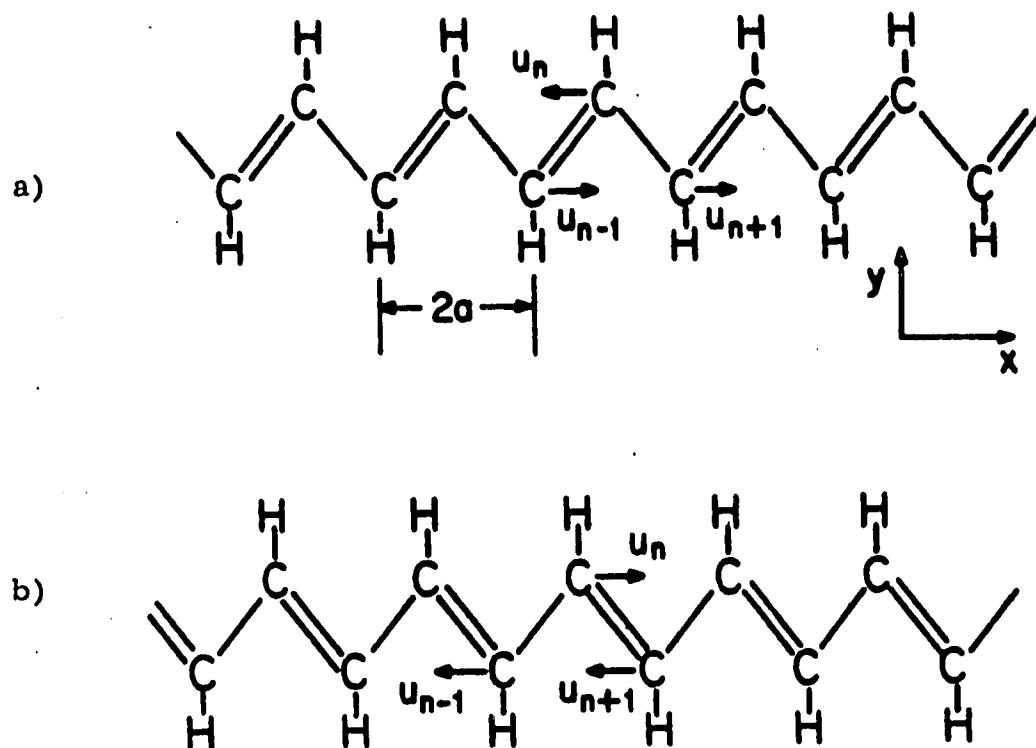


Fig. 1.3 Perfectly dimerized Trans-Polyacetylene (after ref. Su79).  
 a) A phase,  
 b) B phase



$$t_{n+1,n} = t_0 - \alpha (u_{n+1} - u_n). \quad (1.2)$$

$M$  is the mass of the CH unit,  $K$  is the spring constant for the  $\sigma$  energy when expanded to second order about the equilibrium undimerized systems, and  $c_{ns}^+$  ( $c_{ns}$ ) creates (annihilates) a  $\pi$  electron of spin  $s$  on the  $n^{\text{th}}$  CH group. The band structure of the perfect infinite dimerized Trans-Polyacetylene is shown in Figure (1.4). In this perfect structure, the displacements are of the form

$$u_{n0} = \pm (-1)^n u_0, \quad (1.3)$$

where  $\pm$  corresponds to the two possible degenerate structures A and B as shown in Figures (1.3a) and (1.3b) respectively. The transfer integrals for the perfect chain are

$$t_{n+1,n} = \begin{cases} t_0 - t_1 & \text{"single" bond} \\ t_0 + t_1 & \text{"double" bond.} \end{cases} \quad (1.4)$$

The overall bandwidth is  $4t_0 \sim 8-10$  eV. The energy gap  $E_g = 4t_1$  depends on the magnitude of the distortion of the chain. For example if  $E_g = 1.4$  eV, the value of  $u_0$  which minimizes the ground state energy is  $u_0 = 0.042 \text{ \AA}$ . The ground state energy as a function of the displacement of the CH group is shown in Figure (1.4). It is degenerate with respect to two dimerized structures of alternating single and double bonds, A and B, as shown in Figure (1.3).

In the above discussion, the band calculations are done for a one dimensional trans-polyacetylene chain. The interchain coupling is expected to give a transverse bandwidth of the order of a few tenths of an eV. In contrast with the trans structure, the cis structure has an even bandgap for uniform bonds. This suggests that the energy gap of the cis structure is greater than that of the trans structure.

### 1.3 Solitons In Polyacetylene.

As we have seen in the previous section, in trans-polyacetylene, ground state energy is degenerate with respect to two dimerized structures A and B (Figures (1.3),(1.4)). Hence one expects excitations to exist in the form of a topological soliton, or moving domain wall, separating the A and B domains. This has been studied theoretically by Su, Schrieffer and Heeger (Su79), and by Rice (Ri79). In this section we briefly describe their work.

Consider a situation where the A phase and B phase coexist in a chain with a domain wall or a soliton separating the two phases as shown in Figure (1.5a). The soliton is at rest at the origin  $n = 0$ . As one moves to the far right (left), the displacement pattern reduces to that of the A phase (B phase). The displacements in a segment of  $N$  CH groups located symmetrically about  $n = 0$  vary, but, they are matched onto perfect A and B phases on either sides. The ground state

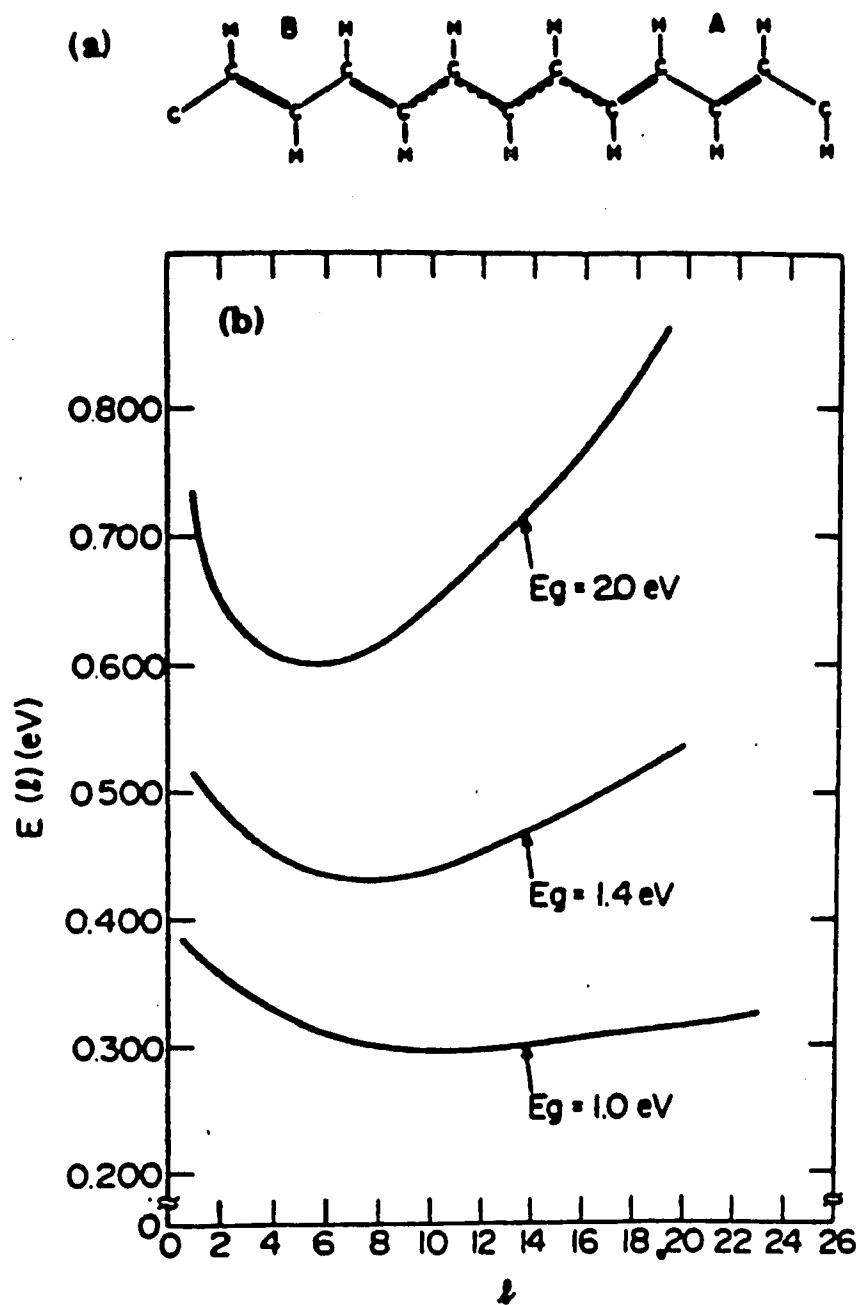


Fig. 1.5 a) Schematic diagram of soliton separating A and B phases.  
 b) Soliton energy as a function of wall width for three values of  $E_g$ .

energy is then calculated for any set of displacements  $u_n$  in the segment. The system energy  $E(\ell)$  can be determined by defining the staggered order parameter

$$\psi_n = (-1)^n u_n, \quad (1.5)$$

and by choosing the trial function as

$$\psi_n = u_0 \tanh(n/\ell). \quad (1.6)$$

$E(\ell)$  as a function of width of the wall  $\ell$ , is shown in Figure (1.5b) for  $4t_1 = 1.0, 1.4, \text{ and } 2.0$  eV. The minimum occurs at  $\ell \sim 7$  for  $4t_1 = 1.4$  eV (for  $4t_1 = 2.0$  eV,  $\ell \sim 5$  and for  $4t_1 = 1.0$  eV,  $\ell \sim 9$ ). The energy to create the soliton at rest is  $E_s \sim 0.4$  eV for  $E_g = 1.4$  eV. The effective mass of the soliton is  $M_s = 6m_e$  where  $m_e$  is the electron mass.

The electronic structure of the soliton shows a single sharp state  $\phi_0$  at the center of the gap, containing one electron for neutral kink. This localized state is spin unpaired but the distorted valence band still has spin 0. Hence the neutral soliton has spin  $\frac{1}{2}$ .

The relevance of solitons in the case of doped  $(\text{CH})_x$  can be seen as follows. The energy for creation of a soliton  $E_s$  must be compared with the energy for freeing an electron (or hole)  $\Delta$ . For  $E_g = 1.4$  eV,  $E_s = 0.4$  eV  $<$   $\Delta = 0.7$  eV therefore, soliton doping is favoured in  $(\text{CH})_x$ . For each donor or acceptor, which transfers an electron or a hole to

the chain, one charged soliton is formed. The charged solitons have spin zero and hence, no spin resonance and Curie-law susceptibility is associated with the charge carriers, as is experimentally observed.

#### 1.4 Electrical Transport Properties.

As we have seen in previous sections, all conjugated organic polymers, in their pure state, are best described as electrical insulators. The room temperature conductivity of undoped Cis is Cis-Polyacetylene about  $10^{-9} \Omega^{-1} \text{cm}^{-1}$  and it increases to  $10^{-5} \Omega^{-1} \text{cm}^{-1}$  on isomerization to Trans-Polyacetylene. This conductivity, however, is attributable to defects and impurities in the polymer. When pure polyacetylene is doped with a donor or an acceptor, the electrical conductivity increases dramatically over many orders of magnitude. It then saturates at higher dopant levels above approximately 1 %. The typical behaviour of the conductivity as a function of dopant concentration ( $y$ ) is shown in Figure (1.6). The general features appear to be the same for various dopants, but they differ in saturation values and critical concentrations above which conductivity depends weakly on  $y$ . The transport studies indicate a change in behaviour at a critical concentration  $y_c$  which may be characterized as a semiconductor to metal transition.

A great deal of effort has been devoted to the understanding of electrical transport in conducting polymers. A qualitative model (Fr85)

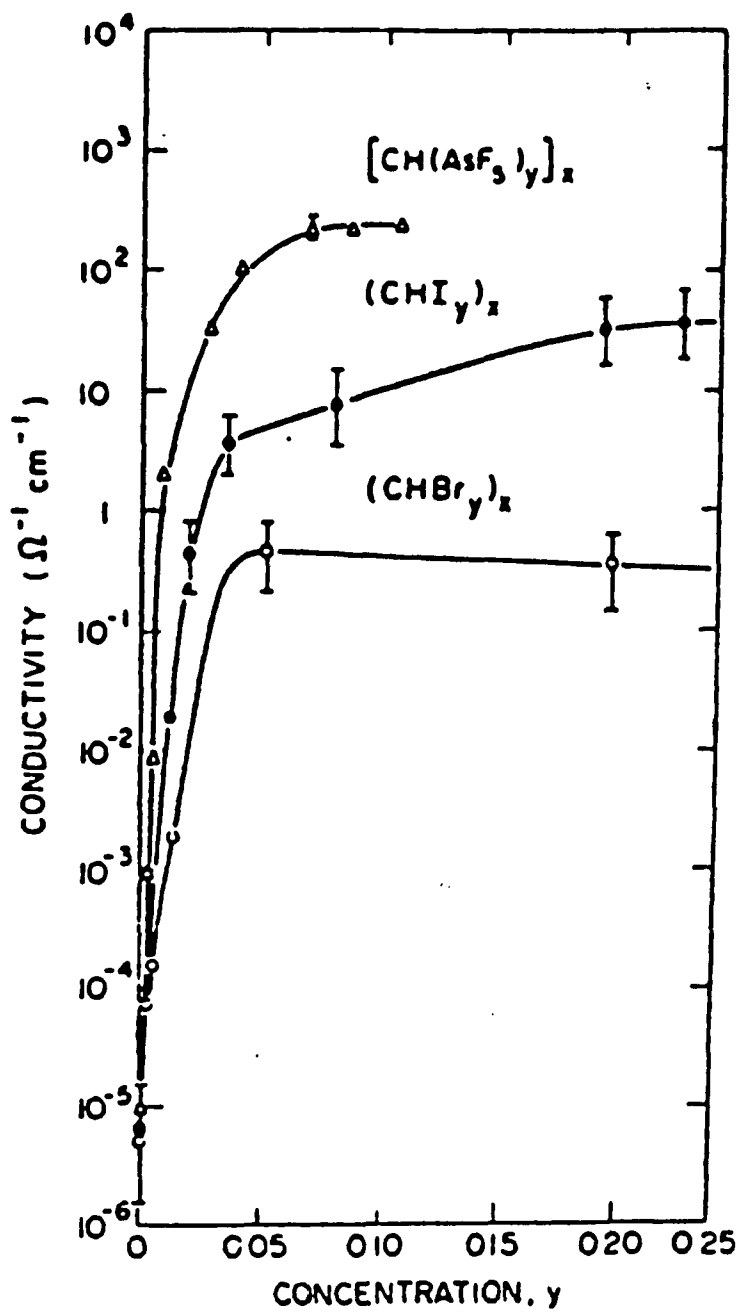


Fig. 1.6 Electrical conductivity (room temperature) as a function of dopant concentration (after ref. Ch77).

for conduction suggests that, there are at least three processes contributing to the conductivity : (i) Interchain transport (ii) Intrachain transport (iii) Interfiber transport. Thus, the conductivity is determined both by microscopic (interchain, intrachain) and macroscopic (interfiber) processes. Since, the relative importance of these processes is influenced by dopant concentrations, it is very difficult to develop a unique quantitative model. Various authors have proposed different models wherein attention is focussed on a particular feature of the conduction process. The Miller Abrahams model (Mi60) of hopping transport of electrons between localized sites, which is valid for lightly doped semiconductors, has been applied to polyacetylene by Summerfield et al (Su85). On the other hand, Kivelson (Ki82) has developed a variable range hopping model, in which it is assumed that, the conduction takes place via hopping of charge from charged solitons to neutral solitons. The large values of conductivity at high dopant concentrations suggest that, in this case, the fibers become essentially metallic and only the interfiber resistance is relevant for the overall conductivity (Eh86). Sheng (Sh80) has proposed a model for disordered materials with large conducting regions separated by small insulating barriers; in which, the conduction takes place via fluctuation induced tunneling of electrons between the conducting regions. This has been applied to heavily doped Polyacetylene (Pa80, Ph80). Tomkiewicz et al (To81) have developed a model in which it is assumed that the doping is highly

inhomogenous and dopants form metallic islands. In this model, the semiconductor-metal transition is related to a threshold for percolation between these islands. We will describe some of these models in some detail in the next chapter.

### 1.5 Other Conducting Polymers.

Besides Polyacetylene, polymers which can be made highly conducting by doping, are Polypyrrole, Polythiophene, and Polyphenylene and its derivatives. The molecular building units of these polymers are either the six membered phenylene rings or the five-membered hetero rings which are linked together by  $C_2H_2$  group and an S atom in the case of polyphenylene vinylene and polyphenylene sulphide.

The electrical conductivity of these polymers in the undoped state is low ( $10^{-10}$  to  $10^{-16} \Omega^{-1} \text{ cm}^{-1}$ ). Upon doping, the conductivity can be raised by many orders of magnitude to values between 1 and  $10^3 \Omega^{-1} \text{ cm}^{-1}$ . Because of the complexity in the chemical structure of these materials, they are not studied as extensively as polyacetylene. Since in many respects their properties are similar to polyacetylene, the concepts developed for polyacetylene may hopefully be generalized to accommodate this wider class of polymers.

## Chapter 2.

**ELECTRONIC CONDUCTION IN POLYMERS:  
THEORETICAL TOOLS.**

**2.1 Hopping of electrons between localized states.**

In doped semiconductors, at sufficiently low temperatures, the number of free carriers is small, and the conduction mechanism is dominated by charge transport in impurity states. When the impurity concentration is high, the impurity states overlap forming an impurity band and the conduction takes place in this band. At low concentration, however, banding does not occur and conduction takes place by hopping of electrons from occupied to unoccupied localized donor states (Mo56).

Miller and Abrahams (Mi60) have developed a model for the hopping process and have shown that this may be represented by an electrical network. The spatial locations of the nodes of this network are at the randomly distributed impurity sites, and the value of individual node to node conductance depends in general on the site separation and the site energies. We describe their model briefly.

Consider a semiconductor with  $N_D$  donors and  $N_A$  acceptors,  $N_D > N_A$ . At low temperatures acceptors will compensate  $N_A$  of the donors, and there will be  $N_A$  ionized donors,  $N_A$  ionized acceptors and  $N_D - N_A$

electrons in remaining donor states. If one of the  $N_D - N_A$  donor electrons is close to one of the  $N_A$  donor vacant sites, it can hop to this site. This transfer is accompanied by emission or absorption of a phonon in order to conserve energy. In absence of an electric field the charge transfer is random and net current is zero. The electric field introduces an average gradient in the donor state energy along the field direction. This increases the transfer rate to sites of lower field energy and hence a net current flows in the field direction.

Consider a simple model system consisting of equivalent sites, each of which can be either unoccupied or occupied by a single electron. The average transition rate for an electron from site  $i$  to site  $j$  is given by

$$\Gamma_{ij}^0 = \langle n_i (1 - n_j) \gamma_{ij} \rangle. \quad (2.1)$$

Here  $n_i$  are the occupation probabilities,  $\gamma_{ij}$  is the intrinsic transition rate from site  $i$  to site  $j$ ; the angular brackets denote an average over time. In thermal equilibrium, the occupation probabilities for different sites are statistically independent, hence  $\langle n_i n_j \rangle = \langle n_i \rangle \langle n_j \rangle$ , and

$$\langle n_i \rangle = [1 + \exp(E_i/kT)]^{-1}, \quad (2.2)$$

where energy  $E_i$  is measured from the Fermi level. Since we are considering a tunneling process, the dependence of  $\gamma_{ij}$  on  $\vec{R}_{ij}$ , the distance between the sites  $i$  and  $j$  must be exponential. The energy depen-

dence is less obvious but, when  $kT$  is small compared to  $|E_i - E_j|$  and when  $|E_i - E_j|$  is smaller than or of the order of Debye energy, one can write

$$\begin{aligned}\gamma_{ij} &= \gamma_0 \exp[-2\alpha R_{ij} - (E_j - E_i)/kT] && \text{for } E_j > E_i, \\ &= \gamma_0 \exp[-2\alpha R_{ij}] && \text{for } E_j \leq E_i,\end{aligned}\quad (2.3)$$

where  $\gamma_0$  is a constant that depends upon the electron phonon coupling strength.  $\Gamma_{ij}^0$  can then be simplified to (Am71)

$$\Gamma_{ij}^0 = \gamma_0 \exp[-2\alpha R_{ij} - (|E_i| + |E_j| + |E_i - E_j|)/2kT]. \quad (2.4)$$

In the presence of weak external electric field the site energies are modified as  $E_i \rightarrow E_i + e\vec{E} \cdot \vec{R}_i$ . The intrinsic transition rate  $\gamma_{ij}$  can now be written as

$$\begin{aligned}\gamma_{ij}(\vec{E}) &= \gamma_0 \exp[-2\alpha R_{ij} - (E_j - E_i + e\vec{E} \cdot \vec{R}_{ij})/kT] && \text{for } E_j > E_i, \\ &= \gamma_0 \exp[-2\alpha R_{ij}] && \text{for } E_j \leq E_i.\end{aligned}\quad (2.5)$$

The modified occupation number  $n_i(\vec{E})$  can be expressed in terms of the changes  $\delta\mu_i$  in the chemical potential at various sites:

$$n_i(\vec{E}) = [1 + \exp\{(E_i - \delta\mu_i)/kT\}]^{-1}. \quad (2.6)$$

By retaining only the first order terms in the electric field, the average net flow from site  $i$  to site  $j$  can be written as

$$\Gamma_{ij}(\vec{E}) - \Gamma_{ji}(\vec{E}) = [1/kT] [e\vec{E} \cdot \vec{R}_{ij} + \delta\mu_i - \delta\mu_j] \Gamma_{ij}^0. \quad (2.7)$$

The factor in the second parenthesis of equation (2.7) is the total potential difference between sites  $i$  &  $j$ . Hence the quantity

$$G_{ij} = [e^2/kT] \Gamma_{ij}^0 \quad (2.8)$$

can be recognized as the conductance between two sites.

The overall electrical conductivity can then be calculated by reducing the electrical network problem to a percolation problem. The conductivity  $\sigma$  is given by

$$\sigma = G_c/R_c. \quad (2.9)$$

$R_c$  has dimension of length, and it depends on some typical length scale of the network.  $G_c$  is the critical percolation conductance. It is defined as the largest conductance such that the subset of network with  $G_{ij} > G_c$  still contains a connected network which spans the entire system. Since the analysis involved in calculations of  $G_c$  and  $R_c$  is complex; they are generally determined by Monte Carlo Simulation Techniques.

## 2.2 Electron Hopping in a Soliton Band.

As we have seen in section 1.3, the elementary excitations in Trans-Polyacetylene are in the form of topological solitons [Figure (1.5)]. In undoped polyacetylene there is a small number of neutral solitons. Upon

doping, charge is transferred from dopant to polyacetylene chain, either by changing pre-existing neutral solitons into charged solitons or by creating new charged solitons. This charged soliton formation is favoured in  $(\text{CH})_x$  over freeing an electron from the dopant.

Since the solitons are topological excitations of the polymer chain, the free solitons can diffuse along the chain, however, they cannot hop between chains. Their motion is thus highly one dimensional. The neutral solitons are mobile, whereas the charged solitons, which are formed by transfer of charge between dopant atom and the polymer chain, are bound to the ionized dopant atom with binding energy  $E_b \sim 0.3$  eV. At high temperatures some of the charged solitons become free, and then the charge transport is presumably dominated by charged soliton diffusion. At low temperatures, however, there are not many free charged solitons available. Kivelson (Ki82) has explained the conduction at such temperatures, and low doping levels, in terms of phonon assisted hopping of charge from charged solitons to neutral solitons.

Consider a negatively charged soliton bound to a positively charged impurity on one of the chains [Figure (2.1)]. If a neutral soliton on a nearby chain has an impurity atom in its vicinity then phonon assisted hopping of an electron from the charged soliton to the neutral soliton is energetically favoured as compared to liberating the charged soliton from the impurity. To determine the net conductivity of a fiber using

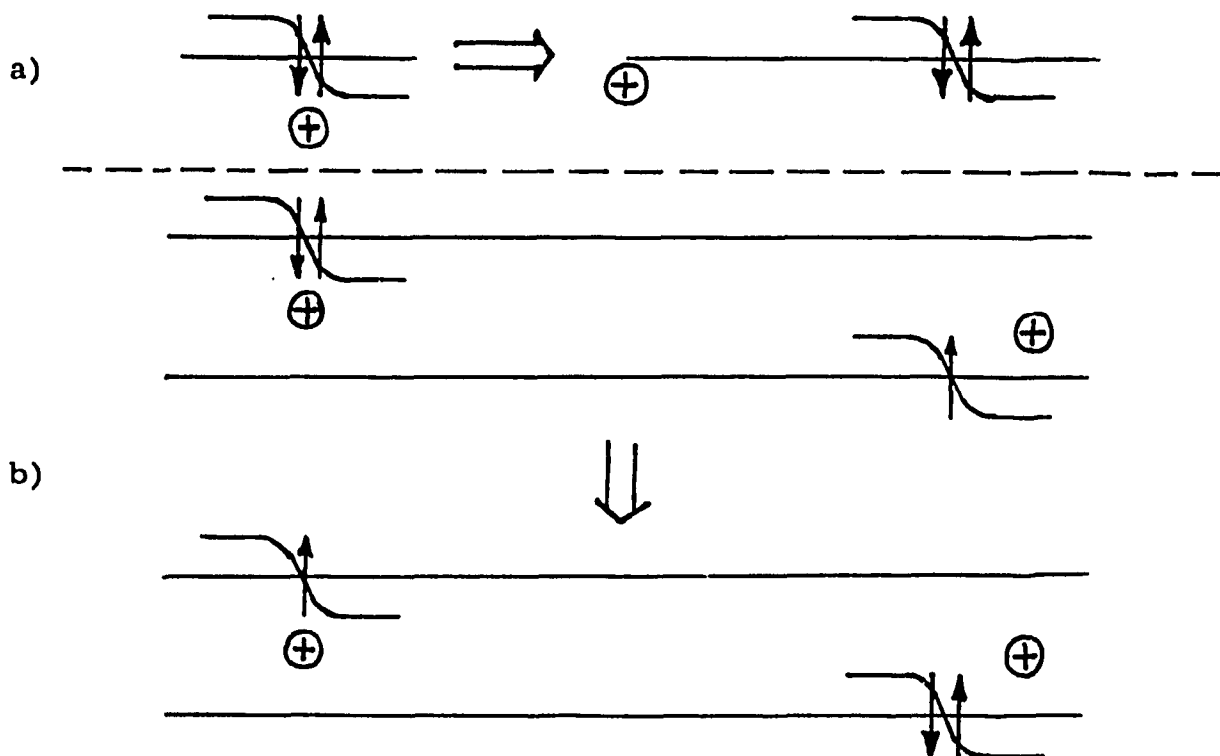


Fig. 2.1 Schematic representation of soliton conduction.  
 a) Free-soliton conduction in which a bound charged soliton is thermally liberated.  
 b) Electron hopping between soliton bound states.

this model, the method of the last section is followed. Consider a simple model system consisting of charged and neutral solitons. In thermal equilibrium, the average transition rate from the  $i^{\text{th}}$  soliton to the  $j^{\text{th}}$  soliton is given by

$$\Gamma_{ij}^{(0)} = v_{ij} n^{(0)} (1-n^{(0)}), \quad (2.10)$$

where  $v_{ij}$  is the transition rate from charged soliton at the  $i^{\text{th}}$  soliton site to neutral soliton at the  $j^{\text{th}}$  soliton site,  $n^{(0)}$  is the fraction of solitons which are charged, and  $(1-n^{(0)})$  is the fraction of solitons which are neutral and have an impurity atom nearby. (For future convenience we have absorbed the factor  $1/N$ , which reflects the probability that the neutral soliton is near an impurity atom, in the expression  $(1-n^{(0)})$ . On the other hand, Kivelson has absorbed it in the expression for transition rate).

To determine  $v_{ij}$ , Kivelson has solved the two soliton problem within the Born-Oppenheimer approximation. He has shown that the transition rate can be expressed as a product of two factors; one depending upon the spatial separation  $\vec{R}_{ij}$  between two solitons  $i$  and  $j$ , and the other one depending upon the electron phonon coupling.

$$v_{ij} = \gamma(T) \exp\{-2[(R_{\parallel}/\xi_{\parallel})^2 + (R_{\perp}/\xi_{\perp})^2]^{\frac{1}{2}}\}, \quad (2.11)$$

where  $R_{\parallel}$  is the component of  $\vec{R}_{ij}$  along the chain and  $R_{\perp}$  is the component perpendicular to the chain.  $\xi_{\parallel}$  and  $\xi_{\perp}$  are the in chain and out of

chain electron decay lengths respectively. To further calculate the characteristic frequency  $\gamma(T)$  appearing in equation (2.11), it is necessary to construct a three dimensional microscopic model of polyacetylene. Su, Shrieffer and Heeger's model as discussed in section 1.3 is purely one dimensional. Kivelson has augmented this model by considering interchain interactions as a perturbation over the three dimensional hamiltonian. He then evaluates the electron phonon coupling function, in terms of which  $\gamma(T)$  becomes,

$$\gamma(T) = (500 \text{ eV}/\hbar) [T/300 \text{ K}]^{10}. \quad (2.12)$$

Using Eq. (2.11) and Eq. (2.12),  $\Gamma_{ij}^{(0)}$  can be written as

$$\Gamma_{ij}^{(0)} = (500 \text{ eV}/\hbar) [T/300 \text{ K}]^{10} n^{(0)} (1-n^{(0)}) \times \exp\{-2[(R_{\parallel}/\xi_{\parallel})^2 + (R_{\perp}/\xi_{\perp})^2]^{\frac{1}{2}}\}. \quad (2.13)$$

In analogy with the last section, in the presence of a weak external electric field, the net flow from site  $i$  to site  $j$  is given by

$$\Gamma_{ij}(\vec{E}) - \Gamma_{ji}(\vec{E}) = [1/kT] [e\vec{E} \cdot \vec{R}_{ij} + \delta\mu_i - \delta\mu_j] \Gamma_{ij}^{(0)}. \quad (2.14)$$

(See Appendix A for details.) The factor in the second parenthesis of the above equation is the potential difference between sites  $i$  and  $j$ , so the quantity

$$G_{ij} = [e^2/kT] \Gamma_{ij}^{(0)}, \quad (2.15)$$

can be identified as the conductance between sites  $i$  and  $j$ . Kivelson has obtained analytical formula for the overall electrical conductivity by using the method of Butcher et al (Bu77). He found

$$\sigma = (Ae^2/kT) n^{(0)} (1-n^{(0)}) \chi(T) (\xi/R_0^2) \exp (-2BR_0/\xi), \quad (2.16)$$

where  $A=0.45$ ,  $B=1.39$ ,  $R_0$  is the typical separation between impurities, and  $\xi$  is the three dimensionally averaged electronic decay length.

### 2.3 Fluctuation-Induced Tunneling Conduction.

As we have seen in section 2.1, in amorphous semiconductors, at low temperatures and at low doping levels, the conduction mechanism can be explained by the hopping transport of electrons between localized sites. However, some disordered materials, such as conductor-insulator composites and heavily doped amorphous or organic semiconductors, are characterized by large conducting regions separated by thin insulating barriers. For these systems the electrical conduction is dominated by electron transfer between large conducting segments rather than by hopping between localized sites. Sheng (Sh80) has introduced a novel mechanism, fluctuation-induced tunneling, in order to explain such electron transfers across insulating gaps in the conducting pathways. We now describe this mechanism briefly.

The conduction electrons in the above mentioned disordered materials are delocalized and free to move over distances very large as compared to atomic dimensions. These electrons tend to tunnel between the conducting regions at the points of their closest approach. The tunnel junctions are usually small in size and are therefore prone to thermally activated voltage fluctuations across the junction. The tunneling probability is affected by these fluctuations since they modulate the potential barrier. The fluctuations introduce characteristic temperature dependence to the normally temperature independent tunneling conductivity.

To determine the conductivity, Sheng has considered a single tunnel junction in the presence of applied electric field  $E_A$  and the thermal fluctuating field  $E_T$ . Since it is equally probable that  $E_T$  is in the same direction as  $E_A$ , or opposite to it; the net current density in the applied field direction, for  $E_T > E_A$ , is given by

$$\Delta j = \frac{1}{2} [ j(E_T + E_A) - j(E_T - E_A) ]. \quad (2.17)$$

Here a partial conductivity can be defined as

$$\Sigma(E_T) = \lim_{E_A \rightarrow 0} (\Delta j / E_A) = dj(E_T) / dE_T. \quad (2.18)$$

The fluctuation-induced tunneling conductivity can then be obtained by thermal averaging  $\Sigma(E_T)$ ,

$$\sigma = \int P(E_T) [dj(E_T) / dE_T] dE_T, \quad (2.19)$$

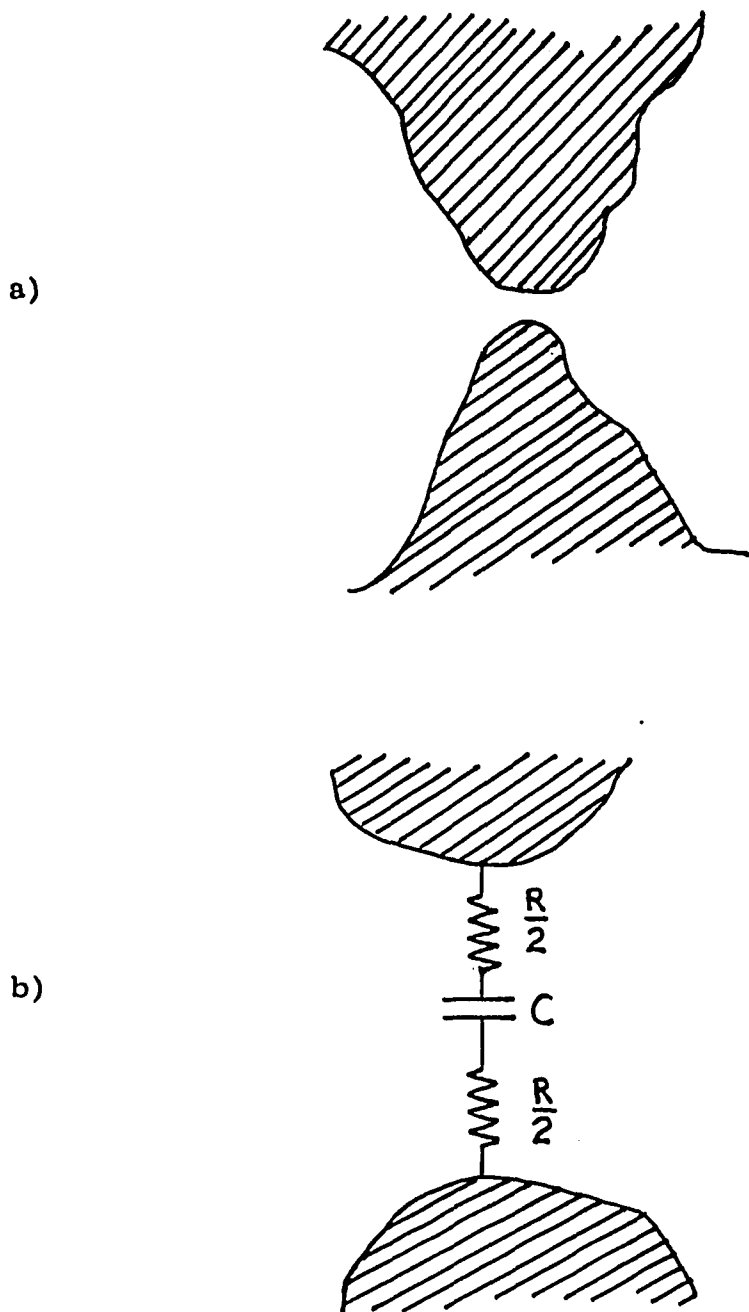


Fig. 2.2 a) Tunneling junction between two conducting segments.  
b) representation of a junction as a parallel plate capacitor.

where  $P(E_T)$  is the fluctuation probability function. To determine  $P(E_T)$ , Sheng has approximated the tunnel junction [Figure (2.2a)] by a parallel plate capacitor with area  $A$  and separation  $w$  as shown in Figure (2.2b).  $R/2$  denotes the resistance connecting to the rest of conducting segments. Using this picture of the junction, and by applying the equipartition theorem assuming the capacitor as a system with one degree of freedom,  $P(E_T)$  can be estimated as ,

$$P(E_T) = (4a/\pi kT)^{\frac{1}{2}} \exp[-aE_T^2/kT]. \quad (2.20)$$

Here  $a = wA/8\pi$  is a measure of the volume of a junction.

To find the field dependent tunneling current  $j(E_T)$  Sheng has used an image force corrected rectangular potential barrier to represent the thin insulating gap between conducting segments. The image force correction makes the potential smoothly varying, and thus removes unphysical infinite fields implied by a rectangular barrier. It allows one to study a variety of barrier shapes, from nearly rectangular to nearly parabolic. For this potential he determines the barrier transmission factor, and then calculates  $j(E_T)$  for low temperatures. By using this expression in Eq.(2.19), alongwith Eq.(2.20), the conductivity can be simplified to

$$\sigma = \sigma_0 \exp [ -T_1(E^{*2}/T + \phi(E^*, \lambda)/T_0) ], \quad (2.21)$$

where  $\sigma_0$  is a constant.  $T_0$ ,  $T_1$ , and  $\lambda$  are microscopic tunneling junction parameters.  $E^*$  is the reduced electric field.

A disordered material contains a large number of tunnel junctions. The voltage fluctuations vary from one junction to another. The behaviour of each junction can be expressed in terms of junction parameters  $T_0$ ,  $T_1$ . Therefore, as far as conductivity is concerned, the disordered material may be regarded as a random resistor network in which the resistors represent the tunnel junctions with distributions in the values of  $T_0$ , and  $T_1$ . The nodes of the network are the conducting pathways connecting the different junctions. Sheng has determined the conductivity of such a network by applying effective medium theory (ki79).

#### 2.4 Effective Medium Theory and Resistor Networks.

In previous sections, we have described various theoretical models which have been applied to a variety of semiconductors in order to understand the conduction mechanism. To determine the conductivity of a physical sample using these models, one has to employ the methods of Effective Medium Theory (EMT) or to solve the problem by reducing it to a random resistor network. Let us first illustrate the method of EMT by applying it to a polymer fiber film.

Consider the film to be a composite medium of polymer and air with conductivities  $\sigma_1$  and  $\sigma_2$  respectively. The conductivity of polymer  $\sigma_1$  can be determined by using a specific model for conduction (for example Kivelson's model.). Our objective is to calculate  $\sigma_e$ , an effective conductivity of the entire composite. We begin (Se85) by considering a small spherical grain inside the material, and treat that grain as if it is embedded in a homogenous effective medium, of conductivity  $\sigma_e$ , to be computed self-consistently. Let the field and current density far from the central grain be  $E_0$  and  $J_0 = \sigma_e E_0$ . We can therefore calculate the fields and current density within the grain to be

$$E_{in} = [3\sigma_e / (\sigma_i + 2\sigma_e)] E_0 \quad (2.22)$$

$$J_{in} = \sigma_i E_{in} \quad (2.23)$$

where  $\sigma_i$  is either  $\sigma_1$  or  $\sigma_2$ . The self consistency for computing  $\sigma_e$  comes from the assumption that

$$\langle J_{in} \rangle = \sigma_e \langle E_{in} \rangle. \quad (2.24)$$

Assuming that the composite is made up of the fraction  $f$  of component 1 and  $(1-f)$  of component 2, we can substitute Equations (2.22) and (2.23) into Eq.(2.24) to yield,

$$f[(\sigma_1 - \sigma_e) / (\sigma_1 + 2\sigma_e)] + (1-f)[(\sigma_2 - \sigma_e) / (\sigma_2 + 2\sigma_e)] = 0. \quad (2.25)$$

Since conductivity of air  $\sigma_2$  is zero, Eq.(2.25) can be simplified to obtain

$$\sigma_e = [(3f-1)/2] \sigma_1 \quad (2.26)$$

This gives the percolation threshold  $f^* = 1/3$ .

Although EMT has proved to be a useful approximation for dealing with systems about which we have very little structural information, the theory fails when a percolating system approaches the percolation threshold. EMT predicts a much higher critical concentration than is observed experimentally or by numerical simulation (K173). The source of this discrepancy can be traced to the number of simplifying assumptions that have been made in arriving at this result. The spherical grain shape is hardly compatible with the geometry of the fibrous film. With an elongated grain shape it is possible to lower the percolation threshold. The EMT is essentially a macroscopic approach to the study of inhomogeneous media, as a result, attention is paid neither to the structural details of the medium nor to the underlying microscopic processes.

An alternative approach to this problem is to simulate the physical system by a percolation model. Percolation models are composed of sites, and of bonds between sites. The relation to the physical model is made by identifying the sites with the sources of interactions, and the bonds

with interactions of some minimum strength or greater. This is the approach we have taken to determine the conductivity properties of polymer fiber films. This enables us to consider the microscopic as well as the macroscopic processes of conduction, thereby allowing us to study the effects of the morphology of the film on its conductivity. The details of our computer simulation model are given in the next chapter.

## Chapter 3.

### A COMPUTER SIMULATION MODEL.

#### 3.1 Search for an alternative.

In the previous chapter we have seen a number of theoretical models for the conduction mechanisms in disordered semiconductors. These models provide us with considerable insight into the physical processes of conduction; however, in order to keep the treatment manageable, each model focusses attention on a particular aspect of the conduction process. This limits their range of validity.

The Miller Abrahams model (Section 2.1) and Kivelson's model (Section 2.2) are appropriate for the description of conduction processes at low temperatures and low impurity concentrations. These models have been applied to lightly doped polymer fiber films, and in this case, they describe the intrafiber conduction mechanism. The conductivity calculations based on these models determine the conductivity of a single fiber. As we have seen in section 1.3, polymer fiber films have characteristic morphology. They contain randomly oriented fibers which occupy only one fourth to one half of the film's volume. This suggests that, in order to compare the theoretical conductivity with the experimental conductivity, one must incorporate interfiber processes along

with intrafiber processes and thus take into consideration the morphology of the film. This aspect of the conductivity calculation seems to have been overlooked so far.

Sheng's model has been employed to describe conduction mechanism in heavily doped films at low temperatures (Sh80). Here the fibers are assumed to be metallic and the details of intrafiber processes are not considered. The interfiber conduction process is attributed to the fluctuation-induced tunneling of electrons between two fibers. For polymer fiber films the different geometries of the junctions have been taken care of by choosing appropriate parameters for the potential barrier representing the junction. However, this still is far from taking all the details of morphology into account.

In the present work we have developed a computer simulated Random Network Model which enables us to study the electrical conduction in a polymer fiber film, paying attention simultaneously to interfiber and intrafiber conduction processes. This model mimics the physical film and allows us to extract the effect of morphology of the film on its conductivity.

The model film consists of randomly oriented straight lines which represent fibers. The conduction along a single fiber is due to intrafiber processes, whereas, the interfiber processes control the conduction between two fibers at their intersection. We use the equivalent electri-

cal network to represent these processes. Our objective is to obtain the net macroscopic conductivity of a film. With a detailed knowledge of the morphology of the film we set out to correlate the conductivity with the morphology. The conductivity of the film is frequency dependent. We calculate the complex conductivity in the frequency range of 1 Hz to 10 MHz.

### 3.2 Random Network Model.

We consider our system as a unit square with thickness equal to the diameter of a fiber. The fibers are represented by randomly generated straight lines. The straight lines can be generated in either of two ways : (i) by generating coordinates of two end points using a random number generator, or (ii) by generating one end point and slope using a random number generator and length using a Gaussian distribution, with some mean length and variance. Our results are independent of the procedure used for the generation of the straight lines. Assuming the diameter of each fiber to be  $250 \text{ \AA}$  , a number of fibers are generated until the desired volume fraction is achieved. Simultaneously the points of intersection are determined. An intersection point between two fibers represents point of closest approach, or junction, between them. The interfiber conduction process is simulated by introducing an R-C parallel combination at the point of intersection; henceforth referred to as

intersection impedance. For lightly doped systems, the conductivity along a fiber can be determined using any one of the hopping models. In our work, we have used the Monte Carlo Simulation of Kivelson's variable range hopping model, for reasons that will be discussed in the next section. For heavily doped systems, the fibers are assumed to be ohmic with conductivities in the metallic regime. The lower and the upper edge of the film are assumed to be equipotential lines.

After having generated all the fibers and having determined all the points of intersection, a check is made to see which fibers can take part in the conduction process on the basis of the following criteria. A fiber can contribute to conductivity if it has: (i) one end-point on the lower edge and the other on the upper edge of the film, or (ii) at least one end-point on either of the edges and at least one intersection point, or (iii) at least two intersection points. [These conditions by no means guarantee participation of the fiber in conduction.]. Only such fibers are considered in the following algorithm. Each fiber is traced from its starting point to its end point, and only the portion of the fiber which takes part in the conduction process is kept. This is similar to the backbone used in percolation clusters. Node numbers are assigned at each intersection point. The upper and the lower edge are assigned the node numbers 1 and 2 respectively. Each intersection point gives rise to a pair of nodes between which the intersection impedance is introduced. An impedance proportional to the length is intro-

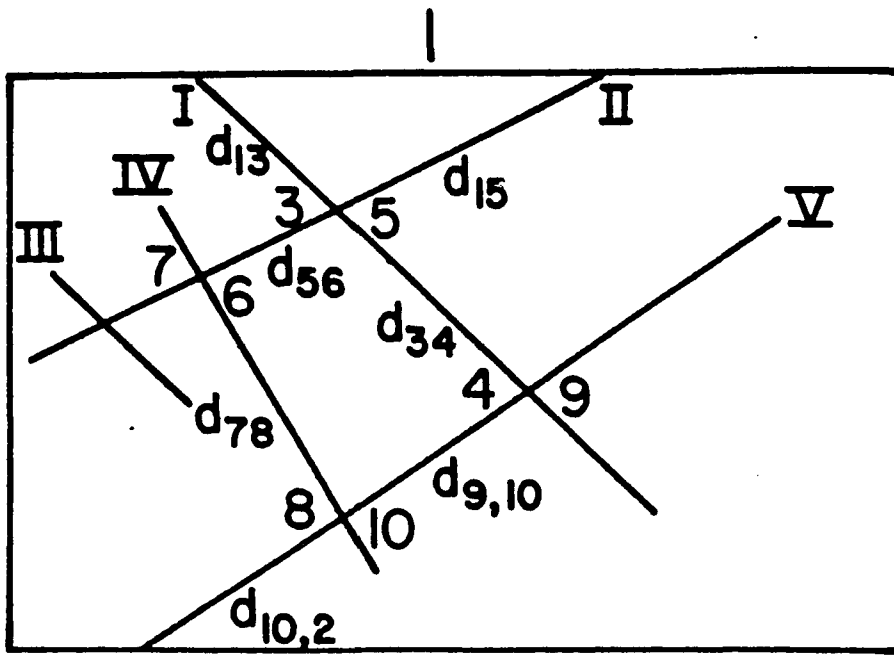
duced between nodes lying on the same fiber. This procedure is then carried out for all fibers. This generates an electrical network.

To illustrate this algorithm let us consider a typical system of five fibers as shown in Figure (3.1 a). First each fiber is checked to see if it takes part in the conduction process. Since Fiber III does not satisfy any of the above mentioned criteria, it does not participate in the conduction. It is not considered in further discussion. All other fibers satisfy at least one of the criteria and hence are analysed as follows.

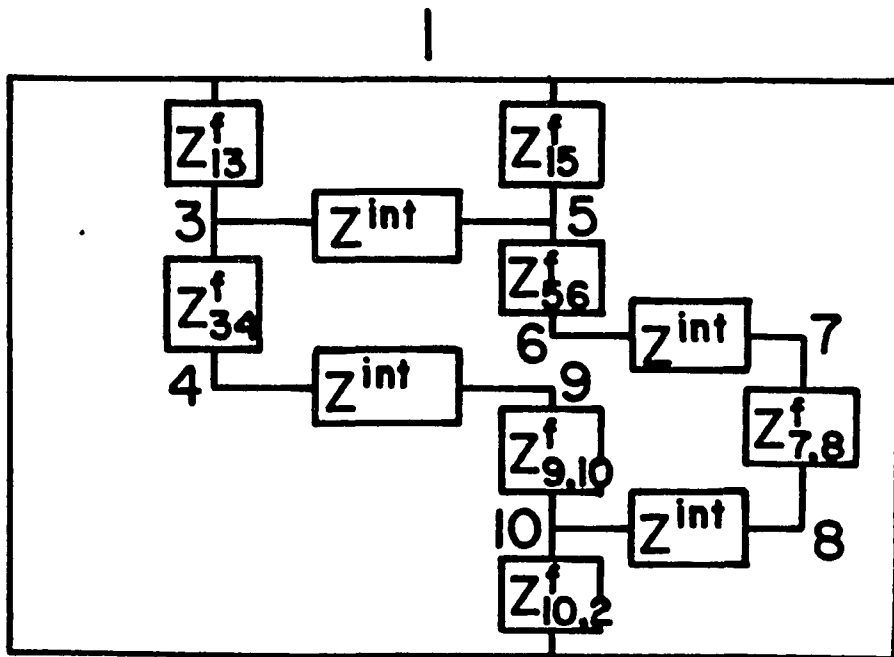
Fiber I : Since it starts from the upper edge, that end point is assigned node number 1. Its intersections with Fiber II and Fiber IV are assigned node numbers 3 and 4 respectively. The impedences  $Z_{1,3}$  and  $Z_{3,4}$  are introduced between nodes 1 and 3, and nodes 3 and 4 respectively; the values of the impedences being proportional to the length of the fiber between them. The portion of Fiber I beyond node number 4 is ignored because it does not contribute to conduction.

Fiber II : Its starting point is node number 1. Its intersections with Fiber I and Fiber IV are assigned node numbers 5 and 6 respectively. An intersection impedance is introduced between the nodes 3 and 5. The impedences, proportional to lengths, are introduced between the nodes lying on Fiber II, similar to Fiber I. The portion of Fiber II beyond node 6 is ignored.

Fiber IV : The portion of this fiber from its starting point to its first intersection point is ignored. Node numbers 7 and 8 are assigned to the points of intersection. The intersec-



2



2

Fig. 3.1 A typical system of fibers with its equivalent network.

tion impedance is introduced between nodes 6 and 7. An impedance proportional to length is introduced between 7 and 8. The tail portion of the fiber is again ignored. The same procedure is adopted for Fiber V. Its endpoint lies on the lower edge which is assigned node number 2. The equivalent electrical representation of this system is shown in Figure (3.1 b).

Once the electrical network has been defined, the conductivity matrix  $G$  is constructed. The computer sets up the Kirchoff's law equations :

$$G V = I \quad (3.1)$$

where matrix  $G$  denotes a conductance matrix, matrix  $V$  represents voltage at each node and matrix  $I$  represents the input current. Due to the fact that the model includes reactive circuit elements, the quantities  $G, V, I$  are complex. Hence the resulting equations may be represented as

$$\begin{pmatrix} G_r & -G_i \\ G_i & G_r \end{pmatrix} \begin{pmatrix} V_r \\ V_i \end{pmatrix} = \begin{pmatrix} I_r \\ I_i \end{pmatrix} \quad (3.2)$$

where subscripts  $r$  and  $i$  denote real and imaginary parts. A known current is sent at the lower edge and the upper edge is grounded. The equations are then solved for the voltages at all the nodes. The impedance is then determined by dividing the voltage at the lower edge by the net current.

A number of techniques exists for the solution of this class of problems. A widely used method for solving simultaneous equations in Random Resistor Networks is the Gauss Seidel iteration procedure with over-relaxation (We75). This is a very economical method, in both execution time and storage space. A serious drawback of this technique is the relatively strict requirements that it places on the coefficient matrix in order for convergence to be achieved, namely that the matrix be either diagonally dominant, or at least positive definite (Ca69). For Kirchoff's law problems with purely resistive components, diagonal dominance is assured, since the diagonal elements of the conductance matrix are simply the sum of the off diagonal elements. In our problem, with complex impedances, we find that at frequencies for which the imaginary conductance approaches the same order of magnitude as the real conductance, the Gauss Seidel procedure does not converge. This is due to the form of the Equations (3.2), where there are many additional off diagonal elements due to the  $G_i$  values. When these imaginary components are large, the matrix is no longer diagonally dominant, and becomes indefinite. For all of our computations, we have used a Gaussian elimination routine, which takes advantage of both the sparseness and the symmetry of the G coefficient matrix (Ki79). Only the nonzero elements in the upper half triangle of the matrix are stored, and an efficient pivoting strategy is chosen to minimize nonzero matrix fill during the pivoting and to minimize the number of multiplications required

in the solution. In practice, the technique is approximately an order of magnitude more expensive to use than Gauss-Seidel in both speed and storage requirements. The advantage of using the Gaussian elimination technique is that a solution is guaranteed for all but the most ill-conditioned problem. We found that it was necessary to solve the equations in double precision. Recursive corrections were necessary especially at higher frequencies. The accuracy of the calculations is checked in two ways : the percentage change in the net impedance in successive iterations and the percentage difference between the net current coming in and going out of the system.

The final step in the model is to choose a minimum size of the film that provides some degree of statistical significance but is still within reasonable limits of available computer time. If the Random Network Model is a true statistical model then the calculation should not be sensitive to the size of the film. Thus the minimum size is chosen by solving the problem on increasingly large sizes until the answer converges to a fixed value. The results of this study are presented in Figure (3.2). It shows the impedance data for the film sizes  $L/d$  ranging from 60 to 160, where  $L$  is edge length of the film, and  $d$  is its thickness.  $L/d = 80$  is used in almost all of the calculations. For this size, the number of fibers necessary to fill the film to a volume fraction of 0.3 is about 50. These give rise to number of nodes  $N \sim 600$ . For a system of 600 nodes, there are approximately 1200 equations to be solved.

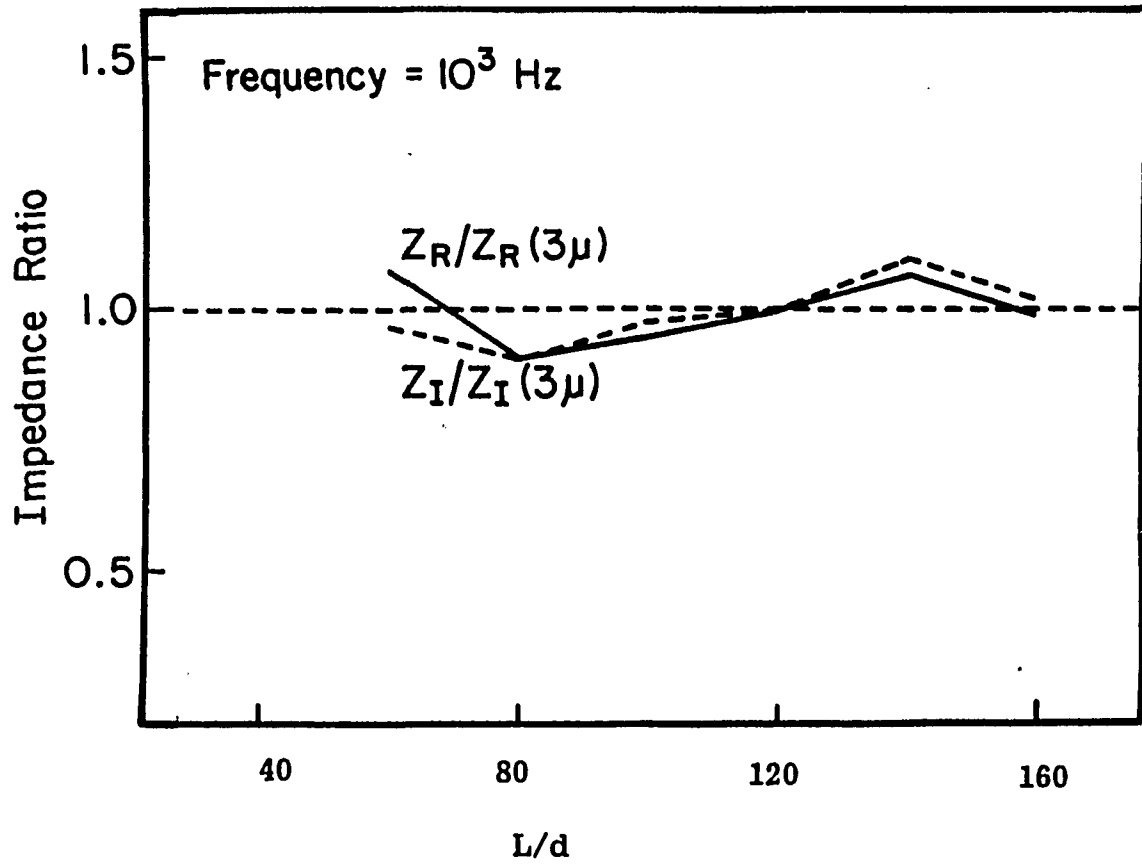


Fig. 3.2 Real and imaginary impedences for different sizes of film, compared with those for a film of size  $L/d = 120$ .  $L$  is the length of the film, and  $d$  is it's thickness.

### 3.3 Computer Simulation of a Single Fiber.

In the previous section we described our random network model. This model is general in its scope and can be applied to any fibrous film. The focus is on the morphology and its effect on the conductivity of the film. It is essentially a macroscopic model; no attention is paid to the microscopic details of conduction inside a fiber. The values of the interfiber and the intrafiber conductivities are the input parameters of this model.

In the present section our simulation of the microscopic conduction process inside a fiber is presented. We concentrate on the conduction in lightly doped Trans-Polyacetylene. As we have stated in Chapter 1, Polyacetylene has a simple chemical structure, and metallic conductivity can be achieved in this material with appropriate doping. Because of its simplicity, it has been studied extensively over the last few years. Despite the enormous amount of experimental data and a number of theoretical investigations, there are still many open questions; especially those concerning the semiconductor-metal transition and the details of electrical transport and magnetic susceptibility. These problems are due partly to experimental difficulties, leading often to conflicting results, and partly to the lack of an established theoretical framework with which to interpret the data.

The leading theory for microscopic process of conduction in Trans-Polyacetylene is Kivelson's variable range hopping model (Section 2.2). It is based on the soliton model of Trans-polyacetylene as developed by Su, Schrieffer, and Heeger (Section 1.4). Solitons are topological excitations of a polymer chain. The charged solitons are spinless; hence they contribute to conductivity but not to spin susceptibility. The neutral solitons are chargeless but carry spin  $\frac{1}{2}$ ; hence they contribute to spin susceptibility but not to conductivity. This separation of electric and magnetic properties is one of the interesting features of solitons in polyene chains and it has been supported by various experiments. The most direct experimental evidence comes from the failure to see a decrease in spin susceptibility, accompanying a great decrease in dc conductivity, when  $\text{AsF}_5$ -doped Trans-Polyacetylene is compensated with  $\text{NH}_3$  (Go79). Also, no increase in spin susceptibility, accompanying a large increase in dc conductivity, is observed when pristine Trans-Polyacetylene is lightly doped with  $\text{AsF}_5$  (We79). These experiments indicate that the principal charge carriers in these systems are spinless. The charged solitons are the perfect candidates for these charged carriers; and hence we believe that any model for conduction in these systems should incorporate the soliton picture. This led us to employ Kivelson's variable range hopping model for the description of the intrafiber conduction.

Kivelson's model has been described in some detail in Section 2.2; here we will summarize it briefly. In the soliton model (Su80), the semiconducting properties of undoped  $(\text{CH})_x$  are attributed to commensurate Peierls distortion. For trans-polyacetylene the two phases of dimerization are degenerate in energy and a soliton is the boundary between the two phases. The energy level associated with a soliton is at midgap. When this level is singly occupied the soliton is neutral with spin  $\frac{1}{2}$  and when it is doubly occupied the soliton is charged and spinless. At high temperatures, the charged solitons are free, and the conduction can be explained in terms of their diffusion. However, at low temperatures, they are bound to the impurities. Kivelson explains the conduction at low temperatures and low doping levels in terms of phonon assisted hopping of charge from charged solitons to neutral solitons. An expression for the hopping rate  $\Gamma_{ij}^{(0)}$  between sites  $i$  and  $j$  is given by

$$\Gamma_{ij}^{(0)} = n^{(0)}(1-n^{(0)}) \gamma(T) \exp \{-2[(R_{\parallel}/\xi_{\parallel})^2 + (R_{\perp}/\xi_{\perp})^2]^{\frac{1}{2}}\}. \quad (3.3)$$

In this equation  $n^{(0)}$  is the fraction of solitons that are charged and  $(1-n^{(0)})$  is the fraction of solitons that are neutral and have an impurity atom nearby.  $\vec{R}_{ij}$  is the vector distance from site  $i$  to site  $j$ .  $R_{\parallel}$  is the component of  $\vec{R}_{ij}$  along the chain and  $R_{\perp}$  is the component perpendicular to the chain.  $\xi_{\parallel}$  and  $\xi_{\perp}$  are the in-chain and out-of-chain electron decay lengths respectively.  $\gamma(T)$  is a frequency defined by

$$\gamma(T) = (500 \text{ eV}/\hbar) [T/300\text{K}]^m. \quad (3.4)$$

Using these expressions the hopping model can be converted into an equivalent electrical network. The conductance between sites  $i$  and  $j$  is given by

$$G_{ij} = [ e^2 \Gamma_{ij}^{(0)} / kT ]. \quad (3.5)$$

For time dependent fields, this method can be generalized following Miller and Abrahams (Mi60) (See Appendix A). This amounts to connecting a capacitance  $C_j$  between site  $j$  and ground, where  $C_j$  is given by

$$C_j = [ e^2 / kT ] n^{(0)} (1 - n^{(0)}). \quad (3.6)$$

The conduction mechanism described above is simulated as follows: A fiber is assumed to be cylindrical in shape with a radius of 125 Å and length of 4000 Å. Polymer chains are represented by straight lines parallel to the cylinder axis extending over the entire length of the fiber. Radial distances and azimuthal angles of the chains are determined using a random number generator. Neutral solitons are represented by randomly chosen points on randomly chosen chains. The impurity atoms are distributed randomly throughout the fiber. It is assumed that a charged soliton is formed whenever an impurity atom comes sufficiently close to a chain (within 2 Å). This determines the positions of charged solitons. The number of carbon atoms in a fiber and the number of carbon atoms in a chain fixes the number of chains. The density of

neutral solitons in lightly doped samples can be deduced from susceptibility data and is of the order of  $3 \times 10^{-4}$  per carbon atom (Wi79). The impurity concentration determines the number of impurity atoms.

For each charged soliton all neutral solitons are considered, and  $G_{ij}$  between the charged soliton and each neutral soliton is calculated using equation (3.5). Only the largest  $n$  conductances originating from each charged soliton are kept (Pi74); the bulk of the current flows through these conductances. The smaller  $G_{ij}$ 's make a negligible contribution to the conductivity of the fiber. It was seen that the conductivity is independent of  $n$  for  $n > 8$ . In our calculations we choose  $n=12$ . The upper end of the fiber is grounded. A capacitance  $C_j$  [as given in Eq.(4)] is introduced between each soliton site  $j$  and ground. This procedure defines an electrical network which simulates the conductivity properties of a fiber.

Once the electrical network has been defined, the conductivity matrix  $G$  is constructed. The Kirchoff's law equations are set up in exact analogy with the previous section. A known current is sent at the lower end of the fiber. The equations are solved for the voltages at all the sites. The impedance is then determined by dividing the voltage at the lower end by the net current entering the system. Having calculated this, and knowing the geometry of the fiber, the conductivity of a fiber can be calculated. Notice that  $G_{ij}$  and  $C_j$  depend on the

temperature and the concentrations of the neutral and the charged solitons. This dependence has been made explicit in Equations (3.4), (3.5), and (3.6). As a result we can calculate the conductivity of a fiber for various frequencies as well as for various temperatures and concentrations.

We use the conductivity of a fiber as calculated using this model, along with specific assumptions about interfiber couplings, in the Random Network Model described in the previous section to calculate the conductivity of a film [At low temperatures and low impurity concentrations]. We have studied the temperature and concentration dependence of a film over a range of temperatures (100 to 300 K) and over a range of concentrations ( $3 \times 10^{-4}$  to  $6 \times 10^{-3}$ ). We present the results of our computations, and some relevant discussion, in the next chapter.

## Chapter 4.

## RESULTS AND DISCUSSION.

## 4.1 Lightly Doped Polyacetylene.

In section 3.3 of the last chapter, we have seen a computer simulation of a single fiber based on Kivelson's variable range hopping model. Utilizing this simulation model we calculate the complex conductivity of a fiber. It is then used as an input parameter in our Random Network Model, in order to determine the conductivity of lightly doped Trans-Polyacetylene film. In this section we discuss the results of our calculations and compare them with the available experimental data on Trans-Polyacetylene.

The expression for the hopping rate (Eq. 3.3) is written in terms of the in-chain and the out-of-chain electron decay lengths ( $\xi_{\parallel}$  and  $\xi_{\perp}$ ) and frequency  $\gamma(T)$ .  $\gamma(T)$  has a power  $m$  dependence on temperature as given in Eq. (3.4).  $\xi_{\parallel}$ ,  $\xi_{\perp}$  and  $m$  are adjustable parameters of the hopping model for the conductivity of a fiber. The Random Network Model introduces two additional parameters : the fractional volume occupied by fibers  $v$ , and the intersection impedance. By varying these parameters we can simulate various physical conditions in the film. Variations in the values of the intersection impedance, and the impedance of a

fiber, correspond to different impurity concentrations and temperatures. Also, by choosing appropriate relative magnitude for these impedences, we can control the relative importance of the interfiber and the intrafiber processes. It is understood that at low doping levels the microscopic (intrafiber) processes dominate the net conductivity of the film, while at high doping levels the fibers become essentially metallic, and the interfiber processes limit the net conductivity. We will discuss the latter case in the next section.

In lightly doped samples the intersection impedance provides high conductivity path for current across two fibers. The results are insensitive to the values of  $R$  and  $C$  of the intersection impedance, as long as the intersection impedance is small as compared to impedance of the fiber. For all our calculations we have used  $R = 10^{10}$  ohms and  $C = 5 \times 10^{-13}$  F per area of intersection.

Kivelson has chosen the following values for the parameters of the hopping model (Ki82)

$$\xi_{\parallel} = 8.54 \text{ \AA}, \quad \xi_{\perp} = 2.3 \text{ \AA}, \quad m = 10. \quad (4.1)$$

Figures (4.1) and (4.2) show the results of our calculations using these parameters, for fractional volume  $v=0.3$ . Figure (4.1) shows the dc conductivity as a function of concentration together with Kivelson's results and the measured conductivities for various concentrations of

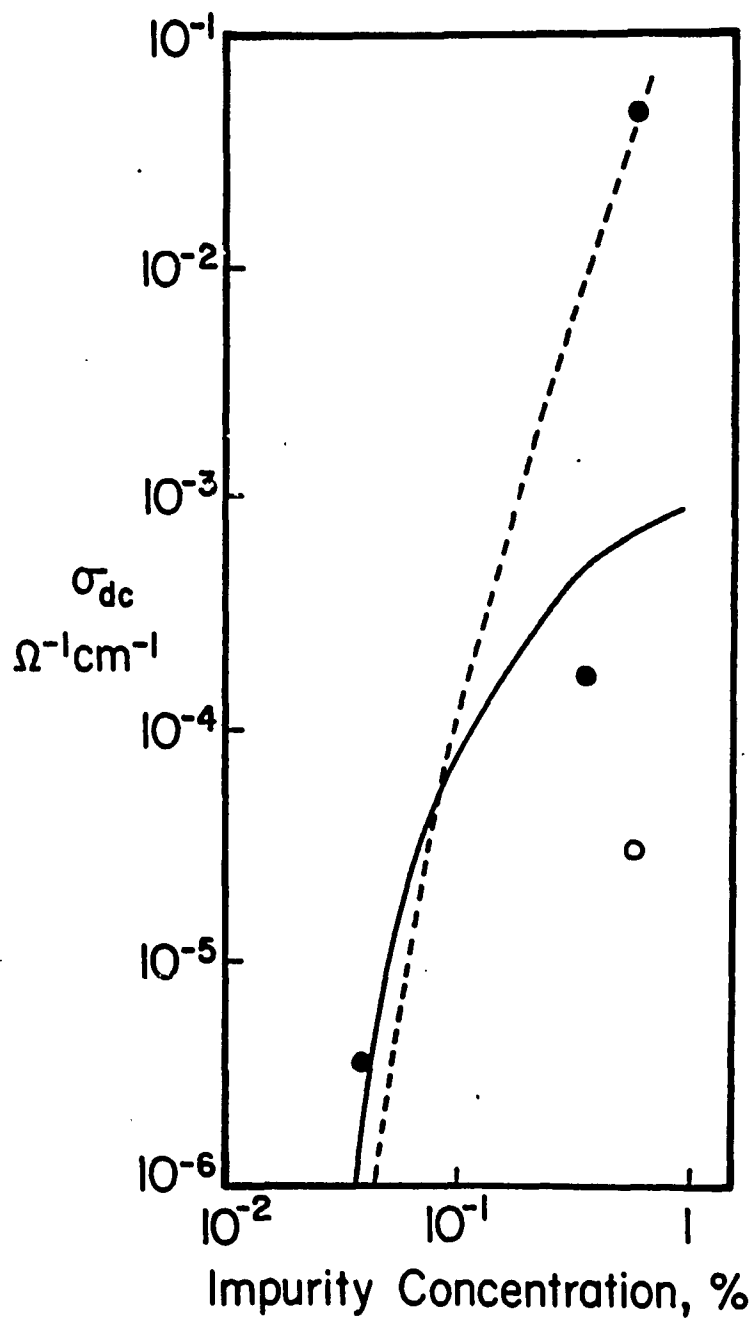


Fig. 4.1

Dc conductivity as a function of concentration. Solid line shows the results of our calculations, the broken one represents Kivelson's results, and the data points are the experimental results of  $\text{AsF}_5$  and Br doped samples.

AsF<sub>5</sub> and Br. As compared to Kivelson's calculations our results are somewhat smaller. Kivelson has overestimated the conductivity because of two reasons. First, he has not taken into account the fibrous nature of the film, hence in his calculations the conductivity of the film is the same as the conductivity of a fiber. In addition, Kivelson assumes 100% charge transfer. In his case each dopant atom gives rise to a charged soliton; however, in our calculation, only those dopant atoms which are within a certain distance from a polymer chain give rise to a charged soliton. One expects, in general, less than one charge to be transferred per dopant atom. The disagreement between our calculations and the experimental conductivities may be due to a variety of causes such as the disordered topology of the actual polyacetylene, the electron-electron interactions or the incomplete charge transfer. Although the charge transfer process is more realistic in our model, it does not account for all the uncertainties associated with various dopants. In Br doped samples, for instance, some Br may be present in the form of Br<sub>2</sub> or Br<sub>3</sub> molecules, reducing substantially the doping efficiency. Due to the scarcity of experimental data, the comparison here is tentative at best, and it is difficult to make definitive statements about the relative merits of different models on that basis.

The relation of the dc conductivity of a film to its morphology can be seen as follows. In the light doping region, the intersection impedance is small as compared to that of the fiber, and hence the current

takes the shortest path across the film. Therefore, as far as electrical conduction is concerned, the film is equivalent to a number of such paths in parallel to each other. This equivalence is illustrated schematically in Figure (4.7b). The resistance of the film is related to that of the fiber by

$$R_{\text{film}} = R_{\text{path}}/N,$$

where  $N = L/p$  is the number of parallel paths and  $L$  is the total length of the fibers and  $p$  is the average path length across the film. In terms of conductivities, this relation becomes

$$\ell/(\sigma_{\text{film}} A_{\text{film}}) = p/(N \sigma_{\text{fiber}} A_{\text{fiber}}),$$

where  $\ell$  is the length of the film, and  $\sigma$  and  $A$  represent the conductivities and areas of the cross section of the film and the fiber. Substituting for  $N$  and simplifying, we get

$$\sigma_{\text{film}} = \sigma_{\text{fiber}} (\ell/p)^2 v, \quad (4.2)$$

where  $v$  is the fractional volume occupied by the fibers. In our random network model, the fibers are represented by straight lines. This gives the average path length to be  $\ell/\cos\theta$ , where  $\theta$  is the average angle made by the fibers with the direction of current flow. In this case the factor  $(\ell/p)$  in Eq.(4.2) is replaced by  $\cos\theta$  and we get,

$$\sigma_{\text{film}} = \sigma_{\text{fiber}} (\cos^2\theta) v. \quad (4.3)$$

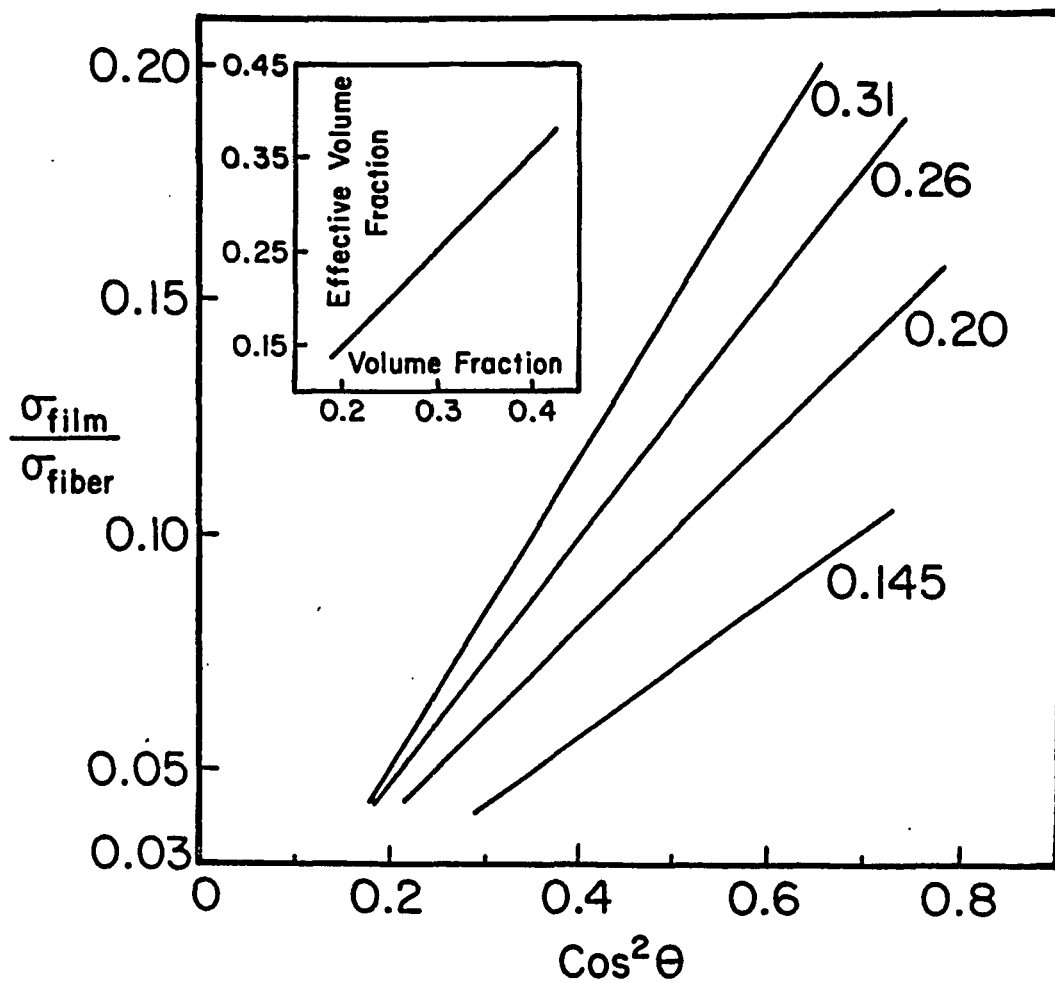


Fig. 4.2 The ratio of the conductivity of the film to that of the fiber as a function of  $\cos^2 \theta$  for various volume fractions. The insert of the figure shows effective volume fraction as a function of volume fraction.

Figure (4.2) shows the ratio of the conductivity of the film to that of the fiber plotted as a function of  $\cos^2\theta$  for different volume fractions. It shows the linear relationship as expected from Eq.(4.3). The slopes, however, are somewhat smaller than the actual volume fraction of the film. This is because only the backbone of the percolation cluster takes part in the conduction process. When the "effective" volume fraction of the backbone is calculated, it is in excellent agreement with the slope. The insert in Figure (4.2) shows the total volume fraction of the percolation cluster as a function of the volume fraction of the film.

The frequency and the temperature dependence of the conductivity of polyacetylene has been measured experimentally by Epstein et al (Ep81). The authors have compared the results of Trans-Polyacetylene with those of Cis-Polyacetylene. They found that in Cis-(CH)<sub>x</sub>,  $\sigma$  is frequency dependent even at 100 Hz.  $\sigma_{dc}$  decreases rapidly with decreasing temperature while  $\sigma_{ac}$  changes very slowly with temperature. This behaviour of  $\sigma(f,T)$  is very similar to that observed in a broad class of disordered semiconductors and insulators. The electrical transport in Cis-Polyacetylene can therefore be understood in terms of Miller-Abrahams hopping model. For Trans-Polyacetylene, however, a large, very strongly temperature dependent  $\sigma_{ac}$  is observed. This behaviour is inconsistent with the usual hopping models for  $\sigma_{ac}$  but Epstein et al found it to be in good agreement with Kivelson's model of phonon assisted hopping of electrons between solitons.

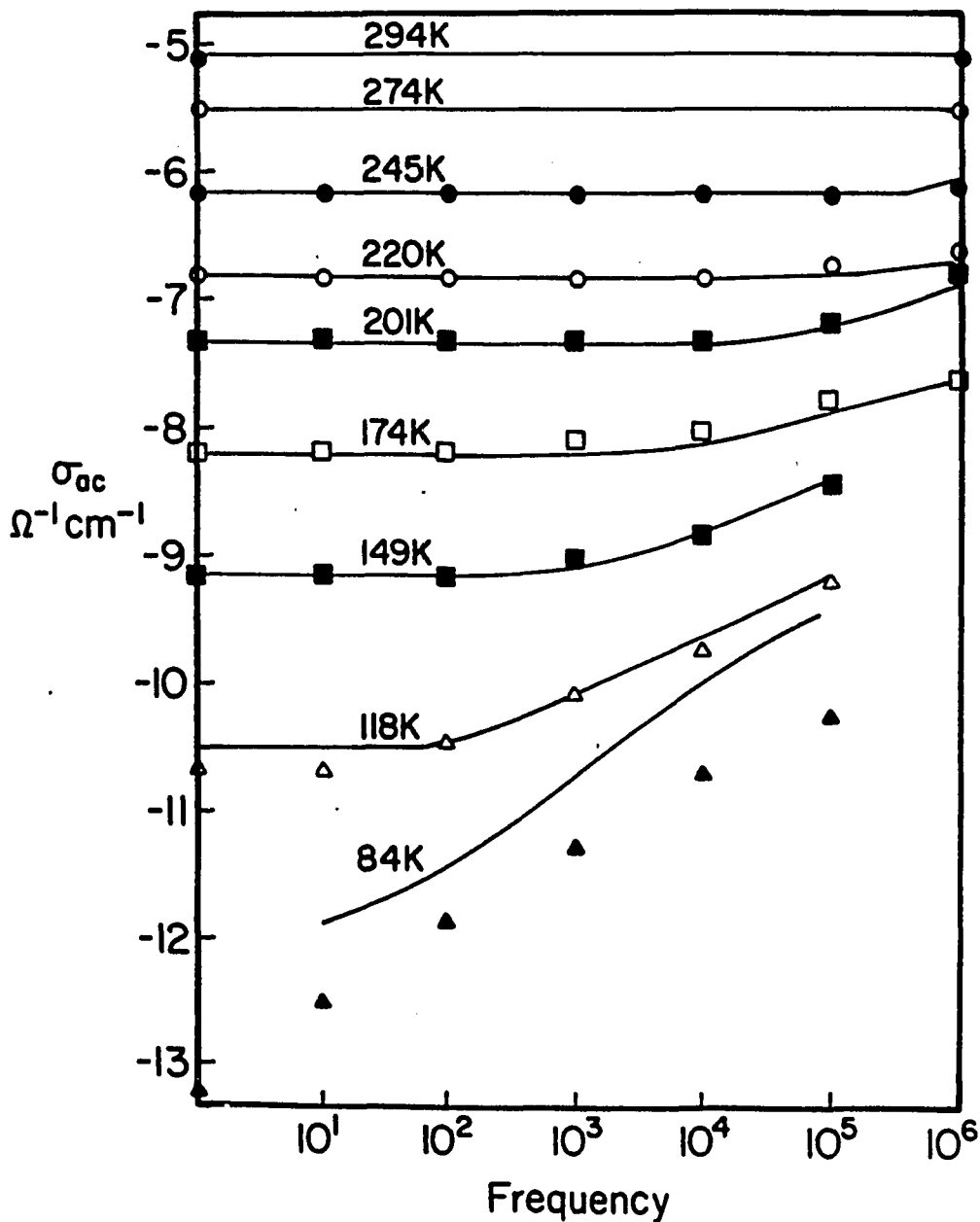


Fig. 4.3 The real part of the conductivity plotted against frequency for various temperatures. Solid lines show the results of our calculations and data points are the experimental results of Epstein et al (Ep81).

The experimental results of the real part of the conductivity as a function of frequency, for various temperatures, are shown in Figure (4.3), along with the results of our calculations. At high temperatures  $\sigma_R$  is independent of frequency upto  $10^6$  Hz. As T is decreased,  $\sigma_{dc}$  decreases rapidly, and a frequency dependent component is revealed. To analyze these results in terms of Kivelson's model, Epstein et al have used the following parameters :

$$\xi_{\parallel} = 10 \text{ \AA}, \quad \xi_{\perp} = 2.5 \text{ \AA} \quad m = 14.7 \quad (4.4)$$

which are somewhat different from the ones chosen by Kivelson [Eq.(4.1)]. They assume the dopant concentration as  $1.3 \times 10^{19} / \text{cm}^3$ , and the concentration of neutral solitons as  $5 \times 10^{-4}$  per C atom. Using these parameters we have calculated the ac conductivity for various temperatures and over the frequency range of 1 Hz to 1 MHz. Our results are in excellent agreement with the experimental work of Epstein et al as can be seen from Figure (4.3).

Summerfield et al (Su85) have also measured the complex conductivity of undoped Trans-Polyacetylene samples at temperatures in the range of 78 °K to 200 °K, and for frequencies in the range of 13 Hz to 50 KHz. They have analyzed their data in terms of the rate equations of Miller and Abrahams (Mi60). The strong temperature dependence of  $\sigma_{ac}$  is explained by adopting an energy dependent model as in the case of disordered semiconductors and insulators. They have claimed that the

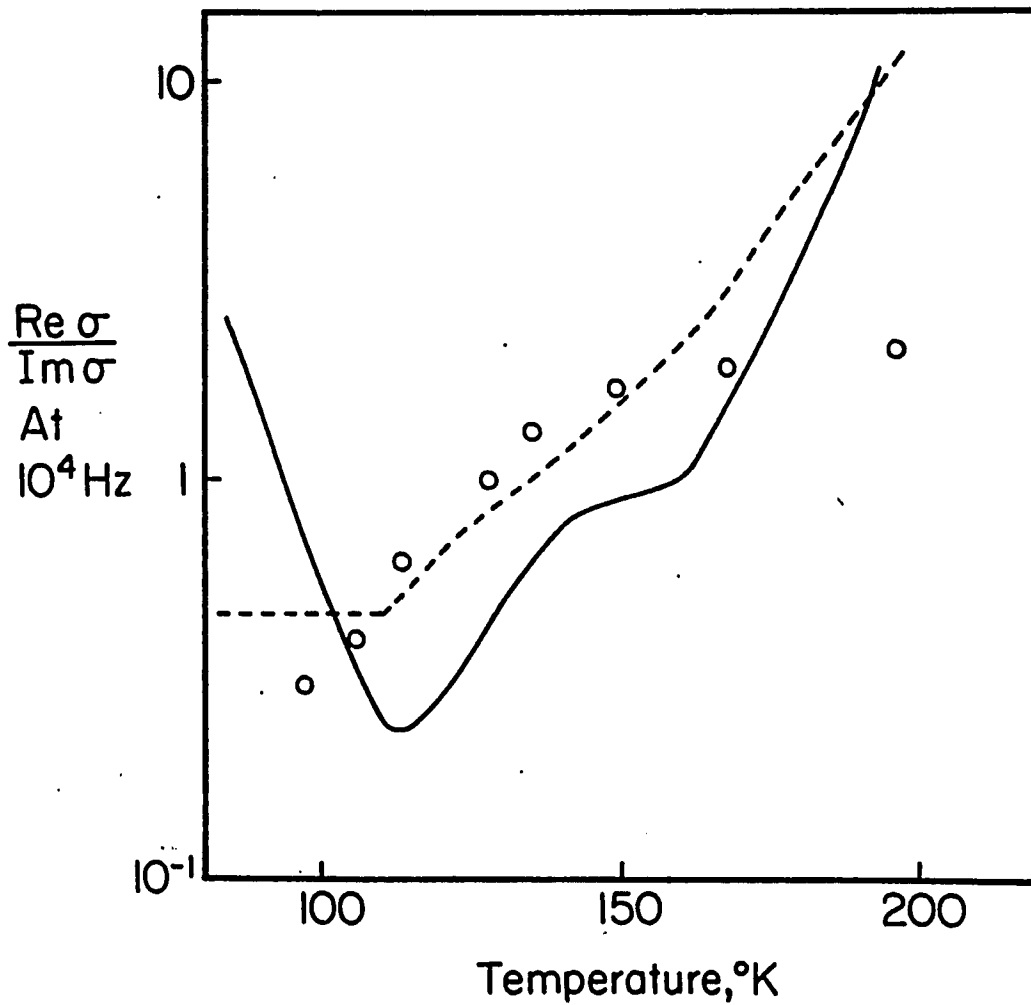


Fig. 4.4 Temperature dependence of the ratio of the real part of the conductivity to the imaginary part at  $10^4$  Hz. Solid line represents results of our calculations, broken one shows the results of theoretical work of Summerfield et al (Su85), and data points represent their experimental work.

energy dependent hopping model provides a better account for the measured conductivity of  $(\text{CH})_x$ , than Kivelson's energy independent model. The model that they have proposed makes less use of specific properties of solitons. The concept of soliton is used to describe the site energy distribution. However, by re-interpreting the density of states, one can equally well use their results to imply non-solitonic levels in the gap.

Figure (4.4) shows our plot of  $\log(\sigma_R/\sigma_I)$  where  $\sigma_R$  and  $\sigma_I$  are the real and the imaginary parts of the conductivity respectively, at frequency  $f=10$  KHz, for various temperatures. On the same graph we have shown the experimental results of Summerfield et al, along with their theoretical results, for comparison. Since we have worked essentially in the framework of Kivelson model, our model is energy independent in contrast with Summerfield et. al. As can be seen from Fig.(4.4) the agreement is reasonable, especially since there are no free parameters in these calculations. The parameters used here are the ones fixed by Epstein et. al. [Eq.(4.4)] by fitting their data of temperature and frequency dependence of the real part of the conductivity.

## 4.2 Behaviour of the Equivalent Electrical Network.

In this section we consider the general response of the model electrical network. The aim of this discussion is to better understand the com-

plex model electric circuit, and the voltage and current distributions under different conditions. It is most useful to begin our discussion with a case where the fibers are ohmic, and the resistance of a fiber is less than the resistance in the intersection impedance. Such a choice is appropriate for heavily doped polyacetylene films because in such films the fibers are nearly metallic. We have therefore chosen the conductivity of fibers in the metallic region. The intersection impedance is represented by an R-C parallel combination. In experimental studies of dc conductivity of heavily doped trans-polyacetylene it is observed that the intersection impedance is at least an order of magnitude larger than the resistance of a fiber (Pa80). A fiber with a typical length of a micron has resistance  $\approx 10^3 \Omega$ . We have therefore chosen the resistance in the intersection impedance to be  $5 \times 10^4 \Omega$ . The value of capacitance in the intersection impedance is obtained from the observed behaviour of metal-insulator composites. The ac conductivity of such composites starts showing a frequency dependence at frequency  $\approx 10^2$  Hz. This suggests that the capacitive reactance at this frequency is of the order of the resistance in the intersection impedance. This gives  $C \approx 10^{-7}$  F. These values of the input parameters are collected in the Fig.(4.5).

Figure (4.6) is a typical result for the Random Network Model at volume fraction  $v=0.3$ , obtained using the input parameters of Figure (4.5). It shows the complex impedance of the system as a function of frequency, for frequencies in the range of 1 Hz to 10 MHz. We categor-

**RESISTIVITY OF A POLYMER FIBER**

$$\rho_f = 2.5 \times 10^{-5} \Omega \text{ cm.}$$

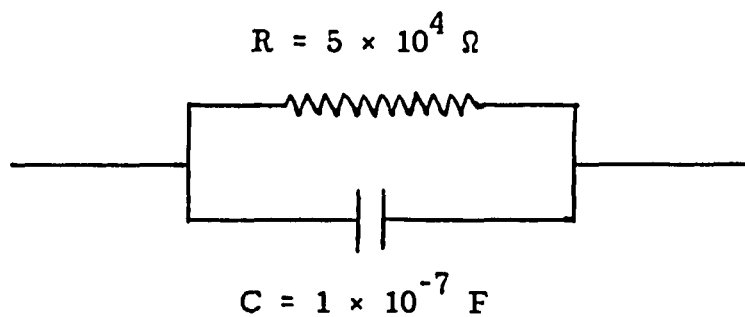
**INTERSECTION IMPEDENCE**

Fig. 4.5 Input parameters of the Random Network Model.

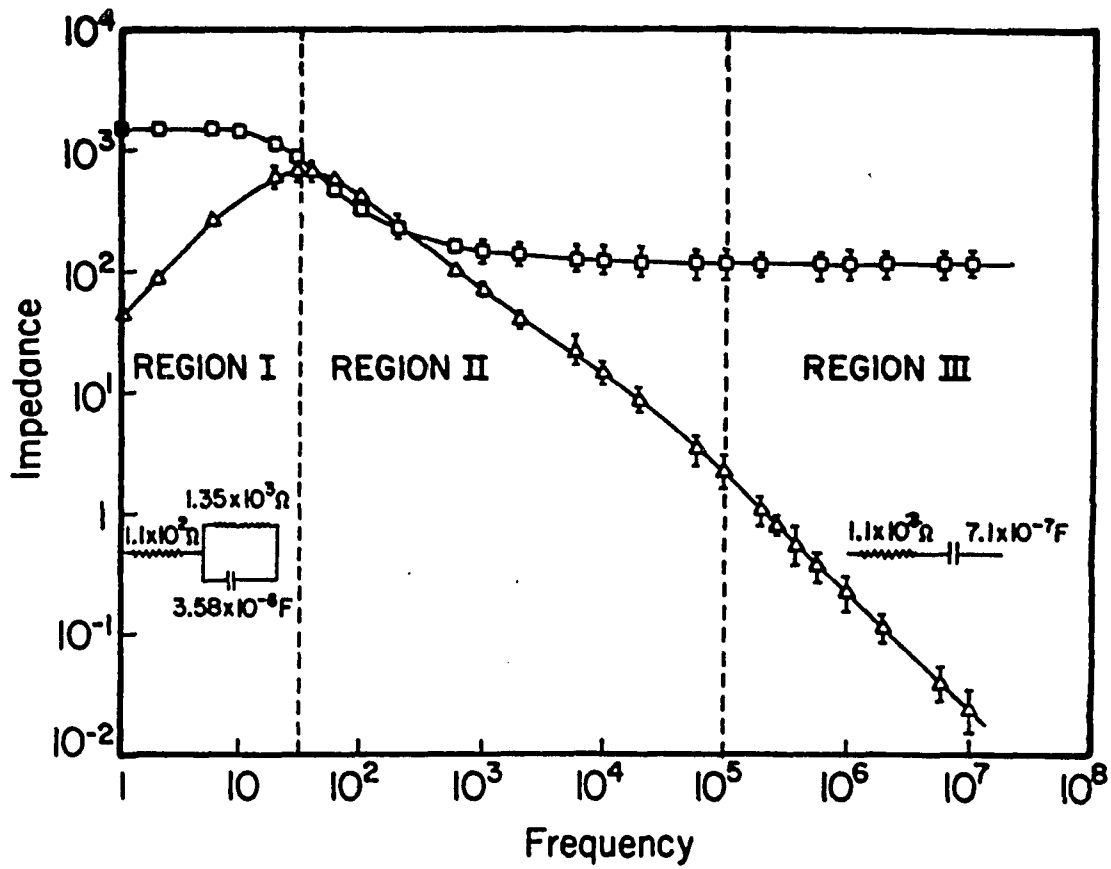


Fig. 4.6 A typical frequency response for fractional volume  $v=0.3$ . The error bars show the variation with random number seed.

ize this behaviour as being composed of three regimes : At low frequency ( $f < 30$  Hz) one can observe a slope 1 behaviour on the log-log plot of the imaginary part of the impedance, whereas at high frequency ( $f > 10^5$  Hz) slope -1 dependence is observed. The mid-frequency region is a transition region and we shall discuss the behaviour of the film in this region, in some detail, in the next section. The low frequency response is the same as that of an R-C parallel circuit ; whereas, the high frequency response resembles that of an R-C series circuit. These equivalent R-C circuits are shown in Figure (4.6) along with the frequency response. The capacitance in the low frequency equivalent circuit,  $C_{lf}$ , is higher in value than that in the high frequency equivalent circuit,  $C_{hf}$ . This general behaviour was found in calculating the impedance of a porous electrode immersed in an electrolyte (Kr84) and in the impedance of a Bruggeman's effective medium dielectricum (Ba86).

In order to understand this behaviour we calculated the current distributions at various frequencies by calculating current flow through each branch of the network. This was done by using the node voltages obtained by solving Kirchoff's law equations, and the impedences between the nodes. It was observed that at low frequencies the current flows through the fibers as far as possible, crossing over to another fiber only when it is necessary for percolation. At high frequencies the current was observed to follow the shortest paths across the film,

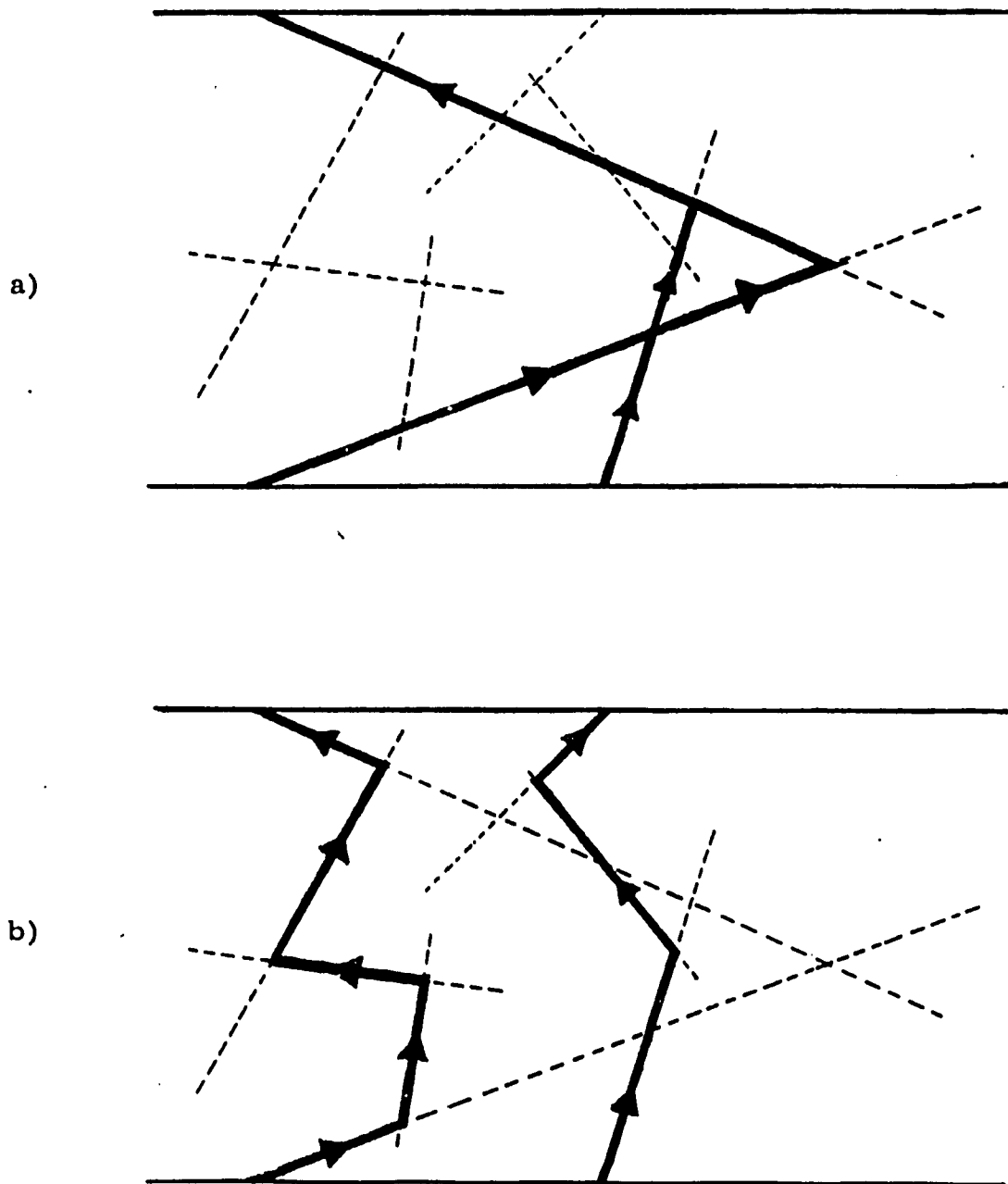


Fig. 4.7 The current flow in a typical system.  
a) At low frequency,  
b) At high frequency.

no matter how many intersections it had to cross. This current flow pattern is understandable on physical grounds. At low frequency, the intersection impedance is much higher than the resistance of the fiber. As a result, the network consists of a number of parallel paths, each containing as few intersection impedances as possible. This is illustrated for a typical system in Figure (4.7 a). In contrast, at high frequency, capacitive reactance and hence the intersection impedance becomes smaller than the resistance of the fiber. The current can cross over to another fiber through an intersection very easily. This produces parallel paths each having number of capacitances in series. This is illustrated for a typical system in Figure (4.7 b). These different current distributions near the low frequency and the high frequency ends lead to different values of capacitances ( $C_{lf}$ ,  $C_{hf}$ ) in the equivalent circuits.

We confirmed these observations by increasing the resistivity of fibers and studying how the value of low frequency capacitance  $C_{lf}$  changes. Figure (4.8) shows that  $C_{lf}$  approaches  $C_{hf}$  as the resistivity of fiber ( $R_f$ ) is increased. The high frequency capacitance  $C_{hf}$ , however, remains constant. This is expected for the following reason. With increase in the fiber resistance, even at low frequency the intersection impedance becomes smaller than the resistance of the fiber and hence, at high values of the fiber resistance, the low frequency response resembles the high frequency response. (The increase in the resistivity of fiber can be viewed as the decrease in the dopant concen-

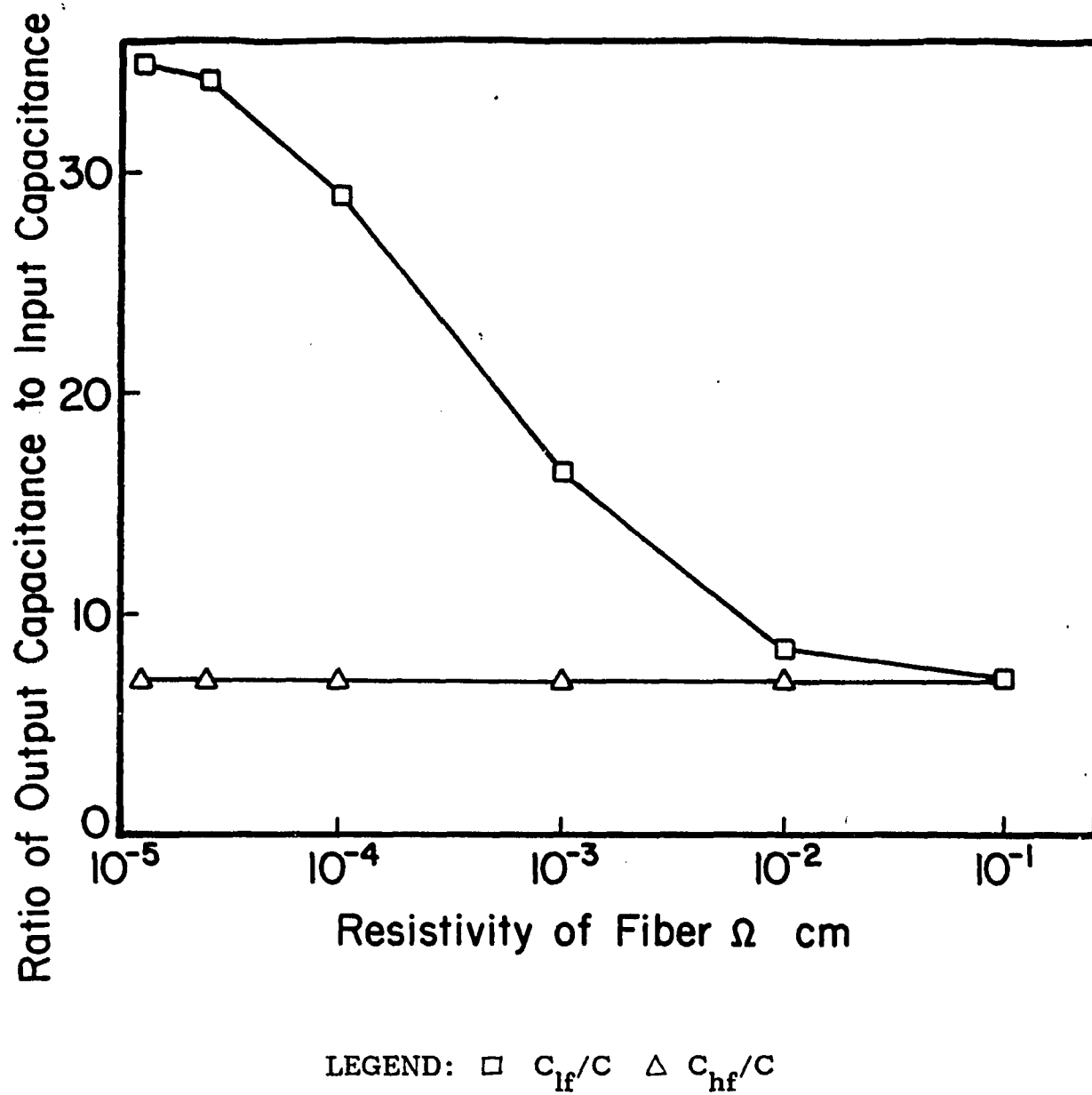


Fig. 4.8 The low and the high frequency capacitances as a function of resistivity of fiber.

tration. Figure (4.8) then represents the transition from heavily doped system to lightly doped system).

To explore the relationship of  $C_{lf}$  and  $C_{hf}$  with the morphology of the film, we calculated  $C_{lf}$  and  $C_{hf}$  for different values of fractional volume  $v$ . As can be seen from Figures (4.9 a) and (4.9 b),  $C_{lf}$  varies linearly with the square of the fractional volume  $v$ , whereas  $C_{hf}$  varies linearly with  $v$ . As we have discussed earlier, at low frequency, the current flows through the fibers as far as possible, crossing over at an intersection point only if it is necessary for percolation. Since a single fiber connecting the lower edge of the film to the upper edge has a very small probability of occurrence, the majority of the current passes through the paths having only one intersection point. The impedance of such a path is series combination of the intersection impedance and resistance of the fiber. The net impedance of the system can therefore be estimated as the average impedance of a path divided by the number of such parallel paths. Hence  $C_{lf} \sim N_p \times C$ , where  $C$  is the capacitance in the intersection impedance, and  $N_p$  is the number of parallel paths. The number of parallel paths increases linearly with the number of intersection points. The number of intersection points, in turn, increases linearly with the square of the number of fibers present, and hence with the square of the fractional volume  $v$ . Therefore  $C_{lf} \propto v^2$ . At high frequency, the capacitive reactance, and hence the intersection impedance becomes smaller than the resistance of a fiber,

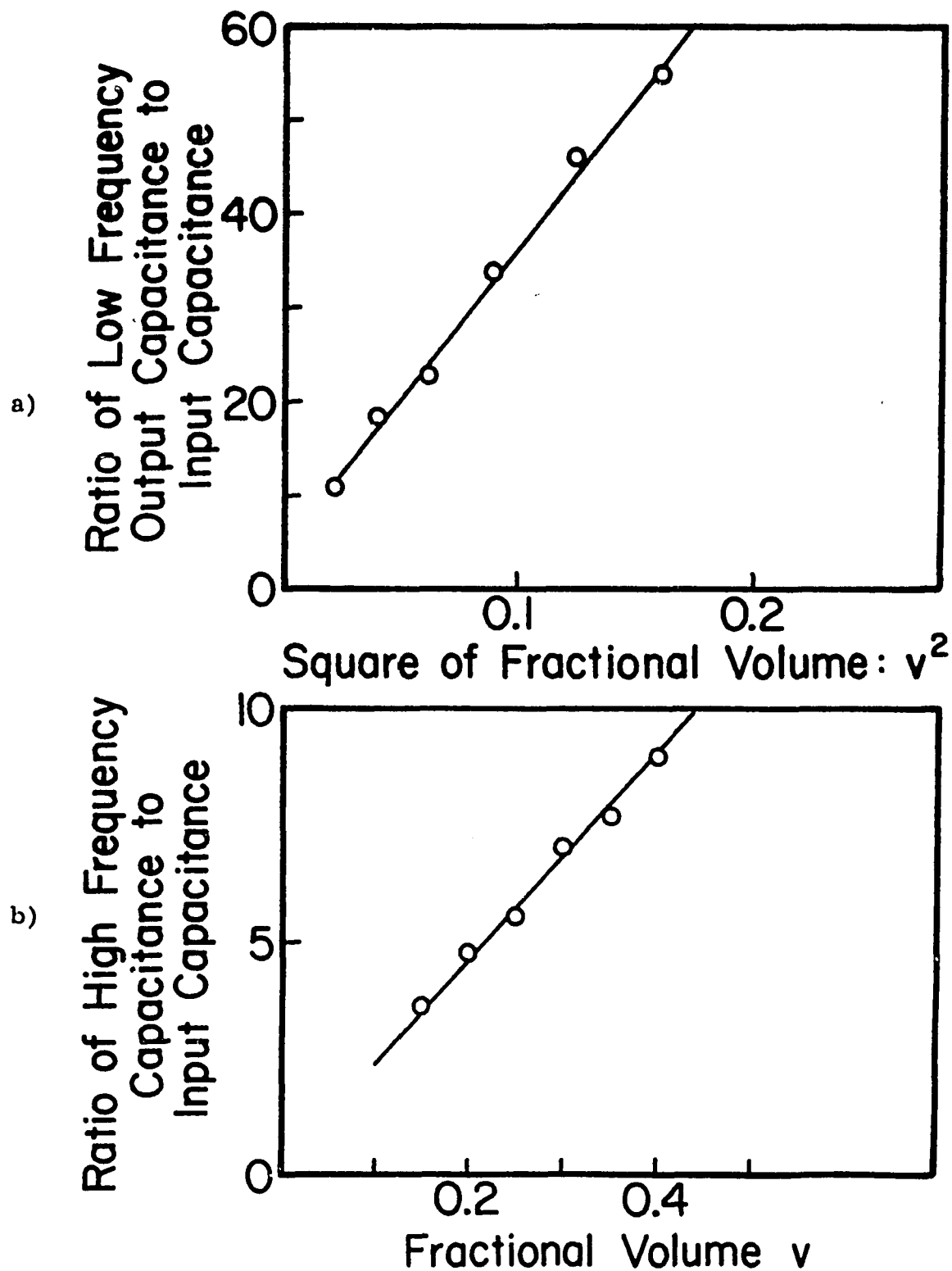


Fig. 4.9 a) The low frequency capacitance as a function of square of fractional volume.  
 b) The high frequency capacitance as a function of fractional volume.

and the current takes shortest path from the lower edge to the upper edge, no matter how many intersection points it has to cross. The impedance of such a path is the resistance of a fiber in series with a number of capacitances. Therefore the net impedance of the system is approximately the average impedance of a path divided by the number of such paths.  $C_{hf} \sim (N_s/M) \times C$ , where  $C$  is the capacitance in the intersection impedance,  $M$  is the average number of intersection points in a path, and  $N_s$  is the number of paths.  $N_s/M$  increases linearly with the number of fibers present in the system and therefore with the fractional volume  $v$ . Hence  $C_{hf} \propto v$ .

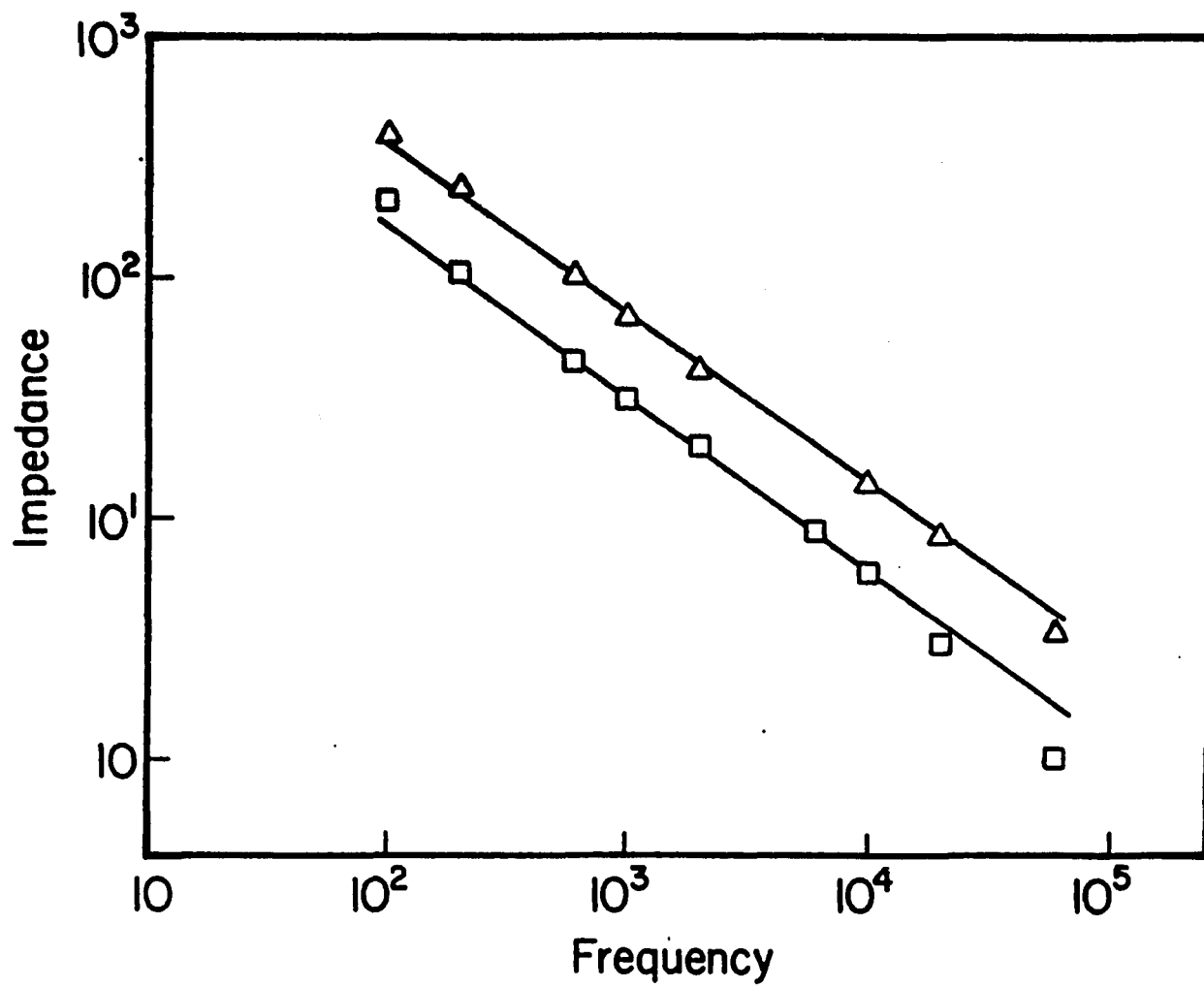
#### 4.3 CPA behaviour and Fractal Nature of the film.

As can be seen from Figure (4.6), in mid-frequency region, the frequency response of the system can not be represented by simple passive circuit. In this regime the real and the imaginary parts of the impedance are observed to obey the following relationships :

$$Z_R = R_s + A/\omega^\beta$$

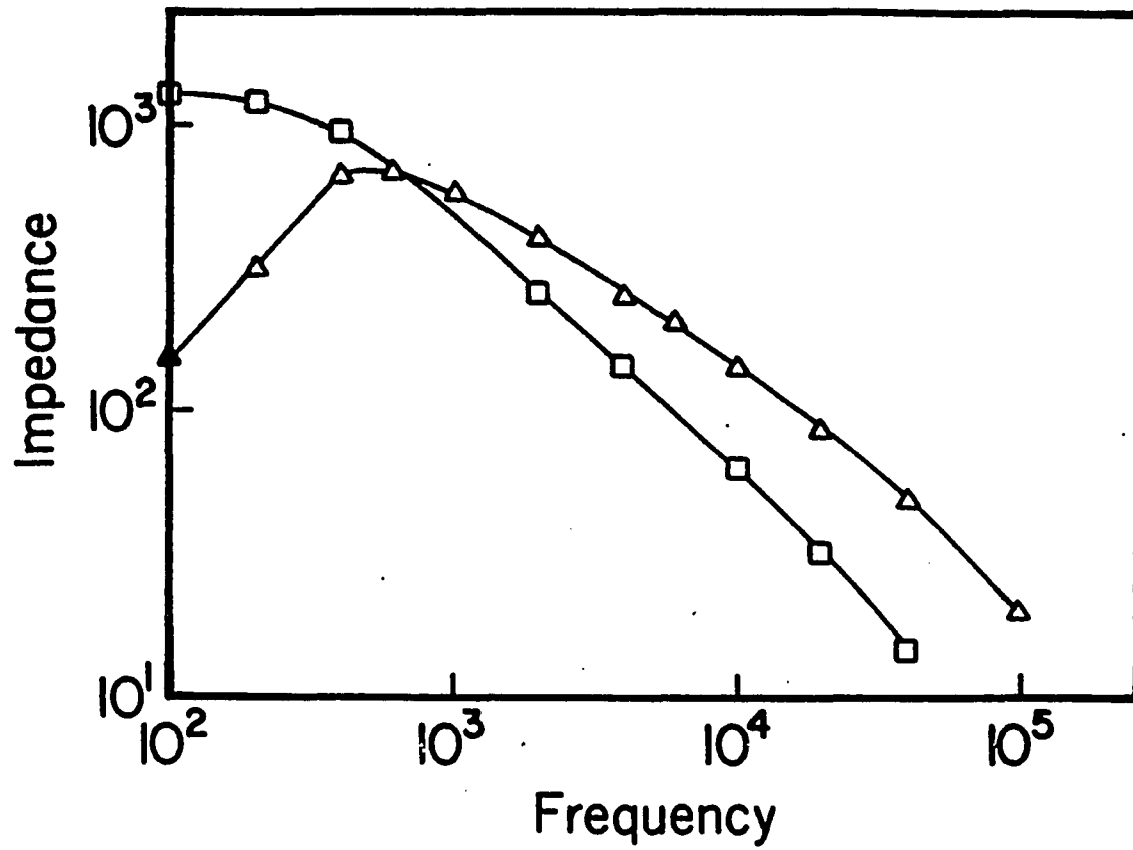
$$Z_I = B/\omega^\beta$$
(4.5)

where  $R_s$ ,  $A$ ,  $B$ ,  $\beta$  are constants independent of frequency, and  $0 \leq \beta \leq 1.0$ . In the literature this fractional frequency scaling has been



LEGEND: □ REAL △ IMAGINARY

Fig. 4.10 CPA behaviour in mid-frequency range.



LEGEND:  $\square$  REAL  $\triangle$  IMAGINARY

Fig. 4.11 Vanishing of CPA behaviour for large values of fiber resistance.

referred to as a Constant Phase Angle (CPA) (Bo76), Constant Phase Element (CPE) (Br84), or Fractional Power Frequency Dependence (FPFD) (Sc74). Such behaviour has been observed in experimental studies of polycrystalline materials (Ly80, Co82). We will hereafter refer to this as CPA behaviour; the constant phase angle refers to the fact that both the real and the imaginary parts scale with the same exponent.

Figure (4.10) shows the log-log plot of  $(Z_R - R_s)$  and  $Z_I$  versus frequency. The CPA slope  $\beta$  in this figure is 0.69. We investigated the relationship between the CPA behaviour and the input parameters by changing the resistance of fiber. As remarked earlier, for large values of fiber resistance the low frequency response resembles the high frequency response and one expects no transition region, and hence no CPA behaviour. Sure enough the CPA behaviour vanishes for large values of the resistance of a fiber as shown in Figure (4.11). When the system does show CPA behaviour, it is observed that the CPA slope is independent of the values of the input parameters. However, it depends upon the morphology of the film. We have calculated the CPA slope for different values of the fractional volume  $v$ . Figure (4.12) shows the relationship between the two to be

$$v = 1 - a\beta, \quad (4.6)$$

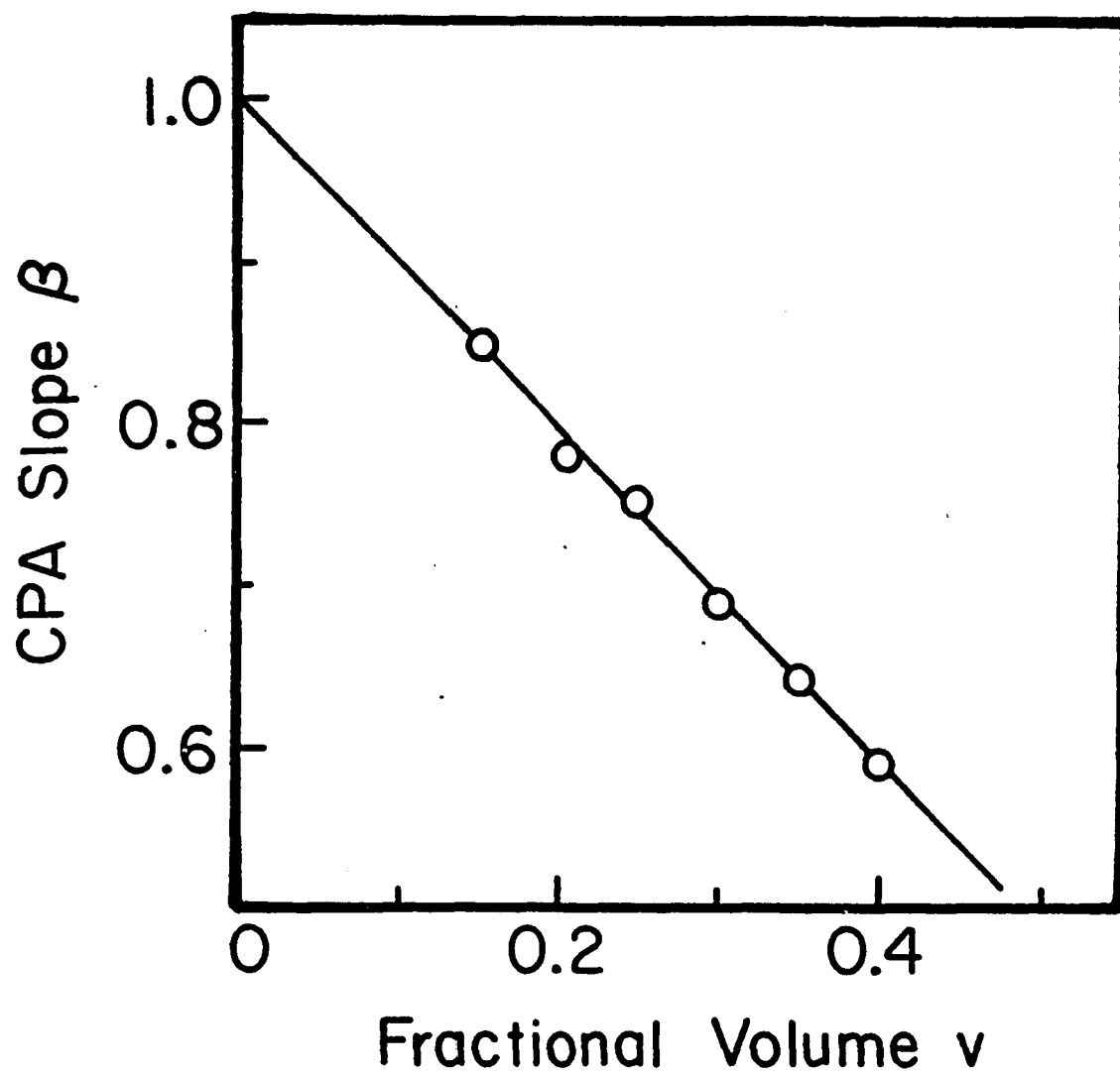


Fig. 4.12 CPA slope as a function of fractional volume.

where  $a$  is close to 1;  $a=1.06$ . Recent studies have shown that the CPA behaviour arises as a natural consequence of fractal structure. Liu (Li85) has constructed a model of the electrode-electrolyte interface out of a "textbook" fractal structure - the Cantor bar. He assumes that the interface is ideally polarizable and that each "prong" in the bar can be represented by a series R-C element that scales with the "prong" width [Figure (4.13)]. By solving for the total impedance of this equivalent circuit, he obtains a CPA behaviour. The exponent  $\beta$  that he measures is related to the fractal dimension  $D$  of the bar by  $\beta = 1-D$ .

To explore the fractal nature of our system, we have used the sandbox method, which consists of constructing squares of increasing lengths and measuring their contents. For our Random Network Model film, the number of intersection points inside a square is a good measure of percolating cluster within it. Figure (4.14) shows a log-log plot of the number of intersection points plotted against the size of the square, for fractional volume  $v=0.3$ . This behaviour can be expressed as :

$$N \propto L_s^D, \quad (4.7)$$

where  $N$  is the number of intersection points,  $L_s$  is the length of a side of the square, and  $D$  is the fractal dimension. For  $v=0.3$ , we found  $D=1.69$  as in Figure (4.14). To study the relationship of the fractal dimension  $D$  with the CPA slope  $\beta$ , we have determined the fractal

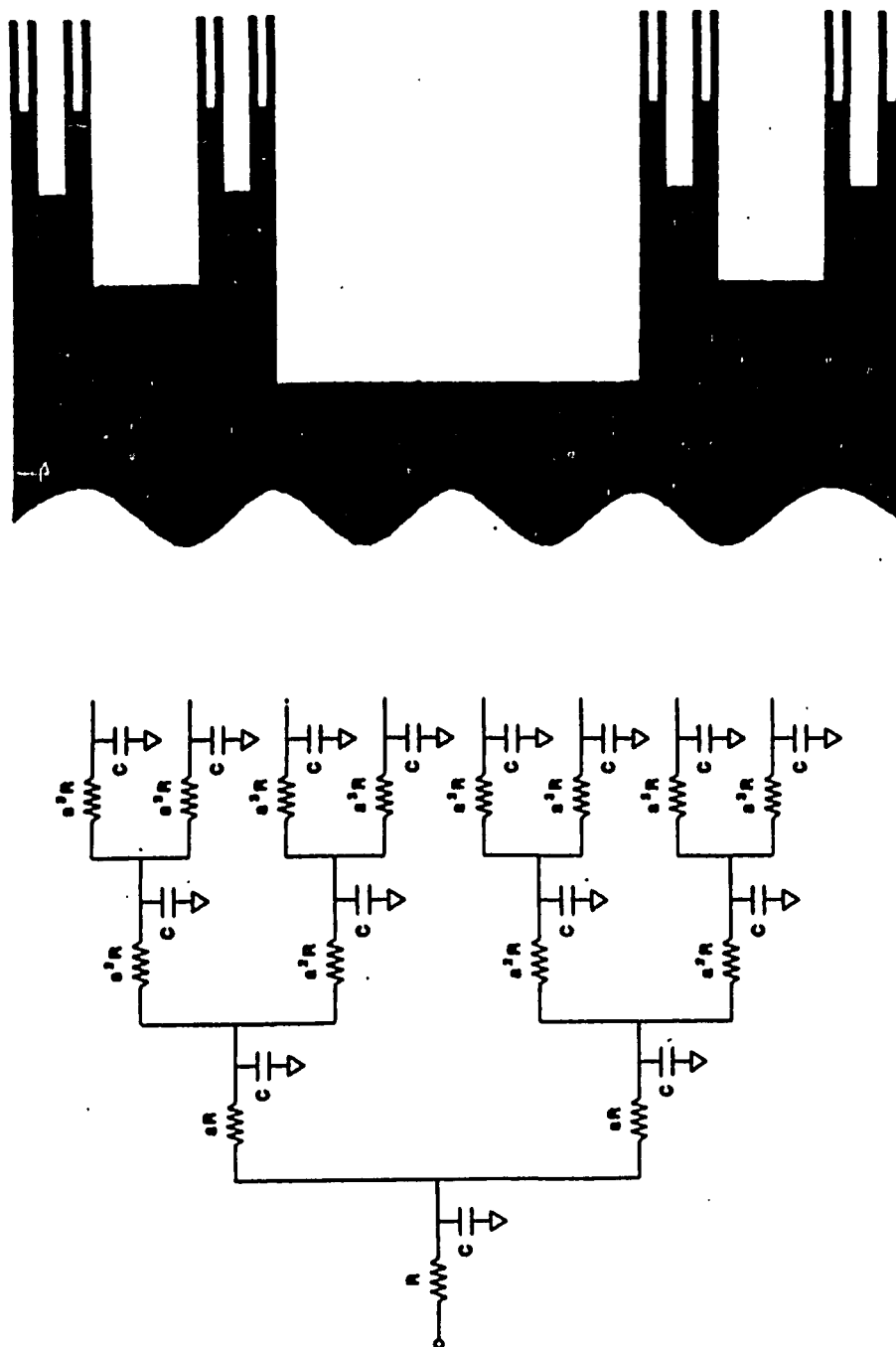


Fig. 4.13 Liu's Cantor bar model of rough electrode and its equivalent circuit [after ref. (Li85)].

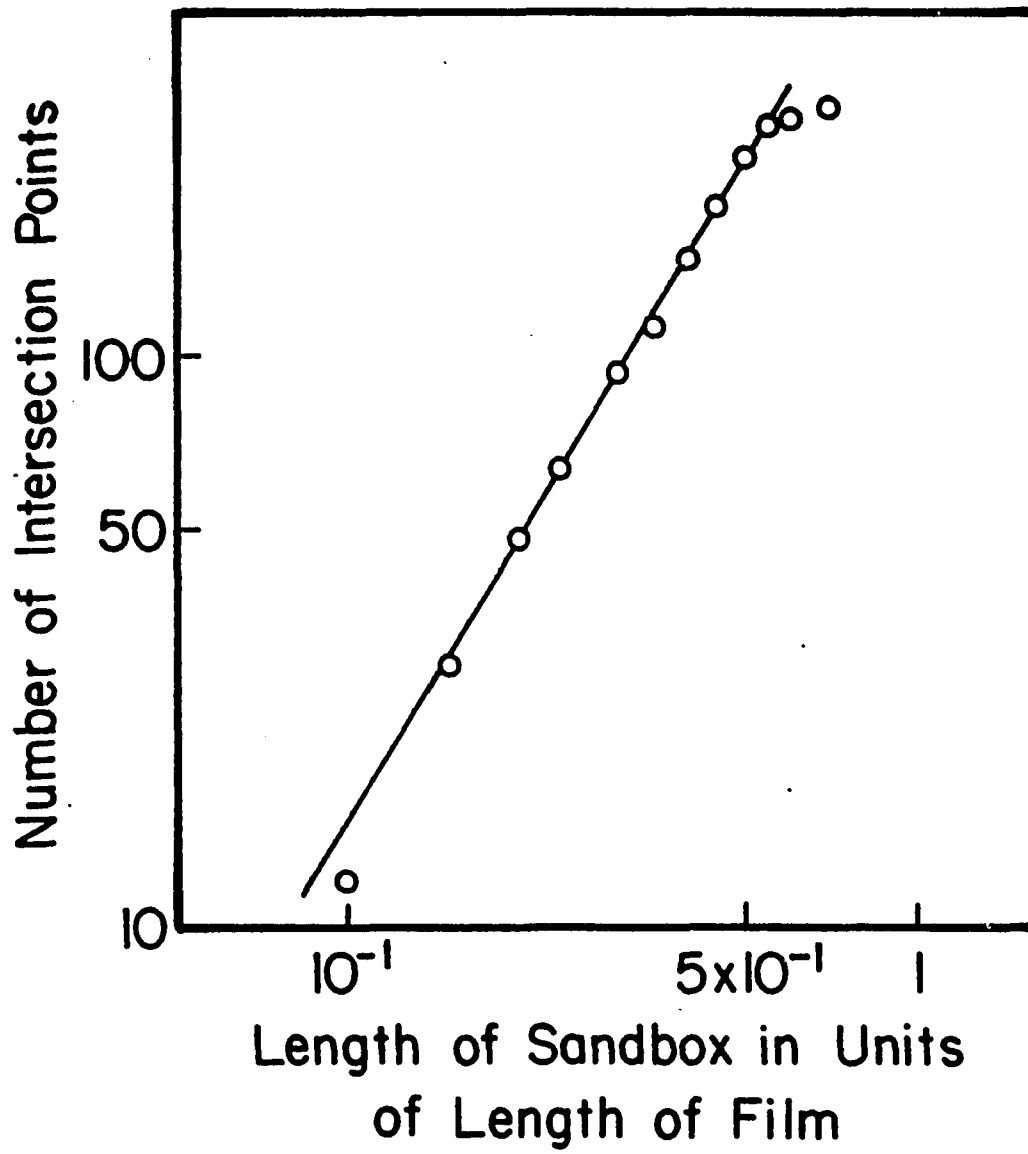


Fig. 4.14 log-log plot of number of intersection points and the size of the square.

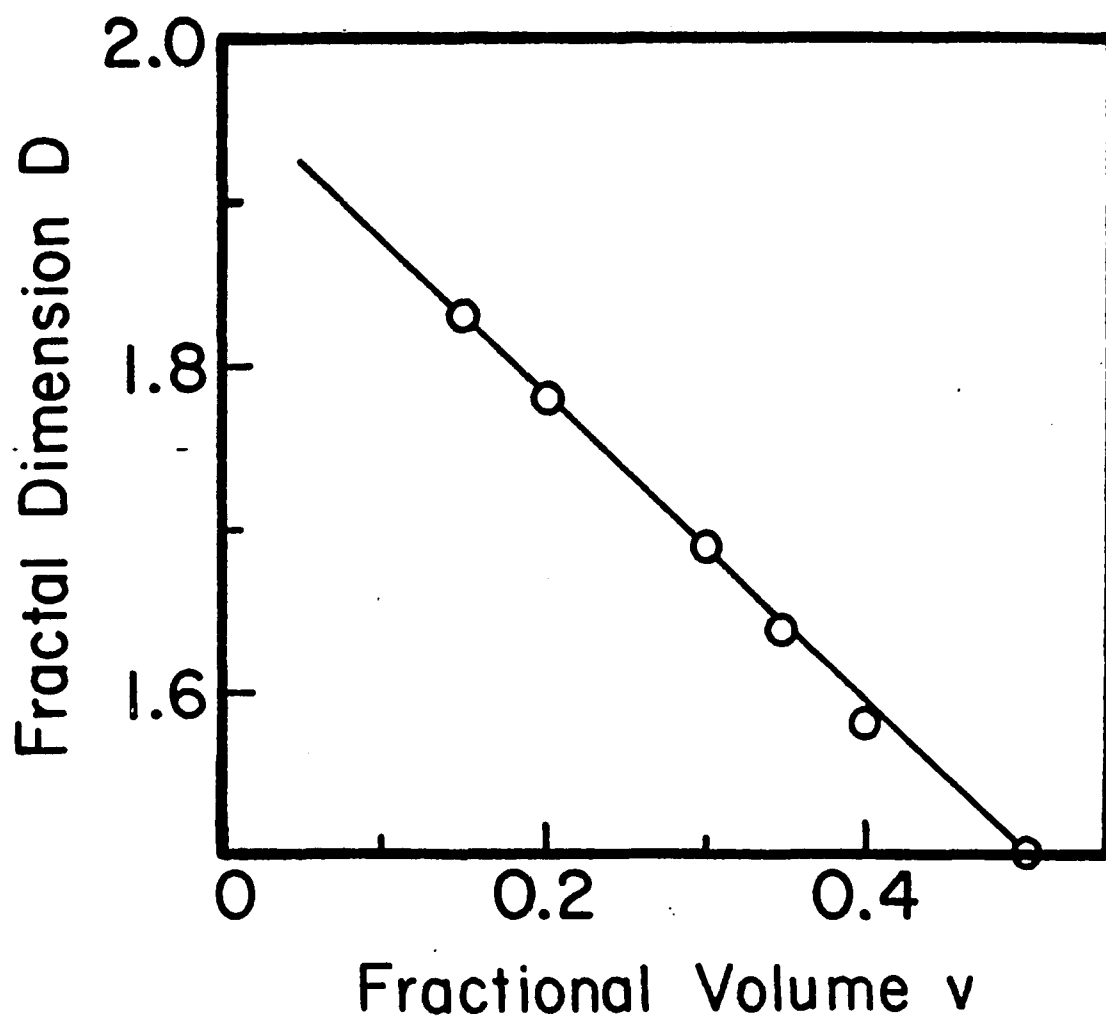


Fig. 4.15 Fractal dimension as a function of fractional volume.

dimension for different fractional volumes, following the same method. As can be seen from Figure (4.15),  $\beta$ ,  $D$ , and  $v$  are related by

$$\beta = bD - 1 = 1 - av, \quad (4.8)$$

where  $b$  is close to 1;  $b=1.03$ . The CPA behaviour in the mid-frequency range, and its relation to morphology, can be understood in terms of the penetration of the ac signal in the film. At low frequencies, the current flows through a fiber as far as possible avoiding intersections (since the intersection impedance is large at low frequencies). At high frequencies the intersection impedance is small and the current follows the shortest paths across the film. In the mid-frequency region the intersection impedance becomes comparable with the resistance of the fibers. As a result the amount of current that crosses over to another fiber at an intersection, and the amount that continues to flow along the same fiber, depends upon the exact resistances of the segments of fibers and hence on the exact positions of the points of intersection. The impedance of the film thus depends upon the details of the distribution of points of intersection. As noted earlier, the number of points of intersection scales with a fractal dimension and this is reflected in the frequency response of the film as the observed CPA behaviour.

The response of the model electrical network discussed so far is for the case where the fibers are ohmic, and the resistance in the intersec-

tion impedance is higher than the resistance of the fibers. For heavily doped polymer fiber films, the fibers become essentially metallic, and the net conductivity is limited by the interfiber conduction processes. Hence the results of this and the previous section can be utilized to understand conduction in this case. Since the Random Network Model is developed to describe ac conduction in the system, all the interesting results have their origin in the frequency response. Unfortunately no experimental data is available for the ac conductivity at high doping levels, hence we can not compare these results with experiments. The observed dc conductivity can be obtained trivially from our model by adjusting the parameter  $R$  in the R-C parallel combination. But this is a meaningless exercise and is insufficient to decide the merits of our model. Hence we have not attempted to reproduce the dc conductivity results. Nonetheless, the response of the model network is interesting in its own right, and sheds light on the effects of morphology on the conductivity of the system.

## SUMMARY AND CONCLUSIONS.

The simulation presented in this work involves three steps : First, a model structure is generated which mimics the morphological features of a polymer fiber film. Second, this model is represented by an appropriate equivalent electrical network by considering different transport mechanisms. Last, utilizing the computer, the complex electrical network problem is solved to extract the net conductivity of the system and then it is analyzed in terms of the morphology of the model film.

The random network model that we have presented is an attempt to portray a typical polymer fiber film. The distribution of interfiber junctions, and the fractional volume occupied by the fibers are the major morphological features of our model which affect our results. A representation of fibers as straight lines is a simplified approximation to the intricate configurations of fibers inside a real film. Additional variations can be considered to explore how different pictures of the geometry and different constraints would affect the results.

The interfiber conduction process is simulated by introducing an R-C parallel combination at the points of intersection of two fibers. For lightly doped polyacetylene, Monte Carlo Simulation is used to determine the conductivity of a single fiber; whereas, for heavily doped systems the fibers are assumed to be ohmic. The equivalent electrical network is

then constructed. The Random Network Model uses no basis lattice, as is usually done for the network simulations. The nodes of the network are the points of intersection, which are determined by the system itself.

Once the network is set up, the net impedance of the system is determined for various frequencies and for different morphologies. The electrical impedance is very useful in analyzing the structure of the model film, since it depends not only on its macroscopic shape and size but on its internal structure as well.

The Random Network Model provides us with a consistent way of observing the macroscopic behaviour of the system for various input parameters representing the microscopic processes in the film. For lightly doped samples we have shown that Kivelson's model, when augmented by systematic considerations of interfiber couplings and morphology of the film, yields very good results. The model gives results, at least as good in agreement with experiments as any other model, if not better. Unfortunately the experimental data available at this time is too scanty to arrive at any decisive conclusions.

For heavily doped systems, the fibers become metallic and the intersection impedance dominates the net impedance of the system. No experimental data is available for ac conductivity in this case and hence, we can not compare our results with experiments. Nonetheless

the response of the system is interesting in its own right. We have demonstrated that the low and the high frequency behaviour of the system can be represented by simple passive networks. The difference in the values of the low and the high frequency capacitances is a direct reflection of the fact that the current distributions are different at different frequencies. At mid-frequency range, we have found that there is a fractional power law relationship between impedance and frequency with an identical scaling exponent for both the real and the imaginary components (CPA behaviour). We have further shown that this exponent ( $\beta$ ) is related to the fractal structure of our model film. The sand box method is utilized to determine the fractal dimension  $D$ , and it is observed that  $D$ ,  $\beta$  and the fractional volume  $v$  are related by a simple relation  $\beta = bD - 1 = 1 - av$ .

#### Future Work.

We have represented the fibers by straight lines in our model. It will be interesting to see how representation by different shapes, for example random curves, affects the results of our calculations. One can attempt to construct the model film by tracing the electron micrograph of polymer fiber film and then solve for the impedance of such a realistic structure. Our model film is fractal and it will be interesting to see how different geometries of the system affect the fractal nature, and thereby the electrical response, of the film.

For lightly doped polyacetylene, we have used a Monte Carlo simulation of the soliton model to determine the conductivity of a single fiber. Extensions of this method can be made by incorporating soliton-soliton interactions, or by using polaron-bipolaron models which are suitable for polymers with a non-degenerate ground state.

New techniques have been introduced to calculate the impedances of the networks by utilizing a transfer matrix algorithm (De83, He84). This method provides a greater accuracy as well as greater efficiency in utilizing computer storage. The method has already been applied to 2-D complex impedance networks on a square lattice (Bu86). Generalization of this to networks with non-lattice geometries, such as ours, should be an interesting exercise.

## Appendix A.

THE DEFINITION OF  
THE EQUIVALENT ELECTRICAL NETWORK.

In this appendix we give, in some detail, the analysis that leads to the definition of the equivalent electrical network. In particular, we present the steps that lead us to the expressions for conductance between two nodes [Eqs.(2.8),(2.15)] and, in case of time varying voltages, the capacitance connected to each node [Eq.(3.7)]. We have followed the work of Miller and Abrahams closely (Mi60).

Miller-Abrahams have defined the average transition rate from the  $i^{\text{th}}$  site to the  $j^{\text{th}}$  site, in absence of an external electric field, as (See Eq.2.1)

$$\Gamma_{ij}^0 = n_i (1-n_j) \gamma_{ij}, \quad (\text{A.1})$$

where  $n_i$  is the occupation probability for site  $i$  and  $n_j$  is that for site  $j$ .  $\gamma_{ij}$  is the intrinsic rate for electron transition from site  $i$  to site  $j$ . An expression for this rate, in terms of the site separation  $\vec{R}_{ij}$  and site energies  $E_i$ , can be written as (See Section 2.1)

$$\begin{aligned} \gamma_{ij} &= \gamma_0 \exp[-2\alpha R_{ij} - (E_j - E_i)/kT] && \text{for } E_j > E_i, \\ &= \gamma_0 \exp[-2\alpha R_{ij}] && \text{for } E_j \leq E_i, \end{aligned} \quad (\text{A.2})$$

The occupation probability is given by

$$n_i = [1 + \exp(E_i/kT)]^{-1}, \quad (\text{A.3})$$

For the case of isoenergetic hopping  $E_i = E_j \equiv E$  and  $n_i = n_j \equiv n^{(0)}$ .

The intrinsic transition rate then reduces to

$$v_{ij} = \gamma_0 \exp(-2\alpha R_{ij}). \quad (\text{A.4})$$

For consistency with Kivelson's notation we have replaced  $\gamma_{ij}$  by  $v_{ij}$ .

Eq.(A.1) is therefore written in the form

$$\Gamma_{ij}^{(0)} = v_{ij} n^{(0)} (1 - n^{(0)}). \quad (\text{A.5})$$

When  $kT$  is small as compared with the site energy, we can approximate Eq.(A.3) so that

$$n^{(0)} \approx \exp[-E/kT]$$

and

$$1 - n^{(0)} \approx 1.$$

In this case we can write the transition rate of Eq.(A.5) as

$$\Gamma_{ij}^{(0)} = v_{ij} \exp[-E/kT]. \quad (\text{A.6})$$

In the presence of a weak external electrical field the site energy changes:  $E \rightarrow E + e\vec{E} \cdot \vec{R}_i$ . The transition rate can therefore be written as

$$\Gamma_{ij}(E) = v_{ij} \exp[-(E + e\vec{E} \cdot \vec{R}_i - \delta\mu_i)/kT], \quad (\text{A.7})$$

where  $\delta\mu_i$  represents the change in the chemical potential at the  $i^{\text{th}}$  site. Thus for the net transition rate from site  $i$  to site  $j$ , we obtain

$$\begin{aligned} \Gamma_{ij}(\vec{E}) - \Gamma_{ji}(\vec{E}) &= v_{ij} \exp[-E/kT] \exp[-(e\vec{E} \cdot \vec{R}_i - \delta\mu_i)/kT] \\ &\quad - v_{ji} \exp[-E/kT] \exp[-(e\vec{E} \cdot \vec{R}_j - \delta\mu_j)/kT]. \end{aligned} \quad (\text{A.8})$$

We now make use of the reciprocity relation

$$v_{ij} = v_{ji}, \quad (\text{A.9})$$

and retain terms upto first order in the weak electric field to obtain

$$\Gamma_{ij}(\vec{E}) - \Gamma_{ji}(\vec{E}) = (1/kT) \Gamma_{ij}^{(0)} [e\vec{E} \cdot \vec{R}_{ij} + \delta\mu_i - \delta\mu_j]. \quad (\text{A.10})$$

We identify

$$eV_{ij} = e\vec{E} \cdot \vec{R}_{ij} + \delta\mu_i - \delta\mu_j,$$

and

$$I_{ij} = e [\Gamma_{ij}(\vec{E}) - \Gamma_{ji}(\vec{E})].$$

Therefore we can write Eq.(A.10) in the form

$$I_{ij} = G_{ij} V_{ij}, \quad (\text{A.11})$$

where the conductance between site  $i$  and site  $j$  is given by

$$G_{ij} = (e^2/kT) \Gamma_{ij}^{(0)}. \quad (\text{A.12})$$

The steady state condition for time independent fields is that the net current arriving at any site be zero (Kirchhoff's first law).

$$\sum_i I_{ij} = 0, \quad \text{for all } j. \quad (\text{A.13})$$

This equation can be written in terms of conductances as

$$\sum_i G_{ij} V_{ij} = 0. \quad (\text{A.14})$$

For the case of time dependent fields the steady state condition must be modified as

$$\sum_i I_{ij} = e (\partial n_j / \partial t). \quad (\text{A.15})$$

Now, the occupation probability  $n_j$  in the presence of external field can be written as

$$n_j(\vec{E}) = [1 + \exp\{(E + e\vec{E} \cdot \vec{R}_j - \delta\mu_j)/kT\}]^{-1}. \quad (\text{A.16})$$

The time derivative of this expression can be easily evaluated as

$$\partial n_j(\vec{E}) / \partial t = -(e/kT) n_j(\vec{E}) (1 - n_j(\vec{E})) \partial V_j / \partial t, \quad (\text{A.17})$$

where  $eV_j = e\vec{E} \cdot \vec{R}_j - \delta\mu_j$  defines the potential of site  $j$  with respect to ground. Using this in Eq.(A.15) we can write

$$\begin{aligned} \sum_i G_{ij} V_{ij} &= \sum_i I_{ij} \\ &= - (e^2/kT) n^{(0)} (1 - n^{(0)}) [\partial V_j / \partial t]. \end{aligned} \quad (\text{A.18})$$

Thus we can identify

$$C_j = - (e^2/kT) n^{(0)} (1 - n^{(0)}) \quad (\text{A.19})$$

as a capacitance connected between site  $j$  and ground.

Appendix B  
PROGRAM LISTINGS







```

C     NODES , AS WELL AS IT TELLS US THE NODES WHICH ARE CONNECTED
C     THROUGH INTERSECTIONS
C
C     CALL COND(NF,G,GU,COL,ND)
C
C     THE ROUTINE REMOV TAKES CARE OF ANY POSSIBLE HANGING NODE.
C
C     CALL REMOV(G,GU,COL,ND)
C
C     TO CONSTRUCT MATRICES A,IA,JA AS NEEDED BY SLMATH.
C
C     CALL CONSTR(G,GU,COL,AA,IA,JA,ND)
C     WRITE(6,122)ND
122   FORMAT(5X,15)
C
C     THE ROUTINE FRACT DETERMINES THE NO. OF POINTS OF
C     INTERSECTIONS INSIDE THE SANDBOXES OF INCREASING LENGTHS.
C
C     CALL FRACT
C
C     CALL EXIT
C     END

```

---

```

C*****
C
C     SUBROUTINE GEN(DSEED,NF)
C
C     THE ROUTINE GEN GENERATES THE END POINTS OF THE FIBERS
C     AND DETERMINES ALL THE POINTS OF INTERSECTIONS.
C
C     DIMENSION X1(200),Y1(200),X2(200),Y2(200)
C     DIMENSION IFIB1(8000),IFIB2(8000),C(200),Z(4)
C     REAL IX(8000),IY(8000),M(200),IXX,IYY
C     DOUBLE PRECISION DSEED
C     COMMON/MGSC/X1,Y1,X2,Y2,A,B,TLEN
C     COMMON/MGSCI/IX,IY,IFIB1,IFIB2,NINT
C     DATA PI/3.14159265/
C
C     INITIALIZATIONS
C     NINT=0
C     NZ=4
C     I=0
C     XLEN=0.0
C     SUMMI=0.0
C     SUMANG=0.0
C     ANGXL=0.0
C     NUMM=0
C     XLIM=0.1*A
C     YLIM=0.1*B
C
C     END OF INITIALIZATIONS.
C
C     LOOP FOR GENERATION OF FIBERS.
C
100   I=I+1

```

```

50      CALL GGUBS(DSEED,NZ,Z)
        X1(I)=A*Z(1)
        X2(I)=A*Z(2)
C      WE WANT Y2 > Y1.
        IF(Z(3).LT.Z(4))THEN
            Y1(I)=B*Z(3)
            Y2(I)=B*Z(4)
        ELSE
            Y1(I)=B*Z(4)
            Y2(I)=B*Z(3)
        ENDIF
C      TO TAKE CARE OF BOUNDRIES.
        IF(X1(I).LE.XLIM)X1(I)=0.0
        IF((A-X1(I)).LE.XLIM)X1(I)=A
        IF(X2(I).LE.XLIM)X2(I)=0.0
        IF((A-X2(I)).LE.XLIM)X2(I)=A
        IF(Y1(I).LE.YLIM)Y1(I)=0.0
        IF((B-Y2(I)).LE.YLIM)Y2(I)=B
        IF((Y1(I).EQ.0.0).AND.(Y2(I).EQ.B))THEN
            WRITE(6,111)I
            STOP
        ENDIF
111     FORMAT(2X,'FIBER',I4,' EXTENDS FROM UPPER TO LOWER EDGE.')
C
C      CALCULATION OF LENGTH, SLOPE, AND Y-INTERCEPT.
        XL=(Y2(I)-Y1(I))*(Y2(I)-Y1(I))
        XL=(XL+(X2(I)-X1(I))*(X2(I)-X1(I)))**.5
C      INFINITE SLOPE AND Y-INTERCEPT IS APPROXIMATED BY 100000
        IF(X1(I).EQ.X2(I))THEN
            M(I)=100000
            C(I)=100000
            THETA=0.0
            GO TO 55
        ENDIF
        M(I)=(Y2(I)-Y1(I))/(X2(I)-X1(I))
        C(I)=Y2(I)-M(I)*X2(I)
        THETA=ATAN(ABS(M(I)))
55     SUMANG=SUMANG+THETA
        SUMMI=SUMMI+ABS(M(I))
        NUMM=NUMM+1
        XLEN=XLEN+XL
        ANGXL=ANGXL+THETA*XL
C
C      FINDING OUT INTERSECTION PTS OF NEWLY GENERATED FIBER
C      WITH ALL PREVIOUSLY GENERATED ONES.
C      LOOP TILL THE LAST GENERATED FIBER.
C
        IM1=I-1
        DO 200 J=1,IM1
C      SAME SLOPE? NO INTERSECTION POINT.
        IF(M(I).EQ.M(J))GO TO 200
C
C      TWO LINES WITH DIFFERENT SLOPES :
C      Y=M1X+C1, Y=M2X+C2

```

```

C      COORDINATE OF INTERSECTION POINT IS GIVEN BY :
C      M1X+C1=M2X+C2
C      X=(C2-C1)/(M1-M2)
C      Y=M1X+C1
C
C      IXX=(C(J)-C(I))/(M(I)-M(J))
C      TO CHECK IF INT. PT. LIES INSIDE THE FILM.
C      IF((IXX.GT.A).OR.(IXX.LT.0.0))GO TO 200
C      TO CHECK IF INT. PT. LIES ON THE FIBER I AS WELL AS J.
C      IF((ABS(IXX-X1(I)).GT.ABS(X2(I)-X1(I))).OR.(ABS(IXX-X2(I)).GT.
1ABS(X2(I)-X1(I))))GO TO 200
C      IF((ABS(IXX-X1(J)).GT.ABS(X2(J)-X1(J))).OR.(ABS(IXX-X2(J)).GT.
1ABS(X2(J)-X1(J))))GO TO 200
C      IYY=M(I)*IXX+C(I)
C      NEW INT. PT. : UPDATING CORRESPONDING ARRAYS.
C      NINT=NINT+1
C      IX(NINT)=IXX
C      IY(NINT)=IYY
C      INTERSECTION OF WHICH TWO FIBERS? IFIB1<IFIB2
C      IFIB1(NINT)=J
C      IFIB2(NINT)=I
200    CONTINUE
C      IF(XLEN.LT.TLEN)GO TO 100
C      WRITE(6,11)XLEN
11     FORMAT(5X,'TOTAL LENGTH OF FIBERS',F13.6)
C      NF=I
C      SUMMI=SUMMI/NUMM
C      SUMANG=SUMANG/NF
C      SUMANG=90.0-180.0*SUMANG/PI
C      ANGXL=ANGXL/XLEN
C      WRITE(6,21)NINT,NF,NUMM,SUMMI,SUMANG,ANGXL
21    FORMAT(3(2X,15),'AVERAGE SLOPE ',F7.3,2X,'THETA=',E13.6,E13.6)
C      RETURN
C      END
C
C*****
C
C      SUBROUTINE SET(NF,FLAG)
C
C      THE CRITERION TO FIND OUT WHETHER A FIBER CONTRIBUTES TO
C      CONDUCTIVITY OR NOT IS AS FOLLOWS. IF FIBER SATISFIES ANY
C      ONE OF THE FOLLOWING CONDITION THEN IT MAY CONTRIBUTE.
C
C      (1) THE FIBER'S Y1,Y2 ARE SUCH THAT Y2=B & Y1=0.
C      (2) Y2=B & FIBER HAS AT LEAST ONE IMPURITY INTERSECTION.
C      (3) Y1=0 & FIBER HAS AT LEAST ONE IMPURITY INTERSECTION.
C      (4) FIBER HAS AT LEAST TWO IMPURITY INTERSECTIONS.
C
C      FLAG IS SET TO .TRUE. FOR THE FIBERS WHICH SATISFY EITHER
C      OF ABOVE CONDITIONS.
C
C      DIMENSION X1(200),Y1(200),X2(200),Y2(200)
C      DIMENSION IFIB1(8000),IFIB2(8000)
C      REAL IX(8000),IY(8000)

```

```

LOGICAL FLAG(200),COND1,COND2,COND3,COND4
COMMON/MGSC/X1,Y1,X2,Y2,A,B,TLEN
COMMON/MGSCI/NINT,IX,IY,IFIB1,IFIB2
C   INITIALIZATION OF FLAG TO .FALSE. FOR ALL FIBERS.
      DO 100 I=1,NF
        FLAG(I)=.FALSE.
100  CONTINUE
C
      DO 200 I=1,NF
C   CHECKING CONDITION 1
        IF((Y1(I).EQ.0.0).AND.(Y2(I).EQ.B))THEN
          COND1=.TRUE.
        ELSE
          COND1=.FALSE.
        ENDIF
C
C   CHECKING REMAINING CONDITIONS
C
      DO 300 J=1,NINT
        IF((IFIB1(J).EQ.I).OR.(IFIB2(J).EQ.I))GO TO 301
300  CONTINUE
        COND2=.FALSE.
        COND3=.FALSE.
        COND4=.FALSE.
        GO TO 199
301  IF(Y2(I).EQ.B)THEN
          COND2=.TRUE.
        ELSE
          COND2=.FALSE.
        ENDIF
        IF(Y1(I).EQ.0.0)THEN
          COND3=.TRUE.
        ELSE
          COND3=.FALSE.
        ENDIF
C
      J1=J+1
      DO 400 K=J1,NINT
        IF((IFIB1(K).EQ.I).OR.(IFIB2(K).EQ.I))GO TO 401
400  CONTINUE
        COND4=.FALSE.
        GO TO 199
401  COND4=.TRUE.
199  FLAG(I)=COND1.OR.COND2.OR.COND3.OR.COND4
200  CONTINUE
C
      RETURN
      END
C
C*****
C
C   SUBROUTINE SORT
C
C   THE ROUTINE SORT SORTS IY IN DESCENDING ORDER USING

```

```

C      BUBBLE SORT.
C
      DIMENSION IFIB1(8000),IFIB2(8000)
      REAL IX(8000),IY(8000)
      COMMON/MGSCI/NINT,IX,IY,IFIB1,IFIB2
C
      NINTM1=NINT-1
      DO 100 I=1,NINTM1
      II=I+1
      DO 100 J=II,NINT
      IF(IY(J).GT.IY(I))THEN
          TX=IX(I)
          TY=IY(I)
          IT1=IFIB1(I)
          IT2=IFIB2(I)
          IX(I)=IX(J)
          IY(I)=IY(J)
          IFIB1(I)=IFIB1(J)
          IFIB2(I)=IFIB2(J)
          IX(J)=TX
          IY(J)=TY
          IFIB1(J)=IT1
          IFIB2(J)=IT2
      ENDIF
100    CONTINUE
C
      RETURN
      END
C
C*****
C
      SUBROUTINE COND(NF,G,GU,COL,ND)
C
      SUBROUTINE TO CONSTRUCT THE CONDUCTANCE MATRIX.
C
      THE ROUTINE TRACES EACH FIBER FROM ITS ENDPOINT (X2,Y2)
      TO ITS OTHER ENDPOINT (X1,Y1) AND LABELS THE INTERSECTION
      POINTS BY THE NODE NUMBERS. THE UPPER AND LOWER EDGE HAVE
      ASSIGNED THE NODE NUMBERS 1 AND 2 RESP. THE CONDUCTANCE
      MATRIX IS SPARSE AND HENCE WE STORE ONLY THOSE ELEMENTS
      WHICH CAN BE NON-ZERO.
C
      G(I,1) : DIAGONAL ELEMENT OF REAL CONDUCTANCE MATRIX.
      G(I,2) : REAL CONDUCTANCE BETWEEN NODE I AND NODE I+1
      IF THEY LIE ON SAME FIBER.
      G(I,3) : REAL CONDUCTANCE BETWEEN NODE I AND SOME NODE J
      (J>I), IF I AND J REPRESENT THE INTERSECTION OF
      TWO FIBERS. COL(I) HOLDS THE NODE NUMBER J.
      G(I,4) : DIAGONAL ELEMENT OF IMAGINARY CONDUCTANCE MATRIX.
      G(I,5) : IMAGINARY CONDUCTANCE BET NODE I AND NODE I+1
      IF THEY LIE ON SAME FIBER.
      GU(1,I) : REAL CONDUCTANCE BETWEEN UPPER EDGE AND NODE I
      IF THE FIBER STARTS FROM UPPER EDGE.
      GU(2,I) : REAL CONDUCTANCE BETWEEN LOWER EDGE AND NODE I

```

```

C           IF THE FIBER ENDS ON LOWER EDGE.
C   GU(3,I) AND GU(4,I) ARE CORRESPONDING IMAGINARY CONDUCTANCES.
C
C
C           DIMENSION X1(200),Y1(200),X2(200),Y2(200),G(3000,5)
           DIMENSION IFIB1(8000),IFIB2(8000),GU(4,3000)
           INTEGER COL(3000),DUMND
           DIMENSION VR(1000),VI(1000)
           REAL IX(8000),IY(8000),NDX(8000),NDY(8000),L
           REAL FRE,CAP,W,ZZ
           LOGICAL FLAG(200),SWITCH
           COMMON/MGSC/X1,Y1,X2,Y2,A,B,TLEN
           COMMON/MC/FLAG
           COMMON/MGSCI/NINT,IX,IY,IFIB1,IFIB2
           COMMON/ELE/GREAL,GIMG
           DATA PI/3.14159265/
C
C   INITIALIZATIONS
           NCOND=0
           TOTCON=0.0
           NINTWO=2*NINT+2
C
           DO 10 I=3,NINTWO
           COL(I)=0
           GU(1,I)=0.0
           GU(2,I)=0.0
           GU(3,I)=0.0
           GU(4,I)=0.0
           G(I,1)=0.0
           G(I,2)=0.0
           G(I,3)=0.0
           G(I,4)=0.0
           G(I,5)=0.0
10  CONTINUE
C
           SUML=0.0
           TOTL=0.0
           ANGL=0.0
           NOL=0
           ND=2
C
C   FOR CURRENT CALCULATIONS : INPUT IS VOLTAGE MATRIX.
C   NODE 1 IS GROUNDED : VR(1)=VI(1)=0
C
           VR(1)=0.0
           VI(1)=0.0
C
C   READ(9,121)(VR(I+1),VI(I+1),I=1,605)
121  FORMAT(4(1X,E15.8))
C
           READ(5,1)FRE,RHO,RHOIM,RC,CAP
           WRITE(6,1)FRE,RHO,RHOIM,RC,CAP
1           FORMAT(5(1X,E13.6))
           TEMP=RHO*RHO+RHOIM*RHOIM

```

```

GRHO=RHO/TEMP
GRHOIM=RHOIM/TEMP
WRITE(4,2)FRE
2   FORMAT(5X,D13.6)
    W=2*PI*FRE
    ZZ=RC/(1.0+W*W*CAP*CAP*RC*RC)**0.5
    GREAL=1.0/RC
    GIMG=W*CAP
C   LOOP TILL ALL FIBERS ARE TRACED
    DO 100 I=1,NF
C   CHECK IF FLAG IS .TRUE.
    IF(.NOT.FLAG(I))GO TO 100
    ND=ND+1
    SX=100.0
    SY=100.0
C
    IF(Y2(I).NE.B)THEN
C   I TH FIBER DOES NOT START FROM THE UPPER EDGE, HENCE GO
C   TO ITS FIRST INTERSECTION POINT.
    DO 200 J=1,NINT
    IF(SX.NE.100.0)GO TO 200
    IF(IFIB2(J).EQ.I)THEN
C   INTERSECTION POINT WITH A FIBER WHICH IS TRACED BEFORE.
    NDM1=ND-1
    DO 300 K=3,NDM1
    IF((NDX(K).EQ.IX(J)).AND.(NDY(K).EQ.IY(
300 1J)))GO TO 325
    CONTINUE
    GO TO 200
C   SET UP AN INTERSECTION IMPEDENCE BETWEEN NODES K AND ND.
325  G(K,3)--GREAL
    COL(K)=ND
    LASTIN=J
    SX=IX(J)
    SY=IY(J)
    NDX(ND)=SX
    NDY(ND)=SY
    J1=J+1
    SWITCH=.FALSE.
    CUR=((VR(ND)-VR(K))*(VR(ND)-VR(K)))+
1(VI(ND)-VI(K))*(VI(ND)-VI(K))**0.5
    CUR=CUR/ZZ
    WRITE(7,111)NDX(K),NDY(K),NDX(ND),NDY(ND),CUR
111  FORMAT(5(1X,F10.6))
    ENDIF
C
    IF(IFIB1(J).EQ.I)THEN
C   INTERSECTION POINT WITH A FIBER WHICH IS NOT YET TRACED.
    SX=IX(J)
    SY=IY(J)
    LASTIN=J
    NDX(ND)=SX
    NDY(ND)=SY
    J1=J+1

```

```

                SWITCH=.FALSE.
                ENDIF
C
C 200          CONTINUE
C
                ELSE
C  I TH FIBER STARTS FROM UPPER EDGE.
                SX=X2(I)
                SY=B
                NDX(ND)=SX
                NDY(ND)=SY
                NDX(1)=SX
                NDY(1)=SY
                J1=1
                SWITCH=.TRUE.
C
                ENDIF
C
C  TO TRACE A FIBER FURTHER TILL OTHER ENDPOINT IS REACHED.
C
                DO 400 K=J1,NINT
                IF(IFIB1(K).EQ.1)THEN
C  INTERSECTION POINT WITH A FIBER WHICH IS NOT YET TRACED.
                L=((SY-IY(K))*(SY-IY(K))+(SX-IX(K))*(SX-IX(K)))**0.5
                TOTL=TOTL+L
                ANGL=ANGL+L*ATAN(ABS((SY-IY(K))/(SX-IX(K))))
                IF(L.LT.1.OE-06)THEN
                    L=1.OE-06
                ENDIF
                IF(SWITCH)THEN
C  FIBER STARTS FROM UPPER EDGE : SET UP GU.
                GU(1,ND)=-GRHO/L
                GU(3,ND)=-GRHOIM/L
                NCOND=NCOND+1
                TOTCON=TOTCON+GU(1,ND)
                TEMPR=L*RHO
                CUR=((VR(ND)-VR(1))*(VR(ND)-VR(1))+(VI(ND)-VI(1))*
1(VI(ND)-VI(1)))**0.5
                CUR=CUR/TEMPR
                DUMND=1
                ELSE
C  TAKE CARE OF IMPEDENCE OF A SECTION OF FIBER
C  BETWEEN TWO INTERSECTION POINTS.
                G(ND,2)=-GRHO/L
                G(ND,5)=-GRHOIM/L
                NCOND=NCOND+1
                TOTCON=TOTCON+G(ND,2)
                TEMPR=L*RHO
                CUR=((VR(ND)-VR(ND+1))*(VR(ND)-VR(ND+1))+
1(VI(ND)-VI(ND+1))*(VI(ND)-VI(ND+1)))**0.5
                CUR=CUR/TEMPR
                DUMND=ND
                ND=ND+1
                ENDIF

```

```

        NDX(ND)=IX(K)
        NDY(ND)=IY(K)
        SX=IX(K)
        SY=IY(K)
        SWITCH=.FALSE.
        WRITE(3,111)NDX(DUMND),NDY(DUMND),NDX(ND),NDY(ND),CUR
    ENDIF
C
        IF(IFIB2(K).EQ.1)THEN
C
        INTERSECTION POINT WITH A FIBER WHICH IS ALREADY TRACED.
C
        HENCE FIND OUT CORRESPONDING NODE NUMBER.
            DO 500 JJ=3,ND
                IF((NDX(JJ).EQ.IX(K)).AND.(NDY(JJ).EQ.IY(K)))GO TO 5
125
500          CONTINUE
C
                GO TO 400
C
525          L=((SY-IY(K))*(SY-IY(K))+(SX-IX(K))*(SX-IX(K)
1)))**0.5
                TOTL=TOTL+L
                ANGL=ANGL+L*ATAN(ABS((SY-IY(K))/(SX-IX(K))))
                IF(L.LT.1.0E-06)THEN
                    L=1.0E-06
                ENDIF
                IF(SWITCH)THEN
C
                FIBER STARTS ON UPPER EDGE : SET UP GU.
                    GU(1,ND)=-GRHO/L
                    GU(3,ND)=-GRHOIM/L
                    NCOND=NCOND+1
                    TOTCON=TOTCON+GU(1,ND)
                    TEMPR=L*RHO
                    CUR=((VR(ND)-VR(1))*(VR(ND)-VR(1))+(VI(ND)-VI(1))*
1(VI(ND)-VI(1)))**0.5
                    CUR=CUR/TEMPR
                    DUMND=1
                ELSE
C
                TAKE CARE OF IMPEDENCE OF A SECTION OF FIBER
C
                BETWEEN TWO INTERSECTION POINTS.
                    G(ND,2)=-GRHO/L
                    G(ND,5)=-GRHOIM/L
                    NCOND=NCOND+1
                    TOTCON=TOTCON+G(ND,2)
                    TEMPR=L*RHO
                    CUR=((VR(ND)-VR(ND+1))*(VR(ND)-VR(ND+1))+
1(VI(ND)-VI(ND+1))*(VI(ND)-VI(ND+1)))**0.5
                    CUR=CUR/TEMPR
                    DUMND=ND
                    ND=ND+1
                ENDIF
                NDX(ND)=IX(K)
                NDY(ND)=IY(K)
                SX=IX(K)
                SY=IY(K)

```

```

        SWITCH=.FALSE.
        WRITE(3,111)NDX(DUMND),NDY(DUMND),NDX(ND),NDY(ND),CUR
        G(JJ,3)=-GREAL
        COL(JJ)=ND
        CUR=((VR(ND)-VR(JJ))*(VR(ND)-VR(JJ))+(VI(ND)-VI(JJ))
1*(VI(ND)-VI(JJ)))**0.5
        CUR=CUR/ZZ
        WRITE(7,111)NDX(JJ),NDY(JJ),NDX(ND),NDY(ND),CUR
    ENDIF
400  CONTINUE
C
C  ALL INTERSECTION POINTS OF A FIBER ARE CONSIDERED.
C  CHECK IF ITS OTHER ENDPOINT LIES ON THE LOWER EDGE.
C
        IF(Y1(I).EQ.0.0)GO TO 100
        NDX(2)=X1(I)
        NDY(2)=0.0
        L=(SY*SY+(SX-X1(I))*(SX-X1(I)))**0.5
        TOTL=TOTL+L
        ANGL=ANGL+L*ATAN(ABS(SY/(SX-X1(I))))
        IF(L.LT.1.0E-06)THEN
            L=1.0E-06
        ENDIF
        GU(2,ND)=-GRHO/L
        GU(4,ND)=-GRHOIM/L
        NCOND=NCOND+1
        TOTCON=TOTCON+GU(2,ND)
        TEMPR=L*RHO
        CUR=((VR(ND)-VR(2))*(VR(ND)-VR(2))+(VI(ND)-VI(2))*
1(VI(ND)-VI(2)))**0.5
        CUR=CUR/TEMPR
        WRITE(3,111)NDX(ND),NDY(ND),NDX(2),NDY(2),CUR
C
100  CONTINUE
C
        AVG=TOTCON/NCOND
        WRITE(6,222)AVG,NCOND,TOTCON
222  FORMAT(5X,'AVERAGE CONDUCTIVITY BET TWO INT-PTS',1X,E13.6,
12X,I5,2X,E13.6)
        ALSUML=ALOG10(-SUML+24.0254)
        ANGL=ANGL*180.0/(PI*TOTL)
        VOLFRA=9.817477E-03*TOTL
        WRITE(6,999)VOLFRA,ANGL,NOL
999  FORMAT(10X,'EFF.VOL.FRACTION = ',E13.6,2X,E13.6,2X,I5)

        RETURN
        END
C
C*****
C
        SUBROUTINE REMOV(G,GU,COL,ND)
C
        DIMENSION G(3000,5),GU(4,3000)
        INTEGER COL(3000)

```

```

C
      DO 100 I=3,ND
      IF((G(I,2).EQ.0.0).AND.(G(I,3).EQ.0.0).AND.(G(I-1,2).EQ.0.0))
1THEN
      DO 200 K=3,ND
      IF(COL(K).EQ.I)GO TO 100
200  CONTINUE
C
      IF((GU(1,I).NE.0.0).OR.(GU(2,I).NE.0.0))GO TO 100
C
C
C      IF FLOW OF PROGRAM REACHES THIS POINT THEN IT MEANS THAT
C      NODE I IS HANGING NODE. HENCE REMOVE IT.
C
      ND=ND-1
      DO 300 J=I,ND
      G(J,2)=G(J+1,2)
      G(J,3)=G(J+1,3)
      G(J,5)=G(J+1,5)
      GU(1,J)=GU(1,J+1)
      GU(2,J)=GU(2,J+1)
      GU(3,J)=GU(3,J+1)
      GU(4,J)=GU(4,J+1)
      IF(COL(J+1).EQ.0)THEN
          COL(J)=COL(J+1)
      ELSE
          COL(J)=COL(J+1)-1
      ENDIF
300  CONTINUE
      ENDIF
100  CONTINUE
C
      RETURN
      END
C
C*****
C
      SUBROUTINE CONSTR(G,GU,COL,A,IA,JA,ND)
C
      DIMENSION G(3000,5),GU(4,3000),A(30000),IA(3000),JA(30000)
      INTEGER COL(3000)
      REAL CAP,FRE,W
      COMMON/ELE/GREAL,GIMG
      DATA PI/3.14159265/
C
C      CONSTRUCT DIAGONAL ELEMENTS OF CONDUCTANCE MATRIX.
C
      DO 100 I=3,ND
      G(I,1)=-G(I,2)-G(I,3)
      G(I,4)=G(I,5)+G(I-1,5)
      IF(COL(I-1).NE.I)THEN
          G(I,1)=G(I,1)-G(I-1,2)
      ENDIF
      IF(COL(I).NE.0)THEN

```

```

        G(I,4)=G(I,4)-GIMG
    ENDIF
    DO 200 J=3,I
    IF(COL(J).NE.I)GO TO 200
    G(I,1)=G(I,1)-G(J,3)
    G(I,4)=G(I,4)-GIMG
200  CONTINUE
    IF(GU(1,I).NE.0.0)THEN
        G(I,1)=G(I,1)-GU(1,I)
        G(I,4)=G(I,4)+GU(3,I)
    ENDIF
    IF(GU(2,I).NE.0.0)THEN
        G(I,1)=G(I,1)-GU(2,I)
        G(I,4)=G(I,4)+GU(4,I)
    ENDIF
100  CONTINUE
C
C   CONSTRUCT MATRICES A, IA, JA IN THE FORM NEEDED BY
C   SLMATH SUBROUTINES.
C   AN ARRAY A CONTAINS ONLY THE NON-ZERO ELEMENTS OF CONDUCTANCE
C   MATRIX STORED ROWWISE. AN ARRAY JA CONTAINS THE CORRESPONDING
C   COLUMN INDICES OF THE NON-ZERO ELEMENTS. AN ARRAY IA INDICATES
C   THE END OF THE LAST ROW. A(K), FOR K=IA(I) IS THE FIRST
C   NON-ZERO ELEMENT OF THE I-TH ROW OF A, JA(K) BEING THE
C   CORRESPONDING COLUMN INDEX.
C
    K=1
    NR=1
    IA(1)=1
    A(1)=0.0
C
C   UPPER EDGE : NODE 1 : GROUNDED
C   LOWER EDGE : NODE 2 : GIVES FIRST ROW OF COND. MATRIX
C
    DO 300 I=3,ND
    A(1)=A(1)-GU(2,I)
300  CONTINUE
    JA(1)=1
    N=ND-1
    DO 400 I=3,ND
    IF(GU(2,I).EQ.0.0)GO TO 400
    K=K+1
    A(K)=GU(2,I)
    JA(K)=I-1
400  CONTINUE
    K=K+1
    A(K)=0.0
    DO 450 I=3,ND
    A(K)=A(K)+GU(4,I)
450  CONTINUE
    JA(K)=N+1
    DO 460 I=3,ND
    IF(GU(4,I).EQ.0.0)GO TO 460
    K=K+1

```

```

        A(K)=-GU(4,I)
        JA(K)=I-1+N
460    CONTINUE
        NR=NR+1
        IA(NR)=K+1
        DO 501 I=3,ND
        K=K+1
        A(K)=G(I,1)
        JA(K)=I-1
        IF(G(I,2).EQ.0.0)GO TO 497
        K=K+1
        A(K)=G(I,2)
        JA(K)=I
497    IF(COL(I).EQ.0)GO TO 498
        K=K+1
        A(K)=G(I,3)
        JA(K)=COL(I)-1
        IF(GU(4,I).NE.0.0)THEN
            K=K+1
            A(K)=-GU(4,I)
            JA(K)=N+1
        ENDIF
        K=K+1
        A(K)=-G(I-1,5)
        JA(K)=I-2+N
        K=K+1
        A(K)=G(I,4)
        JA(K)=I-1+N
        IF(COL(I).GT.(I+1))THEN
            K=K+1
            A(K)=-G(I,5)
            JA(K)=I+N
            K=K+1
            A(K)=GIMG
            JA(K)=COL(I)-1+N
        ELSE
            K=K+1
            A(K)=GIMG
            JA(K)=COL(I)-1+N
        ENDIF
        GO TO 500
498    IF(GU(4,I).NE.0.0)THEN
        K=K+1
        A(K)=-GU(4,I)
        JA(K)=N+1
    ENDIF
    DO 499 J=3,ND
        IF(COL(J).EQ.I)GO TO 600
499    CONTINUE

```

HERE IT MEANS THAT I TH NODE IS NOT CONNECTED TO ANY  
NODE BY R-C PARALLELL COMBINATION.

K=K+1

```

        A(K)=-G(I-1,5)
        JA(K)=I-2+N
        GO TO 650
600    K=K+1
        A(K)=G(I,N)
        JA(K)=J-1+N
        IF(J.LT.(I-1))THEN
            K=K+1
            A(K)=-G(I-1,5)
            JA(K)=I-2+N
        ENDIF
650    K=K+1
        A(K)=G(I,4)
        JA(K)=I-1+N
        IF(JA(K).EQ.(2*N))GO TO 500
        K=K+1
        A(K)=-G(I,5)
        JA(K)=I+N
500    NR=NR+1
        IA(NR)=K+1
501    CONTINUE
C
        IAM1=IA(2)-1
        DO 510 I=1,IAM1
        IF(JA(I).GT.N)GO TO 510
        K=K+1
        A(K)=-A(I)
        JA(K)=JA(I)+N
510    CONTINUE
        NR=NR+1
        IA(NR)=K+1
        DO 550 I=3,ND
        K=K+1
        A(K)=-G(I,1)
        JA(K)=I-1+N
        IF(G(I,2).EQ.0.0)GO TO 525
        K=K+1
        A(K)=-G(I,2)
        JA(K)=I+N
525    IF(COL(I).EQ.0)GO TO 535
        K=K+1
        A(K)=-G(I,3)
        JA(K)=COL(I)+N-1
535    NR=NR+1
        IA(NR)=K+1
550    CONTINUE
C
        N2=N*2
800    WRITE(4,111)K,N2
111    FORMAT(20X,I5,5X,I5)
        WRITE(4,222)(A(I),JA(I),I=1,K)
222    FORMAT(3(2X,D15.8,2X,I5))
        WRITE(4,333)(IA(I),I=1,NR)
333    FORMAT(12(1X,I5))

```

RETURN  
END

C

C\*\*\*\*\*

C

SUBROUTINE FRACT

C

C

SUBROUTINE TO DETERMINE WHETHER OUR SYSTEM IS FRACTAL

C

DIMENSION X1(200),Y1(200),X2(200),Y2(200)  
DIMENSION IFIB1(8000),IFIB2(8000)  
REAL IX(8000),IY(8000)  
COMMON/MGSC/X1,Y1,X2,Y2,A,B,TLEN  
COMMON/MGI/IX,IY,IFIB1,IFIB2,NINT

C

C

A1,A2 GIVES US THE SIZE OF THE SANDBOX.

C

SQUARE FILM : A = B IS ASSUMED.

C

NCOUNT GIVES US NUMBER OF INTERSECTION POINTS LYING

C

INSIDE OUR SANDBOX.

C

NCOUNT=0  
D=A/40.0  
A1=A/2.0-D  
A2=A/2+D

C

50

DO 100 I=1,NINT  
IF((IX(I).LE.A2).AND.(IX(I).GE.A1))THEN  
IF((IY(I).LE.A2).AND.(IY(I).GE.A1)) THEN  
NCOUNT=NCOUNT+1  
ENDIF  
ENDIF

100

CONTINUE  
SL=A2-A1  
ALSL=ALOG10(SL)  
ANCOUNT=ALOG10(FLOAT(NCOUNT))  
WRITE(4,111)SL,NCOUNT,ALSL,ANCOUNT  
111 FORMAT(5X,F6.3,2X,I5,2X,E10.4,2X,E10.4)  
NCOUNT=0  
A1=A1-D  
A2=A2+D  
IF(A1.GE.0.0)GO TO 50  
RETURN  
END





```

C
C   SUBROUTINE GENNEU GENERATES POSITIONS OF ALL NEUTRAL SOLITONS
C
C       CALL GENNEU(DSEED,NNEU,NCHAIN)
C
C   SUBROUTINE GENCHA GENERATES POSITIONS OF ALL CHARGED SOLITONS
C   ALONG WITH THE IMPURITIES CORRESPONDING TO THEM.
C
C       CALL GENCHA(DSEED,NIMP,NFLIMP,NCHA,NCHAIN)
C
C       FACT=FLOAT(NCHA*NNEU)/FLOAT(NCHA+NNEU)**2
C       CAP=CAPCON*FACT*(TEMP/300.000)**M
C       WRITE(6,22)CAP
22  FORMAT(10X,D13.6)
C       NEUIMP=NNEU
C       DO 150 I=1,NEUIMP
C           XMPNEU(I)=XNEU(I)
C           YMPNEU(I)=YNEU(I)
C           ZMPNEU(I)=ZNEU(I)
150  CONTINUE
C
C   SUBROUTINE COND CREATES THE CONDUCTIVITY MATRIX G(I,J)
C
C       CALL COND(NVCHA,NVNEU,NCHA,NEUIMP,NFLIMP)
C
C   TO CONSTRUCT MATRICES NECESSARY FOR SLMATH
C
C       READ(5,5)FRE
C       FORMAT(5X,D13.6)
C       WRITE(8,123)FRE
123  FORMAT(5X,D13.6)
C       W=2.000*PI*FRE
C       CALL CONST(NVCHA,NVNEU,CAP,W)
C
C       CALL EXIT
C       END
C
C *****
C   SUBROUTINE CHAINS GENERATES NCHAIN NUMBER OF CHAINS
C   PARALLEL TO Z AXIS FROM LOWER PLATE TO UPPER PLATE.
C   HENCE ONE (X,Y) COORDINATE DEFINES THE CHAIN.
C
C       SUBROUTINE CHAINS(DSEED,NCHAIN)
C
C       IMPLICIT REAL*8 (A-H,O-Z)
C       DIMENSION XCHAIN(3000),YCHAIN(3000)
C       REAL P(2)
C       COMMON/CHAIN/XCHAIN,YCHAIN
C       COMMON/ALL/A,B,C
C
C       NP=2
C       DO 100 I=1,NCHAIN
C           CALL GGUBS(DSEED,NP,P)

```

```

C          THE RANDOM NUMBER P(1) IS USED FOR RADIUS & P(2) FOR THETA.
C
          P(1)=P(1)*A
          P(2)=P(2)*B
          XCHAIN(I)=P(1)*COS(P(2))
          YCHAIN(I)=P(1)*SIN(P(2))
100      CONTINUE
C
          RETURN
          END
C
C
C*****
C
          SUBROUTINE GENNEU(DSEED,NNEU,NCHAIN)
C
C          GENERATES THE SITES FOR THE NEUTRAL SOLITONS
C          ALONG THE CHAINS.
C
          IMPLICIT REAL*8 (A-H,O-Z)
          DIMENSION XNEU(3000),YNEU(3000),ZNEU(3000)
          DIMENSION XCHAIN(3000),YCHAIN(3000)
          REAL P(2)
          LOGICAL FLAG(3000)
          DOUBLE PRECISION DSEED
          COMMON/NEUT/XNEU,YNEU,ZNEU
          COMMON/CHAIN/XCHAIN,YCHAIN
          COMMON/ALL/A,B,C
C
          DO 10 I=1,NCHAIN
              FLAG(I)=.FALSE.
10      CONTINUE
          NP=2
          DO 100 I=1,NNEU
              CALL GGUBS(DSEED,NP,P)
50
C
          P(1) IS USED TO CHOOSE A CHAIN RANDOMLY & P(2) IS
          USED TO FIX Z COORDINATE OF A NEUTRAL SOLITON.
C
          K=P(1)*NCHAIN
          IF((K.LE.0).OR.(K.GT.NCHAIN))GO TO 50
          IF(FLAG(K))GO TO 50
          P(2)=P(2)*2.0D0-0.5D0
          IF((P(2).LT.0.0D0).OR.(P(2).GT.1.0D0))GO TO 50
          XNEU(I)=XCHAIN(K)
          YNEU(I)=YCHAIN(K)
          ZNEU(I)=C*P(2)
          FLAG(K)=.TRUE.
100     CONTINUE
C
          RETURN
          END
C
C

```

```

C*****
C
      SUBROUTINE GENCHA(DSEED,NIMP,NFLIMP,NCHA,NCHAIN)
C
C      GENERATES SITES FOR THE CHARGED SOLITONS
C      ALONG THE CHAINS.
C
      IMPLICIT REAL*8 (A-H,O-Z)
      DIMENSION XCHA(6000),YCHA(6000),ZCHA(6000)
      DIMENSION XCHAIN(3000),YCHAIN(3000)
      DIMENSION XFLIMP(8000),YFLIMP(8000),ZFLIMP(8000)
      INTEGER LPOS(3000),LPOSFL(3000)
      REAL P(3)
      DOUBLE PRECISION DSEED
      COMMON/CHARG/XCHA,YCHA,ZCHA
      COMMON/FLO/XFLIMP,YFLIMP,ZFLIMP,LPOS,LPOSFL
      COMMON/CHAIN/XCHAIN,YCHAIN
      COMMON/ALL/A,B,C,FR
C
      READ(5,11)XYNEAR
11      FORMAT(5X,D13.6)
      NCHA=0
      NFLIMP=0
      NP=3
      DO 100 I=1,NIMP
50          CALL GGUBS(DSEED,NP,P)
              P(3)=P(3)*2.0D0-0.5D0
              IF((P(3).LT.0.0D0).OR.(P(3).GT.1.0D0))GO TO 50
C
C      P(1),P(2),P(3) REPRESENT X,Y,Z COORDINATE OF AN
C      IMPURITY ATOM RESPECTIVELY.
C
      P(3)=C*P(3)
      P(1)=A*P(1)
      P(2)=B*P(2)
      TEMP=P(1)
      P(1)=P(1)*COS(P(2))
      P(2)=TEMP*SIN(P(2))
      DO 200 J=1,NCHAIN
1          DIST=(XCHAIN(J)-P(1))*(XCHAIN(J)-P(1))+
              (YCHAIN(J)-P(2))*(YCHAIN(J)-P(2))
              DIST=DSQRT(DIST)
              IF(DIST.LE.XYNEAR)THEN
                  NCHA=NCHA+1
                  XCHA(NCHA)=XCHAIN(J)
                  YCHA(NCHA)=YCHAIN(J)
                  ZCHA(NCHA)=P(3)
                  GO TO 100
      ENDIF
200      CONTINUE
      NFLIMP=NFLIMP+1
      XFLIMP(NFLIMP)=P(1)
      YFLIMP(NFLIMP)=P(2)
      ZFLIMP(NFLIMP)=P(3)

```

```

100      CONTINUE
C
          RETURN
          END
C
C
C*****
C
          SUBROUTINE COND(NVCHA,NVNEU,NCHA,NEUIMP,NFLIMP)
C
C          IT CONSTRUCTS THE CONDUCTANCE MATRIX, AND TAKES CARE
C          OF THE LOWER AND UPPER EDGES OF THE FIBER.
C
          IMPLICIT REAL*8 (A-H,O-Z)
          DIMENSION G(1000,1000),XCHA(6000),YCHA(6000),ZCHA(6000)
          DIMENSION XMPNEU(3000),YMPNEU(3000),ZMPNEU(3000)
          DIMENSION XFLIMP(8000),YFLIMP(8000),ZFLIMP(8000)
          INTEGER LPOS(3000),LPOSFL(3000)
          INTEGER LU(100),LW(100),NL(100),NU(100)
          DIMENSION GL(2000),GU(2000)
          COMMON/CHARG/XCHA,YCHA,ZCHA
          COMMON/NEAR/XMPNEU,YMPNEU,ZMPNEU
          COMMON/MC/TEMP,FACT
          COMMON/FLO/XFLIMP,YFLIMP,ZFLIMP,LPOS,LPOSFL
          COMMON/ALL/A,B,C
          COMMON/MCC/G,GL,GU
C
          ZLIM=C*0.05
C          FIRST TAKE CARE OF CHARGED SOLITONS LYING ON LOWER PLATE.
          DO 50 I=1,NCHA
              IF(ZCHA(I).LT.ZLIM)GO TO 51
50          CONTINUE
51          TX=XCHA(2)
              TY=YCHA(2)
              TZ=ZCHA(2)
              XCHA(2)=XCHA(I)
              YCHA(2)=YCHA(I)
              ZCHA(2)=ZCHA(I)
              XCHA(I)=TX
              YCHA(I)=TY
              ZCHA(I)=TZ
              IP1=I+1
              NLWC=1
              LW(NLWC)=2
              JLIM=NCHA
              J=IP1
              IF(J.GT.NCHA)GO TO 70
60          IF(ZCHA(J).LT.ZLIM)THEN
              K=NCHA-NLWC+1
61          IF(K.EQ.J)GO TO 65
              IF(ZCHA(K).LT.ZLIM)THEN
                  K=K-1
                  NLWC=NLWC+1
                  LW(NLWC)=K+1

```

```

        GO TO 61
        ENDIF
        TX=XCHA(J)
        TY=YCHA(J)
        TZ=ZCHA(J)
        XCHA(J)=XCHA(K)
        YCHA(J)=YCHA(K)
        ZCHA(J)=ZCHA(K)
        XCHA(K)=TX
        YCHA(K)=TY
        ZCHA(K)=TZ
65      NLWC=NLWC+1
        LW(NLWC)=K
        JLIM=NCHA-NLWC+1
        ENDIF
        J=J+1
        IF(J.LE.JLIM)GO TO 60
C
C      TAKE CARE OF CHARGED SOLITONS LYING ON THE UPPER PLATE.
C
70      DO 80 I=1,NCHA
        IF(ZCHA(I).GT.(C-ZLIM))GO TO 81
80      CONTINUE
81      TX=XCHA(1)
        TY=YCHA(1)
        TZ=ZCHA(1)
        XCHA(1)=XCHA(I)
        YCHA(1)=YCHA(I)
        ZCHA(1)=ZCHA(I)
        XCHA(I)=TX
        YCHA(I)=TY
        ZCHA(I)=TZ
        IP1=I+1
        NUPC=1
        LU(NUPC)=1
        JLIM=NCHA-NLWC+1
        J=IP1
        IF(J.GT.JLIM)GO TO 99
90      IF(ZCHA(J).GT.(C-ZLIM))THEN
        K=NCHA-NLWC-NUPC+2
91      IF(J.EQ.K)GO TO 95
        IF(ZCHA(K).GT.(C-ZLIM))THEN
        K=K-1
        NUPC=NUPC+1
        LU(NUPC)=K+1
        GO TO 91
        ENDIF
        TX=XCHA(J)
        TY=YCHA(J)
        TZ=ZCHA(J)
        XCHA(J)=XCHA(K)
        YCHA(J)=YCHA(K)
        ZCHA(J)=ZCHA(K)
        XCHA(K)=TX

```

```

          YCHA(K)=TY
          ZCHA(K)=TZ
95      NUPC=NUPC+1
          LU(NUPC)=K
          JLIM=NCHA-NLWC-NUPC+2
      ENDIF
      J=J+1
      IF(J.LE.JLIM)GO TO 90
      WRITE(6,14)NUPC
C
C
99      NVCHA=NCHA-NLWC-NUPC+2
          DO 20 I=1,NCHA
              GL(I)=0.0DO
              GU(I)=0.0DO
20      CONTINUE
C
C      NOW FIND OUT THE NEUTRAL SOLITONS LYING ON THE LOWER
C      AND THE UPPER PLATES.
C
      NLWN=0
      J=1
      JLIM=NEUIMP
410     IF(ZMPNEU(J).LT.ZLIM)THEN
          K=NEUIMP-NLWN
420     IF(J.EQ.K)GO TO 450
          IF(ZMPNEU(K).LT.ZLIM)THEN
              NLWN=NLWN+1
              NL(NLWN)=K
              K=K-1
              GO TO 420
          ENDIF
C
          TX=XMPNEU(J)
          TY=YMPNEU(J)
          TZ=ZMPNEU(J)
          ITEMP1=LPOS(J)
          ITEMP2=LPOSFL(J)
          XMPNEU(J)=XMPNEU(K)
          YMPNEU(J)=YMPNEU(K)
          ZMPNEU(J)=ZMPNEU(K)
          LPOS(J)=LPOS(K)
          LPOSFL(J)=LPOSFL(K)
          XMPNEU(K)=TX
          YMPNEU(K)=TY
          ZMPNEU(K)=TZ
          LPOS(K)=ITEMP1
          LPOSFL(K)=ITEMP2
450     NLWN=NLWN+1
          NL(NLWN)=K
          JLIM=NEUIMP-NLWN
      ENDIF
      J=J+1
      IF(J.LE.JLIM)GO TO 410

```

```

C
C
      NUPN=0
      JLIM=NEUIMP-NLWN
      J=1
510  IF(ZMPNEU(J).GT.(C-ZLIM))THEN
      K=NEUIMP-NLWN-NUPN
520  IF(J.EQ.K)GO TO 550
      IF(ZMPNEU(K).GT.(C-ZLIM))THEN
      NUPN=NUPN+1
      NU(NUPN)=K
      K=K-1
      GO TO 520
      ENDIF
C
      TX=XMPNEU(J)
      TY=YMPNEU(J)
      TZ=ZMPNEU(J)
      ITEMP1=LPOS(J)
      ITEMP2=LPOSFL(J)
      XMPNEU(J)=XMPNEU(K)
      YMPNEU(J)=YMPNEU(K)
      ZMPNEU(J)=ZMPNEU(K)
      LPOS(J)=LPOS(K)
      LPOSFL(J)=LPOSFL(K)
      XMPNEU(K)=TX
      YMPNEU(K)=TY
      ZMPNEU(K)=TZ
      LPOS(K)=ITEMP1
      LPOSFL(K)=ITEMP2
550  NUPN=NUPN+1
      NU(NUPN)=K
      JLIM=NEUIMP-NLWN-NUPN
      ENDIF
C
      J=J+1
      IF(J.LE.JLIM)GO TO 510
C
C      READ ELECTRON'S MEAN FREE PATHS.
C      ZETPL : ALONG THE CHAIN
C      ZETPD : PERPENDICULAR TO THE CHAIN
C
      READ(5,111)ZETPL,ZETPD,GCON
111  FORMAT(3(2X,D13.6))
C
      DO 10 I=1,NCHA
      GU(I)=0.0DO
      GL(I)=0.0DO
      DO 10 J=1,NEUIMP
      G(I,J)=0.0DO
10  CONTINUE
      DO 100 I=1,NCHA
      DO 200 J=1,NEUIMP
      RPL=(ZCHA(I)-ZMPNEU(J))*(ZCHA(I)-ZMPNEU(J))

```

```

      RPD=(XCHA(I)-XMPNEU(J))*(XCHA(I)-XMPNEU(J))+
1(YCHA(I)-YMPNEU(J))*(YCHA(I)-YMPNEU(J))
      TI=2.00D0*(RPL/ZETPL+RPD/ZETPD)**0.5D0
      IF(TI.GT.34.0D0)GO TO 200
      TI=DEXP(-TI)
      G(I,J)=TI
200      CONTINUE
100      CONTINUE
C
      NB=0
      DO 300 I=1,NCHA
        DO 301 J=1,NEUIMP
          IF(G(I,J).EQ.0.0D0)GO TO 301
          NB=NB+1
301      CONTINUE
300      CONTINUE
      IVGNB=NB/NCHA
      WRITE(6,12)IVGNB
12      FORMAT(10X,I5)
C
C      TAKE CARE OF HANGING SITES.
C
      NZERO=0
      I=3
340      DO 351 J=1,NEUIMP
        IF(G(I,J).NE.0.0D0)GO TO 350
351      CONTINUE
C      HERE IT MEANS THAT ALL G(I,J)'S ARE ZERO FOR THIS I
      NZERO=NZERO+1
      NCHA=NCHA-1
      DO 352 K=I,NCHA
        DO 352 J=1,NEUIMP
          G(K,J)=G(K+1,J)
352      CONTINUE
      I=I-1
350      I=I+1
      IF(I.LT.(NCHA-NLWC-NUPC+2))GO TO 340
      WRITE(6,41)NZERO
41      FORMAT(20X,I5)
C      WRITE(4,11)((G(I,J),I=100,102),J=1,NEUIMP)
11      FORMAT(3(5X,D13.6))
      DO 375 I=2,NLWC
        LW(I)=LW(I)-NZERO
375      CONTINUE
C
      DO 380 I=2,NUPC
        LU(I)=LU(I)-NZERO
380      CONTINUE
C
      NZNEU=0
      I=1
355      DO 361 J=1,NCHA
        IF(G(J,I).NE.0.0)GO TO 360
361      CONTINUE

```

```

        NEUIMP=NEUIMP-1
        NZNEU=NZNEU+1
        DO 362 K=I,NEUIMP
            DO 362 J=1,NCHA
                G(J,K)=G(J,K+1)
362     CONTINUE
        I=I-1
360     I=I+1
        IF(I.LT.(NEUIMP-NLWN-NUPN))GO TO 355
        WRITE(6,41)NZNEU
C
        DO 390 I=1,NLWN
            NL(I)=NL(I)-NZNEU
390     CONTINUE
        DO 385 I=1,NUPN
            NU(I)=NU(I)-NZNEU
385     CONTINUE
C
C
C
        GMAX=G(1,1)
        GMIN=100.0DO
        DO 125 I=1,NCHA
            DO 125 J=1,NEUIMP
                IF(G(I,J).EQ.0.0DO)GO TO 125
                IF(G(I,J).LT.GMIN)THEN
                    GMIN=G(I,J)
                ENDIF
                IF(G(I,J).GT.GMAX)THEN
                    GMAX=G(I,J)
                ENDIF
125     CONTINUE
        WRITE(6,31)GMIN,GMAX
        31     FORMAT(5X,'GMIN=',D13.6,'GMAX=',D13.6)
        GMETAL=GMAX*5.0DO
C
C
C
        TAKE CARE OF CONDUCTANCES BETWEEN THE SITES AND THE
        LOWER AND THE UPPER PLATES.
C
        NVNEU=NEUIMP-NLWN-NUPN
        DO 500 I=2,NLWC
            DO 525 J=1,NVNEU
                IF(G(LW(I),J).EQ.0.0DO)GO TO 525
                G(LW(1),J)=G(LW(1),J)+G(LW(I),J)
525     CONTINUE
500     CONTINUE
C
        DO 700 I=2,NUPC
            DO 725 J=1,NVNEU
                IF(G(LU(I),J).EQ.0.0DO)GO TO 725
                G(LU(1),J)=G(LU(1),J)+G(LU(I),J)
725     CONTINUE
700     CONTINUE
C

```

```

      WRITE(6,13)NLWC
13     FORMAT(5X,'NLWC=',I5)
      WRITE(6,14)NUPC
14     FORMAT(5X,'NUPC=',I5)
C
      DO 900 I=1,NLWN
        DO 925 J=3,NVCHA
          IF(G(J,NL(I)).EQ.0.0D0)GO TO 925
          GL(J)=G(J,NL(I))
925     CONTINUE
900     CONTINUE
C
      DO 980 I=1,NUPN
        DO 985 J=3,NVCHA
          IF(G(J,NU(I)).EQ.0.0D0)GO TO 985
          GU(J)=GU(J)+G(J,NU(I))
985     CONTINUE
980     CONTINUE
C
      RETURN
      END
C
C*****
C     SUBROUTINE TO CONSTRUCT A,IA,JA NECESSARY TO SOLVE
C     GV=I USING SLMATH ROUTINES.
C
C     SUBROUTINE CONST(NVCHA,NVNEU,CAP,W)
C
C     IMPLICIT REAL*8 (A-H,O-Z)
C     DIMENSION G(1000,1000),A(30000),JA(30000),IA(2500)
C     DIMENSION GL(2000),GU(2000)
C     DOUBLE PRECISION A
C     COMMON/MCC/G,GL,GU
C
C     N=NVNEU+NVCHA-1
C     K=0
C     DO 100 I=2,NVCHA
C       K=K+1
C       IA(I-1)=K
C
C     GL(J) GIVES US COND BET NODE2 & NODE J
C
C     IF (I.NE.2)GO TO 150
C     DO 125 JJ=3,NVCHA
C       IF(GL(JJ).EQ.0.0D0)GO TO 125
C       K=K+1
C       A(K)=-GL(JJ)
C       JA(K)=JJ-1
125     CONTINUE
C
150     DO 200 J=1,NVNEU
C       IF(G(I,J).EQ.0.0D0)GO TO 200
C       K=K+1
C       A(K)=-G(I,J)

```

```

                JA(K)=NVCHA-1+J
200      CONTINUE
          SUM=0.0D0
          DO 300 L=IA(I-1),K
            SUM=SUM+A(L)
300      CONTINUE
C
C          GU(J) GIVES US COND BET NODE1 & NODE J.
C
          SUM=SUM-GU(I)-GL(I)
          A(IA(I-1))=-SUM
          JA(IA(I-1))=I-1
          IF(I.EQ.2)GO TO 100
          K=K+1
          A(K)=-W*CAP
          JA(K)=N+I-1
100     CONTINUE
C
          NT=K
C
          DO 400 J=1,NVNEU
            NT=NT+1
            IA(NVCHA-1+J)=NT
            A(NT)=G(1,J)
            JA(NT)=NVCHA-1+J
            KM1=K-1
            DO 500 I=1,KM1
              IF(JA(I).EQ.(NVCHA-1+J))THEN
                A(NT)=A(NT)-A(I)
              ENDIF
500     CONTINUE
          NT=NT+1
          A(NT)=-W*CAP
          JA(NT)=JA(NT-1)+N
400     CONTINUE
C
          PRINT *,NT, 'ABOVE-600'
          DO 600 I=1,N
            IA(N+I)=NT+1
            JLIM=IA(I+1)-1
            DO 600 J=IA(I),JLIM
              IF(JA(J).GT.N) GO TO 600
              NT=NT+1
              A(NT)=-A(J)
              JA(NT)=JA(J)+N
600     CONTINUE
C
          N=N*2
          IA(N+1)=NT+1
C
C          TO REMOVE ROWS WHICH HAVE ALL ZERO ELEMENTS.
C
          WRITE(8,111)NT,N

```

```
111   FORMAT(20X,I5,5X,I5)
      WRITE(8,222)(IA(I),I=1,N+1)
222   FORMAT(12(1X,I5))
      WRITE(8,333)(A(I),JA(I),I=1,NT)
333   FORMAT(3(2X,D15.8,2X,I5))
C
      RETURN
      END
```



```

      READ(8,3)(IA(I),I=1,N+1)
3     FORMAT(12(1X,I5))
C
      READ(5,44)THETA,CURMAG
44    FORMAT(2(5X,D13.6))
      DO 500 I=1,N
          C(I)=0.0DO
500   CONTINUE
      N2P1=N/2+1
      ITERMX=50
      C(1)=CURMAG*DCOS(THETA)
      C(N2P1)=-CURMAG*DSIN(THETA)
C
      CALL M000(N,NT,IBOT,IA,JA,IPM,IER,IB,LB,JB)
      IBOT=200000
      CALL MSNO(N,IBOT,IA,JA,A,IPM,IU,JU,U,DI,IK,IER,IPMI,IUP,X,IX,
1IP)
      CALL MBSO(N,ISW,IPM,IU,JU,U,DI,C,Y,V)
C
C
C     IN NEXT STEPS WE WILL CHECK OUR ANSWERS.ERR(I) WILL GIVE
C     US MEASURE OF ERROR.
C
C
      DO 50 ITER=1,ITERMX
          RECUR=C(1)
          IMCUR=-C(N2P1)
          TOTCUR=RECUR*RECUR+IMCUR*IMCUR
          VR=Y(1)
          VI=Y(N2P1)
C
          ZR=(VR*RECUR+VI*IMCUR)/TOTCUR
          ZI=(VI*RECUR-VR*IMCUR)/TOTCUR
          SDEN=ZR*ZR+ZI*ZI
          SR=ZR*FACT/SDEN
          SI=-ZI*FACT/SDEN
C
          WRITE(6,23)FRE,ZR,ZI,SR,SI
23    FORMAT(5(1X,D13.6))
C
          DO 100 I=1,N
              CCAL(I)=0.0DO
              IAM=IA(I+1)-1
              DO 200 J=IA(I),IAM
                  CCAL(I)=CCAL(I)+A(J)*Y(JA(J))
200   CONTINUE
C
              I1=I-1
              DO 101 K=1,I1
                  IAM2=IA(K+1)-1
C
                  DO 201 L=IA(K),IAM2
                      IF(JA(L).NE.I)GO TO 201
202   CCAL(I)=CCAL(I)+A(L)*Y(K)

```

```

201          CONTINUE
C
101          CONTINUE
C
          ERR(I)=C(I)-CCAL(I)
C
100          CONTINUE
C
C          TO FIND OUT MAXIMUM ERROR
C
          EMAX=ERR(1)
          DO 52 II=2,N
              IF(ERR(II).GT.EMAX)THEN
                  EMAX=ERR(II)
              ENDIF
52          CONTINUE
          IF(EMAX.LT.1.0E-02)THEN
              WRITE(6,666)ITER,EMAX
              GO TO 55
          ENDIF
666          FORMAT(5X,'ITER=',I5,2X,'EMAX=',D15.6)
C
          CALL MBSO(N,ISW,IPM,IU,JU,U,DI,ERR,R,V)
C
          DO 51 LL=1,N
              Y(LL)=Y(LL)+R(LL)
51          CONTINUE

          RMAX=R(1)/Y(1)
          DO 54 JJ=2,N
              IF(R(JJ)/Y(JJ).GT.RMAX)THEN
                  RMAX=R(JJ)/Y(JJ)
              ENDIF
54          CONTINUE
          IF(ABS(RMAX).LT.1.0E-05)GO TO 55
50          CONTINUE
55          WRITE(6,23)FRE,ZR,ZI,SR,SI
          VR=Y(1)
          VI=Y(N2P1)
C
          N2=N/2
          WRITE(9,121)(Y(I),Y(I+N2),I=1,N2)
121          FORMAT(4(1X,D15.8))
          CALL EXIT
          END

```

## REFERENCES

- Am71 V. Ambegaonkar, B. I. Halperin, J. S. Langer;  
Phys. Rev. B4, 2612 (1971).
- Bo76 P. H. Bottelberghs, G. H. J. Broers;  
J. Electroanal. Chem. 67, 155 (1976).
- Br84 G. J. Brug, A. L. G. Van Den Eeden, M. Sluyters-Rehbach,  
J. H. Sluyters  
J. Electroanal. Chem. 176, 275 (1984).
- Bu77 P. M. Butcher, K. J. Hauden, J. A. McInnes;  
Philos. Mag. 36, 19 (1977).
- Bu86 A. L. R. Bug, G. S. Grest, M. H. Cohen, I. Webman;  
Phys. Rev. B, 19 (1986).
- Ca69 Carnahan, Luther and Wilkes;  
Applied Numerical Methods, P. 300,  
John Wiley and Sons, New York 1969.
- Ch77 C. K. Chiang et al.  
Phys. Rev. Lett. 39, 1098 (1977).
- Co38 C. A. Coulson;  
Proc. Roy. Soc. A164, 383 (1938).
- Co82 M. H. Cohen, M. Tomkiewicz;  
Phys. Rev. B26, 7097 (1982).
- De83 B. Derrida, D. Stauffer, H. J. Herrmann, J. Vannimenus;  
J. Physique Lett. 44, L701 (1983).
- Eh86 K. Ehinger, S. Roth;  
Philos. Mag. B53, 301 (1986).
- Ep81 A. J. Epstein, H. Rommelmann, M. Abkowitz, H. W. Gibson;  
Phys. Rev. Lett. 47, 1549 (1981).
- Fr85 J. E. Frommer, R. R. Chance;  
Encyclopaedia of Polymer Science and Engineering, 2nd Ed. 5,  
462 (1985).
- Go79 I. B. Goldberg, H. R. Crowe, P. R. Newman, A. J. Heeger,  
A. G. MacDiarmid  
J. Chem. Phys. 70, 1132 (1979).

- He84 H. J. Herrmann, B. Derrida, J. Vannimenus;  
Phys. Rev. B30, 4080 (1984).
- It74 T. Ito, H. Shirakawa, S. Ikeda;  
J. Poly. Sci. Poly. Chem. 12, 11 (1974).
- Ki73 S. Kirkpatrick;  
Rev. Mod. Phys. 45, 574 (1973).
- Ki79 S. Kirkpatrick;  
I11 Condensed Matter, Eds. R. Balian, R. Maynard, G. Toulouse  
(North Holland 1979).
- Ki82 S. Kivelson;  
Phys. Rev. B25, 3798 (1982).
- Kr84 M. Kramer, M. Tomkiewicz;  
J. Electrochem. Soc. 13, 1283 (1984).
- Li85 S. H. Liu;  
Phys. Rev. Lett. 55, 529 (1985).
- Le37 J. E. Lennard-Jones;  
Proc. Roy. Soc. A158, 280 (1937).
- Ly80 J. Lyden, M. H. Cohen, M. Tomkiewicz;  
Phys. Rev. Lett. 47, 961 (1980).
- Mi60 A. Miller, E. Abrahams;  
Phys. Rev. 120, 745 (1960).
- Mo56 N. F. Mott;  
Can. J. Phys. 34, 1356 (1956).
- Mo82 J. Mort, G. Pfister;  
Electronic Properties of Polymers, John Wiley and Sons (1982).
- Ov78 A. A. Ovchinnikov, I. I. Ukranski, G. V. Kventsel;  
Sov. Phys. Usp. 15 575 (1978).
- Pa80 Y. W. Park, A. J. Heeger, M. A. Druy, A. G. MacDiarmid;  
J. Chem. Phys. 73, 946 (1980).
- Pe55 R. F. Peierls;  
Quantum Theory of Solids, Clarendon, Oxford 1955.
- Ph82 A. Philipp, W. Mayr, K. Seeger;  
Solid State Comm. 43, 857 (1982).

- Pi74 G. E. Pike, C. H. Seager;  
Phys. Rev. B10, 1421 (1974).
- Ri79 M. J. Rice;  
Phys. Lett. 71A, 152 (1979).
- Sc74 W. Scheider;  
J. Phys. Chem. 79, 127 (1974).
- Sh80 P. Sheng ;  
Phys. Rev. B21, 2180 (1980).
- St85 D. Stroud;  
Proceedings of Symposium on the Chemistry and Physics of  
Composite Media, Eds. P. N. Sen and M. Tomkiewicz Page 27,  
The Electrochemical Society, 1985.
- Su79 W. P. Su, J. R. Schrieffer, A. J. Heeger;  
Phys. Rev. Lett. 42, 1698 (1979).
- Su80 W. P. Su, J. R. Schrieffer, A. J. Heeger;  
Phys. Rev. B22, 2099 (1980).
- Su85 S. Summerfield, J. A. Chroboczek;  
Solid State Comm. 53, 129 (1985).
- To81 Y. Tomkiewicz, T. D. Schultz, H. B. Brom, A. R. Taranko,  
T. C. Clarke, G. B. Street  
Phys. Rev. B24, 4348 (1981).
- We75 I. Webman, J. Jortner, M. H. Cohen;  
Phys. Rev. B11, 2885 (1975).
- We79 B. R. Weinberger, S. Kaufer, A. J. Heeger, A. Pron,  
A. G. MacDiarmid  
Phys. Rev. B20, 223 (1979).
- We80 B. R. Weinberger, S. Kaufer, A. J. Heeger, A. Pron,  
A. G. MacDiarmid  
Phys. Rev. Lett. 45, 1123 (1980).